Association between TSPO-PET measurable microglial activation and soluble GFAP in multiple sclerosis

Institute of Biomedicine
MDP in Biomedical Sciences
Drug Discovery and Development
Master's thesis

Author:
Inke Tirkkonen

Supervisors:
Laura Airas, MD, PhD, Professor
Maija Saraste, PhD

12.04.2023
Turku

Master's thesis

Subject: Institute of Biomedicine, MDP in Biomedical Sciences, Drug Discovery and Development
Author: Inke Tirkkonen, BSc
Title: Association between TSPO-PET measurable microglial activation and soluble GFAP in multiple sclerosis
Supervisors: Laura Airas, MD, PhD, Professor; Maija Saraste, PhD
Number of pages: 77 pages
Date: 12.04.2023

INTRODUCTION Multiple sclerosis (MS) is a chronic, immune-mediated disease that targets the central nervous system (CNS). It is characterized by neuroinflammation, demyelination, and progressive neurodegeneration which are believed to be triggered by an autoimmune reaction. Despite recent advancements, the pathophysiology of MS is still not fully understood.

Microglia and astrocytes are glial cells of the CNS. Microglia participate in the surveillance of the CNS and react accordingly in case of a disturbance, causing them to change their phenotype in a phenomenon called microgliosis. Activated microglia produce various pro- and anti-inflammatory agents, attracting more immune cells to the site. Like microglia, astrocytes can become activated in a process called reactive astrogliosis, characterized by a changed gene expression and hypertrophy. Reactive astrogliosis can result in the formation of a glial scar. Together microglia and astrocytes drive the MS pathophysiology by partaking in lesion formation, causing tissue damage due to the neurotoxic agents they release, and on the other hand by controlling the neuroinflammation.

STUDY OBJECTIVE AND DESIGN The objective of this study was to evaluate microglial and astrocytic activation in MS patients and shed light on the possible connections between the two. Microglial activation was assessed by TSPO-PET imaging using a [^{11}C]PK11195 radioligand, and serum glial fibrillary acidic protein (GFAP) was used as a biomarker of astrocytic activity. The study cohort included 44 MS patients who took part in PET and magnetic resonance imaging, blood sampling, and clinical assessment. In addition, 22 healthy controls (HCs) were included.

RESULTS MS patients had a mean serum GFAP of 98.85 pg/ml and HCs 69.15 pg/ml ($p = 0.006$). The serum GFAP was lower in treated patients compared to non-treated ($p = 0.005$). In MS patients compared to HCs, [^{11}C]PK11195 binding, presented as distribution volume ration (DVR) and the number of active voxels, was higher in whole brain ($p = 0.011$, $p = 0.020$) and normal appearing white matter (NAWM) ($p = 0.046$, $p = 0.010$). MS patients were divided into GFAP(low) and GFAP(high) groups based on the 80th percentile serum GFAP of HCs (90.47 pg/ml). Patients with high serum GFAP levels had fewer active voxels in whole brain ($p = 0.026$) and NAWM ($p = 0.023$), as well as lower DVR in cortical grey matter ($p = 0.003$), compared to patients with low serum GFAP. The DVRs in brain stem ($p = 0.049$), pallidum ($p = 0.042$), and ventral diencephalon ($p = 0.048$) were in turn higher in patients with high serum GFAP.

In MS patients, serum GFAP correlated with Extended Disability Status Scale (EDSS) ($\rho = 0.38$, $p = 0.012$). High GFAP levels were associated with high volume-percentage of overall-active lesions ($\rho = 0.30$, $p = 0.046$) in all MS patients. Serum GFAP correlated negatively with the volume-percentage of inactive lesions in GFAP(high) group ($\rho = -0.50$, $p = 0.012$), and there was a trend towards significance in the whole MS population ($\rho = -0.29$, $p = 0.056$).

CONCLUSION In conclusion, microglial and astrocytic activity are increased in MS as indicated by increased [^{11}C]PK11195 binding and serum GFAP. Serum GFAP correlated with EDSS, suggesting it being indicative of disease progression. However, unambiguous conclusions on the association between serum GFAP and [^{11}C]PK11195 binding cannot be drawn as correlations were quite weak, and both positive and negative in nature suggesting the association could be dependent on the brain region. To confirm these results and fully understand the association between microglial and astrocytic activation, more research is required.

Key words: Multiple Sclerosis, Microglial activation, GFAP, TSPO-PET.

Table of contents

List of Abbreviations

[^{11}C]PK11195	^{11}C-labeled 1-(2-chlorophenyl)-N-methyl-N-(1-methylpropyl)-3-isoquinolinecarboxamide
ARR	Annualized Relapse Rate
BBB	Blood-Brain Barrier
CNS	Central Nervous System
CSF	Cerebrospinal Fluid
DMT	Disease Modifying Therapy
DVR	Distribution Volume Ratio
EDSS	Expanded Disability Status Scale
GFAP	Glial Fibrillary Acidic Protein
GFAP-BDP	GFAP Break-Down Product
GM	Grey Matter
HC	Healthy Control
IF	Intermediate Filament
IQR	Interquartile Range
MRI	Magnetic Resonance Imaging
MS	Multiple Sclerosis
MSSS	Multiple Sclerosis Severity Score
PET	Positron Emission Tomography
PPMS	Primary Progressive Multiple Sclerosis
RRMS	Relapsing-Remitting Multiple Sclerosis
SD	Standard Deviation
SPMS	Secondary Progressive Multiple Sclerosis
TSPO	Mitochondrial 18-kDa Translocator Protein
WM	White Matter
ρ	Spearman's rank correlation coefficient

1 Introduction

1.1 Multiple Sclerosis

1.1.1 Introduction to multiple sclerosis

Multiple sclerosis (MS) is a chronic immune-mediated disease that targets the central nervous system (CNS). The disease is associated with neuroinflammation, multifocal demyelination, and progressive neurodegeneration that are presumably caused by a self-antigen targeting autoimmune reaction (Nylander & Hafler, 2012). MS is the most common, non-traumatic neurological disorder in young patients. Globally the disease affects around 2.8 million people and unfortunately the incidence and prevalence of MS are increasing, especially in developed countries (Walton et al., 2020).

MS damages the brain and spinal cord. Areas with inflammatory cells, demyelinated and damaged axons, and reactive astrogliosis are called MS plaques or lesions, and their location affects the type of symptoms the patients will experience (Ghasemi et al., 2017). These lesions can appear within both grey (GM) and white matter (WM), and virtually anywhere in the CNS, and that is what makes the disease so unpredictable in terms of clinical manifestation. There is variation between patients but also over time as the disease progresses. Although the disease development can be unpredictable and vary between patients to a high degree, most typically MS causes episodes of neurological deficits. These flare ups typically develop within a few days and can last up to multiple weeks, often resolving in approximately eight weeks (Rolak, 2003). Although the relapses can be reversible, over time the neurological deterioration becomes progressive (Goldenberg, 2012). The symptoms and progression of the disease are discussed more in section 1.1.2.

MS has many identified risk factors, both genetic and environmental. Known risk factors include infectious agents such as human herpes virus type 6 and Epstein Barr virus (EBV), vitamin D and B12 deficiencies, diet, smoking, and migration to high risk areas like Europe, for instance (Dobson & Giovannoni, 2019; Ghasemi et al., 2017). It has been suggested that these pathogens might have nuclear antigens that are structurally similar to myelin sheet components, and thus immune cell activation due to the pathogens would result in myelin sheath lesion formation (Ghasemi et al., 2017).

The risk of developing MS is higher if a family member has the disease which supports the idea of MS having a genetic component or predisposition. The most well-known susceptibility region is the human leucocyte antigen (HLA) which includes multiple susceptibility genes: HLA-DR2+, HLA-DQ6, DQA 0102, DQB1 0602, HLA-DRB1, DR15, DRB1*1501, and DRB1*1503 (Ghasemi et al., 2017). However, there are multiple other predisposing genetic factors, since genome-wide association studies have discovered over 150 single nucleotide polymorphisms that are associated with MS susceptibility (International Multiple Sclerosis Genetics Consortium (IMSGC) et al., 2013).

Although many risk factors have been identified, the pathogenesis of MS remains somewhat elusive. What initiates the disease and what the underlying pathogenetic mechanism are, have been debated for a long time. There are many hypotheses ranging from viral infections to autoimmune reactions. Despite the differing views, the immune system, both adaptive and innate, undoubtedly has an important role in the pathogenesis.

Based on modern literature, the current general opinion is that the pathogenesis of MS is an autoimmune-mediated reaction that involves helper T-cells (CD4+) and cytotoxic T-cells (CD8+) as well as autoantibodies to some degree (Baecher-Allan et al., 2018). These myelin-specific autoreactive T-cells cross the blood-brain barrier (BBB) and initiate the formation of new inflammatory lesions (Ciccarelli et al., 2014). The lesions occur when T-cells react with CNS self-antigens, causing an autoimmune reaction that attacks neurons, oligodendrocytes and myelin (Miljkovic & Spasojevic, 2013). However, T-cells are not the only immune cells that migrate to the CNS or contribute to MS pathogenesis. For example, B-cells are known to participate in MS pathogenesis and although they have both anti- and pro-inflammatory effects, the latter ones seem to dominate in most patients (Krumbholz et al., 2012). Also, the innate immune system has an important role which is discussed more in section 1.2.3.

Even though MS is nowadays often stated to be autoimmune-mediated, the autoimmune hypothesis has some limitations. The major reason some scientists disagree with MS being classified as an autoimmune disease is because no MS-specific antigens have been found (Chaudhuri & Behan, 2004; Wootla et al., 2012). In the debate over the autoimmune-origin of MS, there are two competing hypotheses, called “outside-in” and “inside-out”, that aim to explain the course of MS pathogenesis. The previously described traditional view, the “outside-in” model, states that autoimmune inflammation causes myelin degradations whereas the competing “inside-out” model supports the idea that the MS pathogenesis is similar to other

neurodegenerative diseases, meaning that the autoimmune and inflammatory response follows the initial injury to oligodendrocytes and myelin. These competing hypotheses have been thoroughly discussed in prior literature (Baecher-Allan et al., 2018; Miljkovic & Spasojevic, 2013; Preziosa et al., 2021; Stys et al., 2012; Titus et al., 2020).

1.1.2 Progression and subtypes of multiple sclerosis

The clinical manifestation and progression of MS can vary a lot from patient to patient as well as over time within one patient. Being a complex and varied disease, MS can be classified into different subtypes that differ in severity and progression rate (Figure 1). The most common type of MS, causing around 85% of all MS cases, is the relapsing-remitting MS (RRMS) which is characterized by worsening of symptoms followed by remission periods during which the symptoms improve or even disappear (Goldenberg, 2012). These relapses are caused by lesions with extensive lymphocytic inflammation (Dobson & Giovannoni, 2019).

Other main subtypes of MS include primary (PPMS) and secondary (SPMS) progressive MS which are characterized by irreversible clinical progression of the disease (Nylander & Hafler, 2012). The distinction is based on whether the progressive subtype is present from the disease onset (PPMS) or if the progression is preceded by RRMS (SPMS). Around 65% of patients with RRMS develop SPMS, whereas PPMS affects 10-15% of MS patients (Ghasemi et al., 2017). Compared to RRMS lesions, the plaques in progressive subtypes often have inactive cores surrounded by a rim of reactive microglia and macrophages (Dobson & Giovannoni, 2019). Sometimes, a fourth subtype is included in the list of main MS subtypes. This rare form of MS, called progressive-relapsing MS (PRMS) and affecting around 5% of patients, is progressive from the beginning, and the deterioration is accelerated with flare-ups with no remission periods (Goldenberg, 2012).

MS is typically diagnosed between the ages of 20 and 40, more commonly in women (sex ratio 2.5:1) (Ghasemi et al., 2017). However, the first detectable signs of MS often come before the actual disease onset and diagnosis. Before any clinical symptoms, changes associated with MS can be detected with magnetic resonance imaging (MRI), making this often incidentally found phase accordingly named radiologically isolated syndrome (RIS) (Baecher-Allan et al., 2018). The first clinical sing of MS typically manifest as an episode of neurological deficits, and is called a clinically isolated syndrome (CIS) (Miljkovic & Spasojevic, 2013). Neither of these syndromes prove that the person already has or will in the future have MS, but they do increase

the risk. It has been estimated that over a 20-year-long period 63% of those diagnosed with CIS develop MS (Fisniku et al., 2008).

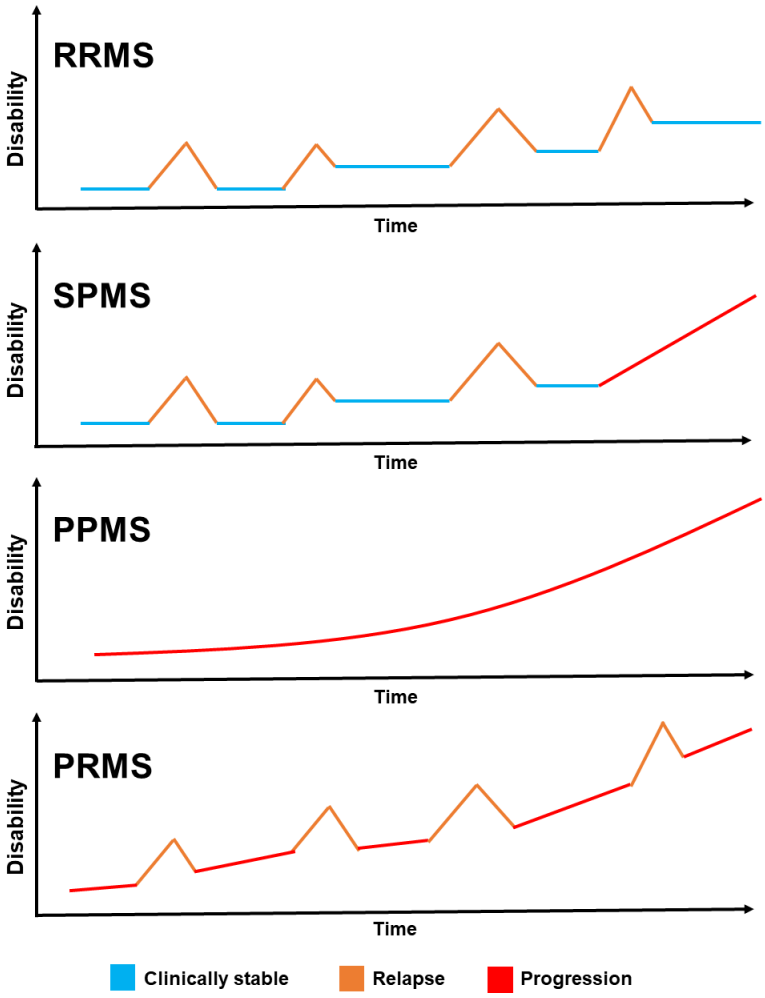

Figure 1. Common multiple sclerosis subtypes and their progression. Multiple sclerosis can be categorised into different subtypes based on the disease progression and severity. Most common subtype is the relapsing-remitting MS (RRMS) in which there are remission periods between flare-ups. However, over time the neurological deterioration worsens. Patients with RRMS can develop secondary-progressive MS (SPMS) in which the clinical progression becomes irreversible. For some patients, the deterioration is irreversible from the beginning which means they have the primary-progressive subtype (PPMS). There is also a progressive-relapsing subtype (PRMS) which is characterized progressive deterioration which is accelerated with relapses. Created by Inke Tirkkonen.

Much like the disease type can vary and progress, the symptoms can also vary between patients or change during the disease course. Typical primary symptoms include issues with vision and walking as well as sensory, gastro-intestinal, and cognitive disturbances, but as the disease progresses, the symptoms become more severe including immobility as well as serious social and psychological complications (Ghasemi et al., 2017).

The multiple subtypes and diverse symptoms make diagnosing MS difficult. The diagnosis is based on the McDonald Criteria (Thompson et al., 2018). According to the criteria, the diagnosis is based on dissemination in time and space, meaning that there must be at least two relapses that have affected at least two regions of the CNS. The diagnosis heavily relies on clinical evaluation as well as MRI which is recommended to all with suspected MS as it helps with not only demonstrating time and space dissemination but also ruling out MS-mimicking conditions (Dobson & Giovannoni, 2019). Similarly, a lumbar puncture is often recommended as cerebrospinal fluid (CSF) analysis can help with diagnosing or ruling out MS and differential diagnoses.

To help with monitoring the patient's level of disability as well as progression and activity of the disease, there are multiple commonly used scales. Extended Disability Status Score (EDSS) can be used to quantify the disability caused by MS (Kurtzke, 1983). The scale ranges from zero to ten with 0.5 intervals; the greater the number the worse the disability. EDSS is determined by neurological exam that tests functional systems. Similar to EDSS, there is a Multiple Sclerosis Severity Score (MSSS) which takes into account the EDSS and disease duration (Roxburgh et al., 2005). MSSS is used to evaluate the progression rate of the disease. There is also an annualized relapse rate (ARR) which measures how many flare-ups the patient has per year. It provides information on disease activity and sustained disability.

1.1.3 Treatment of multiple sclerosis

There is no cure for MS. However, current treatment options may ease the symptoms or manage the disease course. The two available treatment types are disease modifying therapies (DMT), which alter the activity of the immune system, and symptomatic treatments, which aim to ease the complications caused by CNS damage. Commonly used DMTs include interferons such as IFNβ-1a and IFNβ-1b, glatiramer acetate, fumarates, teriflunomide, sphingosine-1-phosphate inhibitors such as fingolimod and siponimod, and monoclonal antibodies such as ofatumumab, natalizumab, and ocrelizumab (Pérez et al., 2023). DMTs have anti-inflammatory effects that lower the annualized relapse rate (ARR), reduce lesion accumulation, and postpone disability (Hauser & Cree, 2020). For example, natalizumab, a second-line treatment that antagonises integrin α4, has been demonstrated to lower ARR by 68% as well as reduce lesion accumulation by 83% and disability progression by 42% in relapsing MS patients during a three-year clinical trial (Polman et al., 2006). On the other hand, the symptoms caused by acute relapses are typically treated with corticosteroids.

Although progress has been made and there are multiple treatment options on the market nowadays, the treatment is still inadequate, especially in the progressive MS subtypes. This is because compared to RRMS pathology, the pathology of progressive MS is not as well understood, in addition to which there are issues with finding reliable and sensitive biomarkers and outcome measures (Ontaneda et al., 2015). Thus, majority of the DMTs on the market are indicated for the treatment of RRMS as the immune response is the most prevalent in the early phases of the disease and starting treatment as early as possible offers the best results.

Fortunately, there seems to be an increasing trend in the research regarding MS treatments and this trend is expected to continue (Aykaç & Eliaçık, 2022). Inhibitors of Bruton's tyrosine kinase, expressed in B-cell and myeloid cells such as microglia, are under investigation for their therapeutic effects (Correale, 2021). Explored neuroprotective treatment options include compounds such as alpha-lipoic acid (ALA), metformin, phenytoin, simvastatin, ibudilast, and amiloride, whereas compound with potential remyelinating properties include biotin, opicinumab, and clemastine fumarate (Pérez et al., 2023). Unfortunately, many of these compounds have failed in clinical trials.

The progressive neurodegeneration is also an issue that is not currently being met. Thus, strategies like stem cell -based therapies have been explored to answer to this issue. For example, one promising candidate are mesenchymal stem cells (MSCs) which secrete cytokines and growth factors that accelerate the tissue repair and regeneration though anti-apoptotic and anti-inflammatory effects while also enhancing angiogenesis, and recruitment, proliferation, and differentiation of stem cells located within the tissue (Joyce et al., 2010). Although promising in theory, there are multiple obstacles, including proving clinical efficacy, ensuring quality, and managing costs, that have to be overcome (Ahmed, 2022).

1.2 Glial cells of the central nervous system

Besides neurons, the nervous system consists of glial cells, also known as neuroglia. For a long time, this group of cells was disregarded as nothing more than glue that holds together the nervous system, hence their name that comes from the Greek word for glue. However, growing interest in this diverse and abundant group of cells has revealed that glial cells contribute to the function of the nervous system in many ways, not just by giving it structure.

Glial cells of mature CNS include oligodendrocytes, microglia, and astrocytes, all of which have essential role in maintaining a healthy and functioning CNS. Oligodendrocytes are

responsible for coating the neuronal axons in myelin, an insulating sheath that enables neuronal impulses to travel faster, which is destroyed in MS. Although oligodendrocytes are greatly affected by MS, the other two types of CNS glial cells, microglia, and astrocytes, are the focus of this thesis.

1.2.1 Introduction to microglia

Microglia, a subclass of parenchymal phagocytes, are part of the innate immune system and the CNS resident macrophages. They are derived from the yolk-sac, are long-lived, and have self-renewing properties (Dong & Wee Yong, 2019). They have small cell bodies and ramified morphology. Microglia are responsible for essential homeostatic functions in the parenchyma; they participate in neural development, synaptic pruning and remodeling, learning, phagocytosis, and neonatal myelination (Dong & Wee Yong, 2019). Homeostatic microglia also produce important growth factors and anti-inflammatory cytokines (Airas & Yong, 2022).

As the resident immune cells, microglia participate in surveillance of the CNS and react accordingly to a disruption in the homeostasis. In case of a disturbance microglia can become mobilized as part of an event called microglial activation, or microgliosis, that causes the cells to change their phenotype. The activation and migration of microglia can be triggered by viruses and other pathogens, tissue damage, or cell debris like degraded myelin. Typical changes include morphological changes as the cells become amoeboid, changes in protein markers to more macrophage-like, increase in cytokine production, and downregulation of homeostatic genes (Kamma et al., 2021).

Activated microglia produce a variety of pro- and anti-inflammatory cytokines and chemokines that attract more immune cells to the site. Together with recruited astrocytes and peripheral immune cells, microglia reinforce the neuroinflammation. Typically in the end, the anti-inflammatory cytokines and neurotropic agents released by microglia suppress the inflammation and aid in tissue repair but a failure to do so can lead to chronic inflammation and neurotoxicity (Notter et al., 2018). However, activated microglia with pro-inflammatory markers have also been found in normal WM of healthy controls (HCs), correlating positively with age, thus dismissing the idea that microglia of healthy CNS are in a “homeostatic” or “steady” state in humans like they are in rodents (Zrzavy et al., 2017).

Activated microglia can be divided into two groups based on their function and expression; M1 microglia are pro-inflammatory and neurotoxic whereas M2 cells have anti-inflammatory and

neuroprotective characteristics. The classically activated M1 cells produce pro-inflammatory agents including tumor necrosis factor α (TNF-α), cytokines and chemokines such as interleukins (IL) 1β, 6 and 12, reactive oxygen species (ROS), nitric oxide (NO), and metallopeptidase 12 (MMP12) (Colonna & Butovsky, 2017). On the other hand, the alternative activation leads to formation of M2 cells which release anti-inflammatory cytokines (IL-4, IL-10, IL-13), growth factors such as transforming growth factor β (TGF-β) and insulin-like growth factor I (IGF-I), and neurotropic factors such as nerve growth factor (NGF).

Although this classic division to M1 and M2 cells is still widely used, it is most likely too generalized and simple to fully explain the microglia activity *in vivo*. This division of different polarization stages is based on cell markers found in *in vitro* research whereas in actuality there could be numerous microglia phenotypes that do not necessarily place on the M1-M2 axis (Ransohoff, 2016).

1.2.2 Introduction to astrocytes

Astrocytes are thought to be the most abundant cell type of the CNS, and they, or similar cells, can be found everywhere in the CNS (Sofroniew & Vinters, 2010). Astrocytes have gotten their name due to their star-like structure. Although they can be divided into multiple subtypes depending on their structure and function, the basic structure consists of a cell body and processes that project out of the soma and allow the cell to form connections to blood vessels and neurons, for instance (Sofroniew & Vinters, 2010).

Astrocytes are an essential part of functioning CNS and BBB. During development, they guide the migration of neurons (Powell & Geller, 1999), contribute to myelin formation (Lutz et al., 2009), and participate in the formation of synapses (Christopherson et al., 2005). In the developed CNS, astrocytes regulate the release of neurotransmitters, modify synapses, produce and release growth factors and neuroactive steroids as well as regulate the ion, pH, transmitter, and liquid balance of the extracellular space (Sofroniew & Vinters, 2010).

Much like microglia can activate when homeostasis is disturbed, this kind of unbalance can also affect the activity of astrocytes, causing a reaction called reactive astrogliosis. Also known as astrocytosis, reactive astrogliosis is a complex and diverse phenomenon that has no precise definition but refers to the morphological, transcriptional, physiological, and metabolic changes astrocytes undergo as an response to CNS pathology (Escartin et al., 2021). It is not an “all or nothing” reaction but rather a continuum of different gene expression patterns and molecular

changes that can differ case to case (Sofroniew, 2009). Typical characteristics of reactive astrogliosis are changes in gene expression and hypertrophy which can be accompanied by astrocyte proliferation and disruption of cell organization when reactive astrogliosis advances (Sofroniew, 2015). Although, reactive astrogliosis can be detrimental for the CNS, as it can form scars and cause degeneration in the CNS, reactive astrocytes are also beneficial as they are essential in wound healing, controlling inflammation, and repairing the BBB as well as protecting neurons and oligodendrocytes (Faulkner et al., 2004).

Like microglia, reactive astrocytes are often divided into two groups based on their phenotype. However, similarly to microglia, this division is rather outdated. The original idea was that there are neurotoxic A1 astrocytes induced by microglia in neuroinflammation and neurodegenerative diseases, and neuroprotective A2 astrocytes induced by ischemia (Liddelow et al., 2017). The same study found that A1 astrocytes, which are abundant in neurogenerative diseases, release a neurotoxin that causes neuronal and oligodendrocyte death, and they have lost the ability to promote formation and function of synapses as well as neuronal survival, and to phagocytose myelin debris and synapses. However, these findings have been misinterpreted to prove universal binary polarization of astrocytes (Escartin et al., 2021). The idea of just two activity phenotypes should be disregarded as single-cell RNA sequencing has shown the reactive astrocytes of a MS mouse model to be molecularly and functionally heterogenous (Wheeler et al., 2020).

1.2.3 Microglia and astrocytes in multiple sclerosis

In MS, the homeostasis of the CNS is disturbed, and microglia and astrocytes become reactive in such events. Trying to maintain a healthy CNS, microglia and astrocytes change their phenotypes. Although these changes are intended to protect the CNS, they can also damage the nervous system if the activation becomes chronic. Thus, microglia and astrocytes can contribute to the MS pathophysiology (Figure 2). Studies regarding MS pathophysiology and the role of glial cells utilize many different *in vitro*, *in vivo*, and *ex vivo* methods. There is also a widely used animal model, the experimental autoimmune encephalomyelitis (EAE), which is considered representative of MS, especially from the pathophysiology point of view.

A study conducted with human brain samples from biopsies and autopsies reported that microglial activation is present early on in the MS lesion development, and microglia nodules, characterized by changed morphology, lack of leukocyte infiltrates, and demyelination, can be found in normal appearing white matter (NAWM) predating lesions (Singh et al., 2013).

Although microglia contribute to the lesion formation, a study conducted with male mice on cuprizone diet found that as an effort to fight the MS pathogenesis, microglia phagocytose myelin debris and aid remyelination, especially in the beginning of the disease (Voß et al., 2012). Phagocytosis, antigen presentation, and oxidative injury are featured in early lesions which indicates the presence of pro-inflammatory M1 cells, however both M1 and M2 markers have been found in active lesions of human autopsy brain tissue (Zrzavy et al., 2017).

Activated microglia can secrete a variety of neurotoxic agents (Venneti et al., 2006). Disease models have demonstrated that in active lesions, rich in microglia, the cells produce excessive amounts of pro-inflammatory agents including NO, IL-β, and TNF-α (Kamma et al., 2021). With time, lesion cores, and eventually whole lesions, become inactive and anti-inflammatory markers can be detected (Zrzavy et al., 2017). These M2 polarized microglia can also be found in the core of classical active lesions as remyelination is attempted.

Like microgliosis, reactive astrogliosis is present in MS. Although neuroinflammation is typically associated with microglia, astrocytes are also its regulators and work together with microglia. Additionally, they participate in the development of MS lesions. The unfavourable effects of astrocytic activity on CNS diseases, including MS, are thought to happen either by loss of essential functions or gain of detrimental ones (Sofroniew, 2009).

Whereas previously astrocytes were considered to react in the post-inflammatory stage by forming glial scars, autopsy-retrieved human CNS tissue samples have demonstrated that astrocytes participate in the early stages of active inflammation with hypertrophy that can result in disruption of astrocyte-oligodendrocyte network (Ponath et al., 2018). A study conducted with human tissue samples reported that in acutely active MS lesions, astrocyte damage and hypertrophy most likely follows the immune cell infiltration playing into the theory that astrocytes are a target of the inflammatory response (Brosnan & Raine, 2013). Additionally, in the parenchyma, astrocyte hypertrophy happens early on in the lesion margins resulting in a layer of swollen astrocytes dividing the actively demyelinating plaques and normal WM. These hypertrophic astrocytes can have multiple fragmented nuclei, that frequently resemble ones in gliomas, and they can engulf other cells, such as oligodendrocytes, in an event called “emperipolesis”, although its role in MS is unclear (Sofroniew & Vinters, 2010).

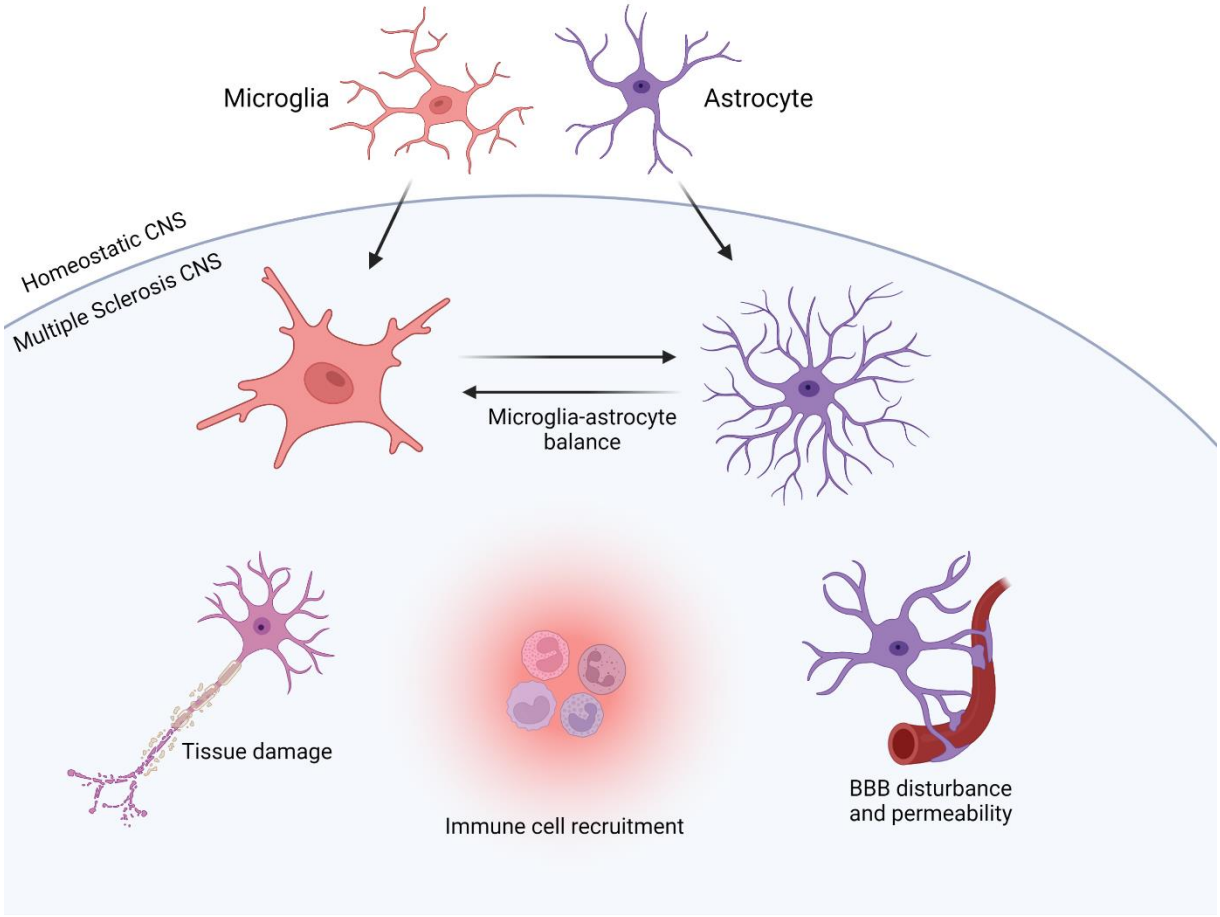

Figure 2. Microglia and astrocytes drive the multiple sclerosis pathogenesis. Microglia and astrocytes are essential part of a well-functioning CNS as they maintain homeostasis and participate in important developmental events. However, if this homeostasis is disturbed, microglia and astrocytes become activated and change their morphology and physiology. These changes can be anti- or pro-inflammatory but unfortunately the latter ones are typically more prevalent in CNS diseases. It has been suggested that there is a microglia-astrocyte balance in immune reaction regulation, and the cells can interact with each other, affecting each other's activity. However, in pathological conditions this balance can be shifted resulting in chronic inflammation. As part of the innate immune system, microglia are typically associated with neuroinflammation and the neurotoxic agents they release are known to induce immune cell recruitment. However, astrocytes contribute to neuroinflammation too by producing and responding to inflammatory agents which cause perivascular astrocytes to increase BBB permeability which in turn further increases immune cell entry to the CNS. Tissue damage, including neuronal degeneration, demyelination, and lesion formation, are also regulated by glial cells. Microglia and astrocytes produce neurotoxic agents that damage neurons and myelin sheets. Active MS lesions are rich in pro-inflammatory microglia which regulate the inflammation. Astrocyte damage and hypertrophy are also detected in active lesions, and swollen astrocytes can be found at the lesion margins. Additionally, the glial scar formed by astrocytes prevents remyelination. CNS; central nervous system. Created by Inke Tirkkonen with BioRender.com.

The effects of astrocytes are not limited to active lesions. In MS tissue samples, reactive astrogliosis is often found in NAWM (Zeis et al., 2008), and although it is not as prominent in chronic and inactive lesions, the astrocytes can still exert pro-inflammatory effects, in addition to which the lesions are characterized by glial scar (Ludwin et al., 2016). The glial scar has both positive and negative effects. On the other hand, it means that there is serious CNS injury,

suggesting remyelination and axon regeneration are not feasible anymore. However, demonstrated with transgenic mice models, the glial scar can also protect the still intact CNS by isolating the damaged area, and thus restricting the inflammation and damage from spreading (Sofroniew & Vinters, 2010). It can also offer structural support secondary to tissue loss (Ludwin et al., 2016).

One hallmark of MS is the disruption of the BBB. Although previously disregarded as a passive barrier, perivascular astrocytes may have an active role in BBB permeability and inflammation due to their ability to produce and respond to inflammatory agents (Brosnan & Raine, 2013). Additionally, these reactive astrocytes can cause damage to the glia limitans in the basal lamina around blood vessels which increases immune cell entry to the CNS, while simultaneously expressing chemokines and adhesion molecules that add to the immune cell recruitment, which further advances the inflammation response.

Despite the detrimental effects reactive astrogliosis can have in MS, the reactive astrocytes actually have many protective and beneficial functions that unfortunately are lost or disturbed in many pathological conditions (Sofroniew & Vinters, 2010). In addition to forming a glial scar that limits the inflammation and neuronal damage from spreading, one key neuroprotective function of astrocytes is remyelination. Studies conducted using both animal models and human MS lesion samples have demonstrated astrocytes to regulate the migration, proliferation, and maturation of oligodendrocyte precursor cells (OPCs), as well as provide an environment where remyelination is possible (Williams et al., 2007). Additionally, reactive astrocytes have been reported to contribute to BBB repair (Sofroniew & Vinters, 2010).

Despite microglia and astrocytes having many independent functions that affect the MS pathophysiology, it is important to remember that they also interact with each other. This cooperation plays a major role in neuroinflammation. There is a suggested microglia-astrocyte balance in immune reaction regulation (Xiao & Link, 1999). This balance is suggested to be regulated through T helper 1 (Th1) and 2 (Th2) responses with mice studies indicating that microglia induce Th1-mediated inflammation whereas astrocytes try to suppress that inflammation though Th2-cells (Aloisi et al., 1998). Furthermore, while IL-6 and TNF released by microglia can cause reactive astrogliosis (Michell-Robinson et al., 2015), *in vitro* research has suggested that astrocytes can prevent the inflammation by inducing antioxidant genes in microglia (Min et al., 2006). However, pathological conditions may shift this balance and alter the outcome (Xiao & Link, 1999).

In MS, the microglia-astrocyte balance has shifted, and inflammation has become chronic. Instead of inhibiting the inflammation, the glial cells seem to intensify the inflammation by activating each other. Research done with mice that lack microglia, revealed that for astrocytes to adapt their pro-inflammatory A1 phenotype, they require the presence of classically activated microglia (Liddelow et al., 2017). Especially important factors in this microglia-astrocyte crosstalk are the complement components 1q (C1q) and 3 (C3), as a study conducted using MS tissue samples, gene expression analysis, and animal models reported that *C1Q* and C3 activator encoding complement factor D (*CFD*), as well as C3 receptors, are expressed in activated microglia whereas activated astrocytes overexpress C1q activators and receptors as well as *C3* (Absinta et al., 2021).

Although MS pathophysiology is typically associated with the adaptive immune system, as early RRMS is mediated by it, there are arguments that CNS inflammation in SPMS could be caused by the CNS resident innate immune cells when activated microglia interact with astrocytes (Nylander & Hafler, 2012). This proposes a question whether the macrophage-like cells detected in MS lesion are recruited macrophages or rather activated microglia from the resident pool. One study showed that 45% of all macrophage-like cells in active MS lesions are part of resident microglia (Zrzavy et al., 2017) supporting the idea of the innate immune system contributing to MS pathogenesis.

1.3 Glial fibrillary acidic protein (GFAP)

1.3.1 GFAP in healthy brain and multiple sclerosis

A cytoskeleton is required for a cell to keep its structure and stability as well as execute important functions such as migration and cell signaling. It is comprised of microfilaments, microtubules, and intermediate filaments (IFs). Glial fibrillary acidic protein (GFAP) is the most common IF in the mature brain, and is typically, but not exclusively, expressed by astrocytes. Other IFs expressed in astrocytes are vimentin, nestin, and synemin. The discovery of GFAP was first announced in 1969 by Dr Eng, who had isolated it from MS plaques (Messing & Brenner, 2020).

GFAP is a type III IF, made-up of 432 amino acids, and encoded by a single gene, located in the chromosome 17q21.1-q25, that can be spliced in multiple ways causing GFAP to have ten isoforms. Besides providing structure and keeping cell organelles in their place, GFAP has been demonstrated to participate in multiple cellular functions including, but not limited to, cell

migration and proliferation, autophagy and vesicle trafficking as well as astrocyte-neuron interactions and myelination (Middeldorp & Hol, 2011).

As astrocytes become reactive, synthesis of GFAP rapidly increases (Eng et al., 2000). This suggests that changed GFAP expression is an indicator of CNS diseases and trauma. As the major IF of astrocytes, GFAP serves as the morphological basis of reactive astrogliosis and the main protein of chronic MS lesions (Eng et al., 1971). A study done with autopsied brains of MS patients revealed that in active lesions, the GFAP-positive reactive astrocytes can be found throughout the demyelinating region, whereas in chronic active lesions these astrocytes are located at the lesion rim (De Groot et al., 2001). However, a CNS disease or trauma is not the only explanation for increased GFAP expression as post-mortem human brain tissue samples have demonstrated GFAP mRNA to increase due to aging regardless of neuropathology (Nichols et al., 1993).

1.3.2 Soluble GFAP as a biomarker

GFAP has been widely used in research as a biomarker of reactive astrogliosis. Although astrocytes express GFAP in their normal state, it can be used to detect specifically reactive astrogliosis, as GFAP expression is upregulated in reactive astrocytes (Zamanian et al., 2012). This overexpression is relative to the activity of astrocytes and severity of reactive astrogliosis (Sofroniew, 2015). It has even been proposed, that GFAP is an early and sensitive marker of neurotoxicity (Eng et al., 2000).

When CNS pathologies prevail, GFAP can become soluble and be released to the CSF, where its increased presence has been thought to be indicative of the neurodegenerative process in MS, making it an attractive biomarker (Axelsson et al., 2011). GFAP and its break-down products, GFAP-BDPs, can even be found in the blood stream (Agostini et al., 2021). However, because of the low concentrations, serum GFAP has been difficult to detect. Fortunately, with highly sensitive assays, like single-molecule array (SIMOA), we are able to detect GFAP from the blood of healthy individuals as well as people with neurological diseases (Abdelhak et al., 2018).

It is not well characterized, at least in terms of MS, how GFAP becomes soluble, as research regarding soluble GFAP has mainly focused on traumatic brain injury (TBI). Glial injury is suggested to accompany neuronal injury, which has been shown to cause the breakdown of intact 50 kDa GFAP into smaller 38-44 kDa GFAP-BDPs by calpain (Yang & Wang, 2015).

Same study suggests that GFAP-BDPs can transfer to extracellular fluid and CSF, possibly passing on to blood stream amid BBB disturbance.

Although the exact mechanism of GFAP and GFAP-BDPs leaking into the circulatory system is not fully understood, there is evidence that it could be the sum of bulk flow via arachnoid villi and along glymphatic system and cervical lymph nodes, as well as the constant bidirectional fluid flow at the CNS barriers (Abdelhak et al., 2022). It has also been suggested that GFAP is at least partly released directly to the bloodstream due to the increased GFAP expression in the astrocyte end feet that are in contact with blood vessels (Sofroniew & Vinters, 2010) and because of the perivascular location of most MS lesions (Tallantyre et al., 2008). CSF and serum GFAP levels have been shown to correlate with each other (Abdelhak et al., 2018; Ayrignac et al., 2020). However, serum GFAP is suggested to be a better biomarker of disease activity in MS due to the reasons mentioned above as well as serum GFAP giving a more prominent correlation to EDSS and MSSS (Abdelhak et al., 2018).

Evidently, MS patients have higher serum GFAP levels than HCs (Högel et al., 2020; Meier et al., 2023) and patients with non-inflammatory neurological diseases (Abdelhak et al., 2018). These studies also reported on serum GFAP levels positively correlating with EDSS, and MS patients with progressive disease type having higher serum GFAP levels compared to RRMS patients. The differences in GFAP levels between MS patients and HCs, as well as its correlation to disease progression, highlight the key role astrocytes have in neuroinflammation.

A recent study suggests that a high serum GFAP could indicate relapse-independent progression as acute disease activity does not seem to increase the serum levels (Meier et al., 2023). However, the effects of relapses on serum GFAP are not entirely known and require more research as serum GFAP levels have been also reported to slowly increase during a relapse (Burman et al., 2014).

1.4 PET imaging and mitochondrial 18-kDa translocator protein (TSPO)

1.4.1 PET imaging and its role in MS research

Positron emission tomography (PET) is an *in vivo* method that utilizes radioactive substances, also known as tracers, to measure metabolic changes in the body and produce 3-dimentional images. With PET, different physiological and pathological processes can be imaged in a quantitative and targeted manner. The main principle of PET is that ligands, marked with

radioisotopes with short half-lives, bind to specific target molecules and accumulate into targeted tissues and structures. These isotopes then decay by positron emission, and the proton they emit travels through tissue until it meets an electron, causing an annihilation and formation of two photons (Poutiainen et al., 2016). The two protons travel in opposite direction and as they meet the imaging device, a line of response (LOR) can be determined for each. The origin point of a LOR is the place of annihilation.

A variety of parameters can be used to measure and quantify the binding of radiotracers. One of the analysis methods is distribution volume ration (DVR), which is a linear function of receptor availability (Logan et al., 1996). Other methods include for example standardized uptake value (SUV), fractional uptake rate (FUR), and non-displaceable binding potential (BP_{ND}).

The development of non-invasive *in vivo* methods has changed how we do research as they allow us to study living organisms and offer real-time information on cellular functions. Although MRI is still the typical method for diagnosing MS and monitoring the disease activity, it has some limitations as it may not detect complex morphological changes and offers poor correlation between imaging result and clinical findings, at least on individual level (Enzinger et al., 2015). Due to the shortcomings of conventional MRI, research of glial activation often relies on PET imaging which allows us to see functional changes even before morphological changes become apparent (Poutiainen et al., 2016). In MS, PET techniques allow imaging of lesion heterogeneity as well as inflammatory and functional changes in the brain of living patients (Högel et al., 2018; Nylund et al., 2021) (Figure 3).

1.4.2 Overview of TSPO

Mitochondrial 18-kDa translocator protein (TSPO) is embedded in the outer mitochondria membrane, consists of 169 amino acids, and has five domains with highly conserved structures. It was formerly known as peripheral benzodiazepine receptor (PBR) as in 1977 it was discovered to be the binding site of benzodiazepine (Braestrup et al., 1977). TSPO has multiple proposed, and debated, functions including cholesterol transport as part of steroidogenesis, monitoring apoptosis and cell survival, participating in inflammation with potent anti-inflammatory actions as well as regulating energy production and oxidative stress (Notter et al., 2018).

In healthy CNS, only minimal TSPO is detected. However, in the presence of CNS damage, its expression is thought to increase. Preclinical studies have reported increase in TSPO expression to be linked to many CNS pathologies and it contributing to both neurodegeneration and neuroinflammation (Rupprecht et al., 2010). However, this view is considered rather old, and as it is based on rodent studies, it is not exactly clear how the increase happens in humans. *In vitro* studies with human microglia suggest that the increase in TSPO is not caused by increased gene expression but rather increased cell density of TSPO-presenting cells (Nutma et al., 2021; Owen et al., 2017).

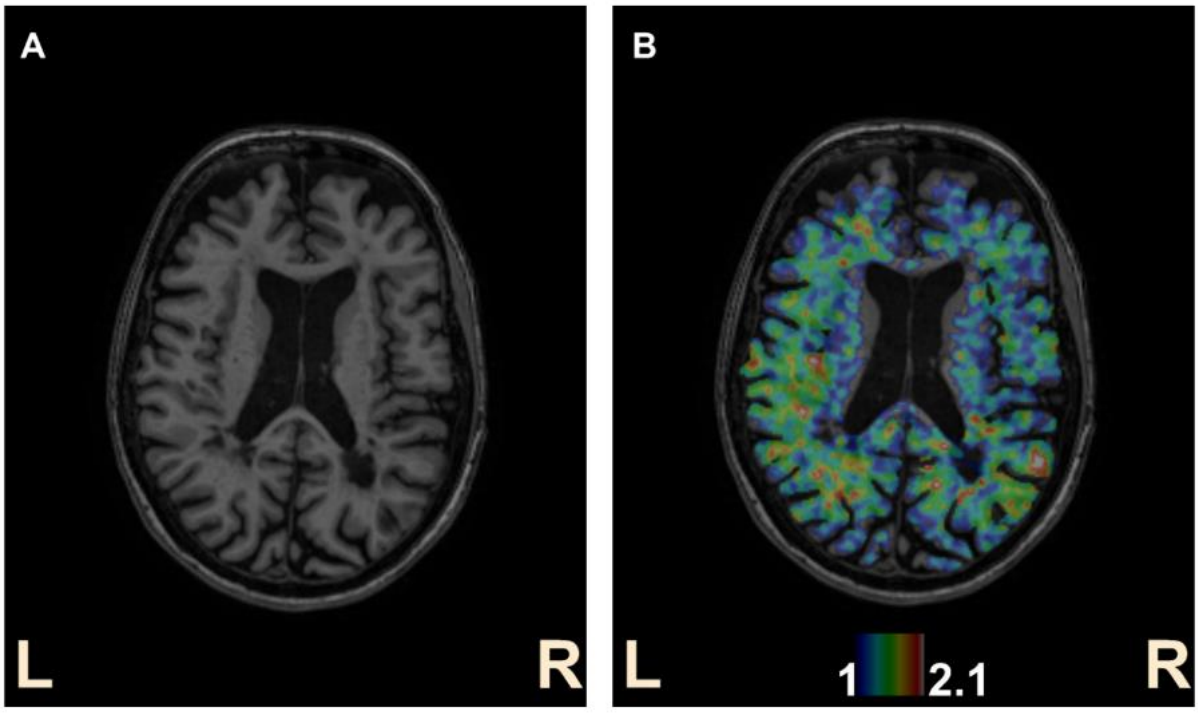

Figure 3. Magnetic resonance and positron emission tomography images of the brain. A) T1 weighted magnetic resonance image of the brain of a MS patient. Lesions can be seen as dark spots. B) TSPO-PET image of the whole brain laid over the magnetic resonance image. [^{11}C]PK11195 was used as the radioligand. Specific [^{11}C]PK11195 is represented on a rainbow scale with blue colour indicating lower DVR and red higher DVR indicating lower and higher microglial activation, respectively. The images are from the brain of a 48-year-old MS patient with a EDSS score of 4. DVR, distribution volume ratio; PET, positron emission tomography; TSPO, mitochondrial 18-kDa translocator protein. Created by Inke Tirkkonen.

TSPO is a popular marker for neuroinflammation and microgliosis (Y. Lee et al., 2020). Older animal studies reported TSPO to be exclusively expressed in microglia which led to the undermining of astrocyte contribution in neuroinflammation (Guilarte, 2019). Although TSPO is commonly used to study microglial activation, it is not an absolute optimum, as apart from microglia, TSPO has been shown to be expressed in astrocytes, endothelial cells of blood vessels, macrophages, and neurons of the olfactory bulb (Jacobs et al., 2012; Kuhlmann &

Guilarte, 2000; Rizzo et al., 2014; Rupprecht et al., 2010; Varlow et al., 2022). In addition, brain tissue from autopsied MS patients has revealed that TSPO-expression is found not only from the pro-inflammatory microglia of active and chronic active lesions, but also from microglia with other phenotypes as well as activated astrocytes in the inactive lesion cores (Nutma et al., 2019). However, in NAWM and active lesions as well as at the rims of chronic active lesions, approximately 95 % of TSPO-expressing cells are microglia and macrophages (Nutma et al., 2021). Also, although TSPO is considered to present neuroinflammation, neuronal activity can affect TSPO levels in the brain which means non-inflammatory pathological processes should also be considered when studying TSPO (Notter et al., 2021).

Despite the diverse variety of cell expressing TSPO, it can still be considered a sensitive and reliable marker of neuroinflammation, that reflects the microglial activation and to a degree, reactive astrogliosis (Cosenza-Nashat et al., 2009; Maeda et al., 2007). Additionally, TSPO's role in neurodegeneration and neuroinflammation has made it an attractive drug target candidate, too (Rupprecht et al., 2010). In fact, animal studies have supported the therapeutic effects of TSPO ligands which has resulted in multiple patent applications for several TSPO ligands that could be used for therapeutic or diagnostic purposes (Kim & Pae, 2016).

1.4.3 TSPO-PET imaging with [^{11}C]PK11195 radioligand

PET imaging utilizes a variety of radiolabeled ligands, one of which is [^{11}C]PK11195. It is an ^{11}C-labeled isoquinoline carboxamide, also known as 1-(2-chlorophenyl)-N-methyl-N-(1-methylpropyl)-3-isoquinolinecarboxamide, that binds to TSPO acting as its antagonist. The ligand was first used to image glial tumors (Bergström et al., 1986; Pappata et al., 1991), but in the 1990s it was discovered that an increase in its R-enantiomer binding is associated with microglial activation (Stephenson et al., 1995). Therefore, research regarding neuroinflammation and CNS pathologies utilizes (R)-PK11195 that can be radiolabeled with different radioactive atoms, such as ^{11}C or ^{3}H.

[^{11}C]PK11195 has been widely used in MS studies. Specific [^{11}C]PK11195 binding, which indicates microglial activation, is greater in MS patients compared to healthy individuals (Banati et al., 2000). A study done with SPMS patients revealed the binding is greatest in the NAWM and thalamus, and could be used to detect widespread inflammation that occurs in the NAWM as well as the active rim of chronic lesions (Rissanen et al., 2014). The [^{11}C]PK11195 ligand allows not only stand-alone measurement, but also a reliable longitudinal research on disease development and effects of different medication on patient level (Kaunzner et al., 2017;

Sucksdorff et al., 2019). A recent study suggests that a high [^{11}C]PK11195 binding in the NAWM indicates later disease progression in MS patients (Sucksdorff et al., 2020). Additionally, higher [^{11}C]PK11195 binding in the NAWM correlates with higher EDSS (Bezukladova et al., 2020; Giannetti et al., 2015; Rissanen et al., 2018; Saraste et al., 2022).

With TSPO-PET, chronic lesions can also be categorized into rim-active, overall-active, and inactive subgroups *in vivo* based on their phenotype, determined by specific [^{11}C]PK11195 binding inside the lesion and at the lesion rim (Nylund et al., 2021). Based on this method, lesions with low DVR in the core and rim are classified as inactive, lesions with low core DVR but comparably high DVR at the rim are classified as rim-active, and lesions with high DVR in both core and lesion rim are classified as overall-active. This type of lesions phenotyping is important as it allows the individual level distinction of rim-active lesions, also known as chronic active or smouldering lesions, which are known to slowly expand and promote relapse-independent disease progression (Beynon et al., 2022).

Although [^{11}C]PK11195 is still the most widely used radioligand in neuroinflammation research (Högel et al., 2018), it has some limitations including poor signal-to-noise ratio, unwanted plasma protein binding, and issues with entering the brain which has led to the development of newer more potent and selective radioligands (Venneti et al., 2006). However, these second and third generation TSPO-ligands have their own disadvantages, such as variability in binding affinity due to genetic polymorphism (Owen et al., 2012). Additionally, overexpression of TSPO is typical for not only microglia, but reactive astrocytes too, which means that some of the increased TSPO levels in neuroinflammation may be due to astrocyte activation as both microglia and astrocytes are activated in neuroinflammation (Lavisse et al., 2012). However, with good image acquisition and high-resolution PET cameras as well as validated post-processing and image analysis, [^{11}C]PK11195 can be considered to be a reliable marker of MS related pathological processes (Sucksdorff et al., 2020).

1.5 Aims and hypotheses

The aim of this master's thesis is to evaluate imaging and soluble biomarkers for microglial and astrocytic activation in MS patients, and shed light on the possible connections between the two. Microglial activation is evaluated as specific [^{11}C]PK11195 binding measured with TSPO-PET imaging, whereas astrocytic activity is determined by serum GFAP. Glial activity is evaluated and compared in HCs and MS patients as well as considering gender, treatment, and serum GFAP levels. More precise aims are the following:

1. Determine the GFAP levels from the blood samples of MS patients and HCs
2. Determine the number and volume of the lesions (MRI)
3. Determine the amount of specific [^{11}C]PK11195 binding (DVR) and the number of active voxels in the different brain regions in MS patients and healthy participants
4. Determine the number and volume of rim-active, overall-active, and inactive lesions in MS patients
5. Determine how serum GFAP correlates with specific [^{11}C]PK11195 binding (DVR) and the number of active voxels in different brain regions including whole brain, cortical GM, NAWM, whole lesions, lesion rims, and different lesion types and volumes in MS patients and HCs as well as GFAP(low) and GFAP(high) patient subgroups
6. Compare specific [^{11}C]PK11195 binding (DVR) as well as GFAP levels and its association to different variables in different cohort subgroups

Hypothesis is that the increased [^{11}C]PK11195 binding, which indicates increased microglial activity, correlates with increased serum GFAP level, which indicates increased astrocytic activity. This hypothesis is supported by the fact that both microglia and astrocytes are known to activate during neuroinflammation (Lavisse et al., 2012). Thus, it is also expected, that microglial activity and serum GFAP levels are greater in MS patients when compared to HCs. Differences could also be detected in microglial activity and GFAP levels when compared to different demographic and clinical variables. For example, rodent studies have shown that microglial transcription and function are affected by sex (Kodama & Gan, 2019), and aging has been suggested to increase microglia-induced inflammation (Wirths et al., 2017).

TSPO and GFAP are important research targets due to their connections to neuroinflammation. This makes them valuable biomarkers and possibly even drug target candidates (Kim & Pae, 2016; Rupprecht et al., 2010). Serum GFAP biomarker could serve as a cost-efficient and only mildly invasive marker of astrocyte activation. Serum GFAP levels are likely associated with the progression of the disease (Abdelhak et al., 2018; Högel et al., 2020; Meier et al., 2023), meaning it could be utilized as an indicator when deciding optimal treatments and estimating disease progression.

Currently, there is no cure for MS. Current therapies aim to modify the disease or help with the symptoms, but despite the advances made in MS drug development, there is still an unmet

medical need when it comes to MS, especially the progressive subtype (Hauser & Cree, 2020). The goal of this master's thesis is to contribute to the understanding of multiple sclerosis by providing information on the MS pathogenesis, and the role microglia and astrocytes play in it.

2 Results

2.1 Demographic and clinical characteristics of the study participants

The cohort included 44 MS patients and 22 HCs. MS patients were further divided into subgroups based on gender and treatments status. Out of the 44 MS patients, 33 were female and 11 were male. 32 patients were on a DMT whereas 12 did not receive disease modifying therapy at the time of study onset. Out of the 32 patients that received a DMT, three were on dimethyl fumarate, four on fingolimod, four on glatiramer acetate, six on interferon beta-1a, and 13 on teriflunomide, while two of the patients received a second-line treatment, natalizumab. Number of subjects as well as statistics of gender and DMT status distribution inside each group can be found in Tables 1 and 2.

The mean age of HCs and all MS patients were 42.2 and 46.3 years, respectively (Table 1). As the HC and MS patient groups were age- and sex-matched, there were no significant differences in age ($p = 0.088$) or gender ($p = 0.85$) between these groups. The mean age at onset for all MS patients was 33.6 years whereas the median disease duration was 13.1. The median EDSS score was 2.5 whereas the mean MSSS was 3.12. The median ARR was 0.30 in MS patient group (Table 1).

At the time of the study, the female patients had a mean age of 47.1 years and male patients 43.7 years ($p = 0.088$) (Table 1). The mean age at onset was 32.2 years for female patients and 34.1 years for male patients ($p = 0.46$). The duration of the disease was significantly longer in female patients compared to male ($p = 0.038$) as median values were 13.8 years and 9.8 years for female and male patients, respectively. The median EDSS score was 2.5 for female patients and 2.5 for male patients whereas the mean MSSS values were 2.85 and 3.94, respectively. There were no statistically significant differences in EDSS ($p = 0.85$) or MSSS ($p = 0.13$) between these groups. The ARR of female patients was 0.30 and 0.30 for male patients ($p = 0.64$).

Patients that received a DMT had a mean age of 46.8 years and those without a DMT had a mean age of 44.8 years ($p = 0.22$) (Table 2). The age at onset was significantly higher ($p = 0.020$) in patients receiving a DMT compared to those who did not as mean values were 34.1 and 28.7 years, respectively. The median disease duration was 12.7 years for patients with DMT and 14.4 years for patients without DMT ($p = 0.13$). The median EDSS was 2.5 for patients with DMT and 2.8 for patients without DMT whereas the mean MSSSs were 3.25 and 2.79,

respectively. There were no statistically significant differences in EDSS (p = 0.88) or MSSS (p = 0.34) between these groups. DMT group had significantly higher ARR compared to no DMT group (p = 0.036). The median ARR values were 0.32 and 0.22 for DMT and no DMT groups, respectively.

Table 1. Demographic and clinical data of HCs, MS patients, and female and male groups. MS patients had higher serum GFAP levels compared to HCs. Comparison of female and male patients revealed a statistically significant difference in disease duration. All p-values have been calculated with Mann-Whitney U test. ARR, annualized relapse rate; EDSS, Expanded Disability Status Scale; GFAP, glial fibrillary acidic protein; HC, healthy control; MS, multiple sclerosis; MSSS, Multiple Sclerosis Severity Score; SD, standard division.

	HC	**MS**	**p (HC vs. MS)**	**Female patients**	**Male patients**	**p (female vs. male)**
Subjects, n	22	44		33	11	
Female/ male, n	16/6	33/11	0.85	33/0	0/11	
Treated/ untreated, n		32/12		24/9	8/3	0.99
Age (years), mean (range)	42.2 (35.4-61.6)	46.3 (34.0-55.1)	0.088	47.1 (35.7-55.1)	43.7 (34.0-53.1)	0.088
Age at onset (years), mean (range)		33.6 (17.1-45.8)		32.2 (17.1-42.8)	34.1 (20.0-45.8)	0.46
Disease duration (years), median (range)		13.1 (2.5-33.1)		13.8 (3.6-33.1)	9.8 (2.5-14.9)	**0.038**
EDSS, median (range)		2.5 (1-6.5)		2.5 (1-6)	2.5 (1-6.5)	0.85
MSSS, mean (range)		3.12 (0.24-7.57)		2.85 (0.24-6.81)	3.94 (0.88-7.57)	0.13
ARR, median (IQR)		0.30 (0.21-0.43)		0.30 (0.21-0.43)	0.30 (0.21-0.44)	0.64
Serum GFAP (pg/ml), mean (SD)	69.15 (24.25)	94.85 (29.89)	**0.006**	96.39 (28.65)	90.24 (34.40)	0.37

Table 2. Demographic and clinical data of DMT, no DMT, GFAP(low), and GFAP(high) groups. Comparison of treated and non-treated patients revealed that DMT group had higher age at onset and ARR, but lower serum GFAP levels compared to no DMT group. GFAP(low) group had a larger portion of treated patients and lower serum GFAP levels compared to GFAP(high) group. Division of MS patients to GFAP(low) and GFAP(high) groups was determined by the 80th percentile of the HC serum GFAP (90.47 pg/ml). All p-values have been calculated with Mann-Whitney U test. ARR, annualized relapse rate; EDSS, Expanded Disability Status Scale; GFAP, glial fibrillary acidic protein; MS, multiple sclerosis; MSSS, Multiple Sclerosis Severity Score; SD, standard division.

	DMT	**no DMT**	**p (DMT vs. no DMT)**	**GFAP(low)**	**GFAP(high)**	**p [GFAP(low) vs. GFAP(high)]**
Subjects, n	32	12		20	24	
Female/ male, n	24/8	9/3	0.99	13/7	20/4	0.17
Treated/ untreated, n	32/0	0/12		18/2	14/10	**0.021**
Age (years), mean (range)	46.8 (34.0-55.1)	44.8 (38.5-53.2)	0.22	45.6 (34.0-53.1)	46.8 (35.7-55.1)	0.39
Age at onset (years), mean (range)	34.1 (18.9-45.8)	28.7 (17.1-38.1)	**0.020**	34.3 (20.0-45.8)	31.3 (17.1-41.3)	0.19
Disease duration (years), median (range)	12.7 (2.5-33.1)	14.4 (9.3-28.7)	0.13	12.6 (2.5-19.9)	13.9 (3.6-33.1)	0.079
EDSS, median (range)	2.5 (1-6)	2.8 (1-6.5)	0.88	2.3 (1-3.5)	3 (1-6.5)	**0.014**
MSSS, mean (range)	3.25 (0.88-7.27)	2.79 (0.24-7.57)	0.34	2.85 (0.64-7.27)	3.35 (0.24-7.57)	0.33
ARR, median (IQR)	0.32 (0.24-0.44)	0.22 (0.19-0.31)	**0.036**	0.28 (0.19-0.44)	0.30 (0.23-0.42)	0.62
Serum GFAP (pg/ml), mean (SD)	86.66 (24.14)	116.70 (33.12)	**0.005**	68.41 (14.37)	117.11 (19.03)	**<0.0001**

2.2 Serum GFAP

2.2.1 Determining the serum GFAP levels

When serum GFAP levels were examined, some discrepancies were noticed. Blood samples of majority of the study cohort were analysed twice (MS, n = 41; HC, n = 6), and this revealed that even though the samples were the same in both analyses and both analyses were done with SIMOA assay kits, the results differed. Additionally, there was no trend in these changes as the

new serum GFAP levels were either higher or lower depending on the patient. Out of the 41 MS patients whose GFAP levels were analysed twice, 28 had higher whereas 13 had lower results in the second analysis compared to the first one. All HCs had higher results in the second analysis. The mean (range) change in serum GFAP was 11.65 (-25.79-64.21) pg/ml in MS patients and 6.40 (1.73-12.85) pg/ml in HCs.

The values retained from the two analyses did correlate strongly in the whole MS population ($\rho = 0.85$, $p < 0.0001$). Still, as an effort to minimize the effects of the inconsistencies in the values, statistical analyses were done with a mean serum GFAP value of the two analyses if both measurements were available. For those with only one analysis result, that value was used. Further analysis established that the newly calculated mean serum GFAP levels had strong correlations to both the first ($\rho = 0.96$, $p < 0.0001$) and second ($\rho = 0.96$, $p < 0.0001$) analysis results.

There was a statistically significant difference in serum GFAP between HCs and MS patients ($p = 0.006$) as the mean values were 69.15 pg/ml and 94.85 pg/ml, respectively (Table 1, Figure 4). Additionally, DMT group had a lower serum GFAP compared to no DMT group ($p = 0.005$) (Table 2). The serum GFAP was 86.66 pg/ml in DMT and 116.70 pg/ml in no DMT group. No statistically significant difference was found between female and male patients ($p = 0.37$) although female patients had slightly higher serum GFAP levels with 96.39 pg/ml as the levels in male patient group were 90.24 pg/ml (Table 1). When the serum GFAP levels of HCs were compared with different subgroups of MS patients, GFAP levels of HCs were found to be significantly lower compared to female ($p = 0.004$), DMT ($p = 0.035$), and no DMT groups ($p = 0.001$).

2.2.2 Division and comparison of MS patients in GFAP(low) and GFAP(high) groups

MS patients were divided into GFAP(low) and GFAP(high) groups based on the 80th percentile serum GFAP of HCs (90.47 pg/ml). There were 20 patients in the GFAP(low) group and 24 in the GFAP(high) group. The mean serum GFAP was 68.41 pg/ml in GFAP(low) and 117.11 pg/ml in GFAP(high) (Table 2, Figure 4). Thus, GFAP(high) group had a significantly higher serum GFAP ($p < 0.0001$). When these groups were compared to HCs, GFAP(high) group was found to have significantly higher serum GFAP levels ($p < 0.0001$). The serum GFAP levels of HCs and GFAP(low) group did not differ significantly ($p = 0.99$).

Comparison of GFAP(low) and GFAP(high) groups revealed no statistically significant differences in age (p = 0.39) or gender (p = 0.17) (Table 2). GFAP(low) group had more treated patients compared to GFAP(high) group (p = 0.021). The mean age at onset was 34.3 years for GFAP(low) and 31.3 years for GFAP(high) group (p = 0.19). The median disease durations were 12.6 and 13.9 in the low and high groups, respectively (p = 0.079). The median EDSS score was 2.3 for GFAP(low) group, and 3 for GFAP(high). Thus, GFAP(high) group had significantly higher EDSS compared to GFAP(low) (p = 0.014). In the GFAP(low) group, the mean MSSS was 2.85 whereas in the GFAP(high) group it was 3.35 (p = 0.33). The median ARR values were 0.28 and 0.30 for GFAP(low) and GFAP(high) groups, respectively (p = 0.62).

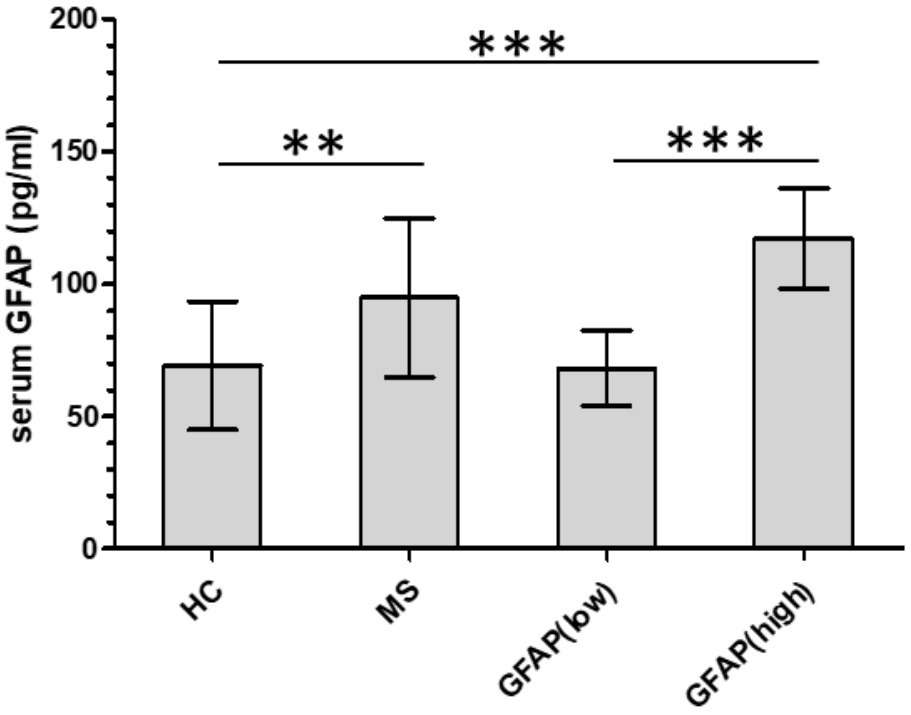

Figure 4. Mean serum GFAP levels with standard deviation of HCs and MS patients as well as GFAP(low) and GFAP(high) subgroups. Serum GFAP levels of HCs were significantly lower compared to MS patients. GFAP(low) group had significantly lower levels compared to GFAP(high) group. Additionally, GFAP(high) group had significantly higher GFAP levels compared to HCs. Division of MS patients to GFAP(low) and GFAP(high) groups was determined by the 80th percentile of the HC serum GFAP (90.47 pg/ml). P-value explanation: * < 0.05; ** < 0.01; *** < 0.001. All analysis were done with Mann-Whitney U test. GFAP, Glial Fibrillary Acidic Protein; HC, healthy control; MS, multiple sclerosis.

2.3 MRI volumes of brain regions and lesions

Volume of whole brain, NAWM, and cortical GM as well as T1 and T2 lesion loads were acquired by MRI. Group-specific statistics are presented in Tables 3 and 4.

In the MS patient population, the median volume of WM was 465.30 cm^3, NAWM 459.29 cm^3, and cortical GM 430.60 cm^3 (Table 3). The median lesion loads were 2.13 cm^3 and 4.58 cm^3 for T1 and T2 lesions, respectively. HCs had higher brain region volumes compared to MS patients, but analysis of the volume of the WM and cortical GM revealed no statistically significant differences between the groups. However, there was a trend towards significance in the NAWM volume ($p = 0.060$).

Table 3. MRI volumes of HCs and MS patients as well as female and male patients. Presented are the volumes of WM, NAWM, and cortical GM as well as T1 and T2 lesion loads. There were no statistically significant differences between HCs and MS patients. Male patients had higher WM, NAWM, and cortical GM volume compared to female patients, but no significant differences were detected in lesion load. All p-values have been calculated with Mann-Whitney U test. GM, grey matter; HC, healthy control; IQR, interquartile range; MS, multiple sclerosis; NAWM, normal appearing white matter; SD, standard division; WM, white matter.

	HC	MS	p (HC vs. MS)	Female (MS)	Male (MS)	p (female vs. male)
WM volume (cm^3), median (IQR)	489.03 (458.31-524.01)	465.30 (426.74-494.02)	0.13	454.29 (412.22-482.60)	520.18 (459.62-605.69)	**0.003**
NAWM volume (cm^3), median (IQR)	489.03 (458.31-524.01)	459.29 (413.74-493.17)	0.060	448.84 (396.21-478.05)	516.36 (451.00-602.07)	**0.005**
Cortical GM volume (cm^3), median (IQR)	465.75 (418.07-485.17)	430.60 (416.23-470.12)	0.19	429.03 (409.39-435.58)	477.82 (441.30-528.20)	**0.002**
T1 lesion load (cm^3), median (IQR)		2.13 (0.94-5.40)		2.12 (0.77-6.32)	2.71 (1.21-3.10)	0.79
T2 lesion load (cm^3), median (IQR)		4.58 (2.64-11.05)		3.65 (2.32-10.25)	4.97 (3.82-11.39)	0.26

Most prevalent differences in MRI volumes were found between male and female patients (Table 3). Male group had significantly higher WM volume ($p = 0.003$), NAWM volume ($p = 0.005$), and cortical GM volume ($p = 0.002$) than female group. In the male group, median WM volume was 520.18 cm^3, NAWM volume was 516.36 cm^3, and cortical GM volume was 477.82 cm^3. In the female group, the volumes of WM, NAWM, and cortical GM were 454.29 cm^3,

448.84 cm^3, and 429.03 cm^3, respectively. There were no statistically significant differences in T1 and T2 lesion load between these two groups.

There were no statistically significant differences in WM, NAWM, and cortical GM volume nor in T1 and T2 lesion load between DMT and no DMT groups (Table 4). Similarly, comparison of GFAP(low) and GFAP(high) groups revealed no difference in WM, NAWM, cortical GM, T1, or T2 volumes (Table 4).

Table 4. MRI volumes of DMT, no DMT, GFAP(low) and GFAP(high) groups. Presented are the volumes of WM, NAWM, and cortical GM as well as T1 and T2 lesion loads. No statistically significant differences were detected between DMT and no DMT or GFAP(low) and GFAP(high) groups. Division of MS patients to GFAP(low) and GFAP(high) groups was determined by the 80th percentile of the HC serum GFAP (90.47 pg/ml). All p-values have been calculated with Mann-Whitney U test. GM, grey matter; IQR, interquartile range; MS, multiple sclerosis; NAWM, normal appearing white matter; SD, standard division; WM, white matter.

	DMT	no DMT	p (DMT vs. no DMT)	GFAP(low)	GFAP(high)	p [GFAP(low) vs. GFAP(high)]
WM volume (cm^3), median (IQR)	474.85 (428.76-512.78)	452.27 (409.73-479.70)	0.29	473.70 (428.76-519.83)	461.92 (425.45-489.17)	0.50
NAWM volume (cm^3), median (IQR)	465.73 (414.22-506.85)	447.60 (400.63-474.26)	0.36	467.21 (419.90-515.03)	454.62 (409.41-482.72)	0.35
Cortical GM volume (cm^3), median (IQR)	430.50 (419.35-475.97)	430.79 (398.98-453.16)	0.54	429.14 (412.85-478.76)	432.67 (416.65-461.65)	0.99
T1 lesion load (cm3), median (IQR)	1.90 (0.94-3.93)	3.03 (0.85-10.12)	0.64	1.88 (0.63-3.38)	2.52 (1.19-11.26)	0.21
T2 lesion load (cm3), median (IQR)	4.00 (2.64-10.36)	6.05 (2.43-15.04)	0.72	3.73 (2.51-7.66)	6.01 (2.75-17.33)	0.23

2.4 [^{11}C]PK11195 binding in different brain regions

2.4.1 Specific [^{11}C]PK11195 binding presented as DVR

Specific [^{11}C]PK11195 binding, suggestive of innate immune cell activity, in different brain regions is presented as DVR. Group-specific statistics are presented in Tables 5 and 6.

MS patients had significantly higher DVR in whole brain ($p = 0.011$) as well as NAWM ($p = 0.046$) compared to HCs (Table 5, Figure 5A-B). In the MS population, the mean whole brain DVR was 1.202 and NAWM DVR was 1.207 whereas the respective values for HCs were 1.185 and 1.182. The difference in NAWM DVR between MS patients and HCs was even greater in

parietal NAWM (p = 0.007) and occipital NAWM (p = 0.0002) (Table 5, Figure 5C-D). Statistically significant differences were not detected in other regions of NAWM between any comparable groups.

MS patients had almost significantly higher DVR in thalamus (p = 0.063) and ventral diencephalon (p = 0.065) (Table 5, Figure 6B, D). The mean values for thalamus and central diencephalon DVRs were, respectively, 1.330 and 1.274 for MS patients and 1.291 and 1.241 for HCs. There were no statistically significant differences in cortical GM, brain stem, amygdala, or pallidum DVRs between MS patients and HCs.

There were no statistically significant differences in the DVRs between female and male MS patients (Table 5). However, there was a trend towards significance in whole brain DVR (p = 0.060) and cortical GM DVR (p = 0.054) with male patients having higher values.

When DMT and no DMT groups were compared, DMT group was found to have significantly higher whole brain DVR (p = 0.002), NAWM DVR (p = 0.044), and cortical GM DVR (p = 0.007) (Table 6). The DMT group had a mean whole brain DVR of 1.209, NAWM DVR of 1.216, and median cortical GM DVR of 1.246. The mean whole brain DVR, NAWM DVR, and median cortical GM DVR in the no DMT group were 1.183, 1.184, and 1.205, respectively. Closer analysis on DVRs of NAWM regions revealed that DMT group had significantly higher occipital NAWM DVR (p = 0.036) in addition to which there was a trend towards significance in parietal NAWM DVR (p = 0.053) (Table 6).

Comparison of GFAP(low) and GFAP(high) groups revealed that GFAP(low) group had a significantly higher cortical GM DVR (p = 0.003) compared to GFAP(high) (Table 6, Figure 5E). The median cortical GM DVR was 1.263 in GFAP(low) and 1.207 in GFAP(high) group. On the other hand, GFAP(low) group had significantly lower DVR in brain stem (p = 0.049), pallidum (p = 0.042), and ventral diencephalon (p = 0.048) compared to GFAP(high) (Table 6, Figure 5F, 6C-D). The mean DVRs of brain stem, pallidum, and ventral diencephalon were, respectively, 1.196, 1.191, and 1.250 in GFAP(low) and 1.233, 1.241, and 1.294 in GFAP(high).

There was no statistically significant difference in NAWM DVR (p = 0.70) between GFAP(low) and GFAP(high) groups but analysis of parietal NAWM DVR showed a trend towards significance (p = 0.079) with GFAP(low) groups having higher mean DVR (Table 6, Figure 5B-C). Trend towards significance was also present in analysis of amygdala DVR (p =

0.088) as GFAP(high) group had higher median DVR (Table 6, Figure 6A). Additionally, there was a trend towards significance when comparing whole brain DVR (p = 0.052) as the mean DVRs were 1.210 and 1.194 for GFAP(low) and GFAP(high) group, respectively (Table 6, Figure 5A).

Table 5. **Specific [^{11}C]PK11195 binding in different brain regions in HC, MS, female, and male groups.** Comparison of MS patients and HCs demonstrated MS patients having significantly higher DVR in whole brain, NAWM, parietal NAWM, and occipital NAWM as well as having more active voxels in whole brain and NAWM. Female and male patients had no statistically significant differences in DVRs, however male patients had more active voxels in whole brain, NAWM, and thalamus. All p-values have been calculated with Mann-Whitney U test. DVR, distribution volume ratio; GM, grey matter; HC, healthy control; IQR, interquartile range; MS, multiple sclerosis; NAWM, normal appearing white matter; SD, standard division.

	HC	MS	p (HC vs. MS)	Female (MS)	Male (MS)	p (female vs. male)
Whole brain DVR, mean (SD)	1.185 (0.025)	1.202 (0.025)	**0.011**	1.198 (0.026)	1.213 (0.020)	0.060
NAWM DVR, mean (SD)	1.182 (0.047)	1.207 (0.049)	**0.046**	1.202 (0.050)	1.221 (0.046)	0.20
Parietal NAWM DVR, mean (SD)	1.246 (0.060)	1.290 (0.058)	**0.007**	1.283 (0.057)	1.314 (0.057)	0.13
Occipital NAWM DVR, mean (SD)	1.210 (0.058)	1.275 (0.056)	**0.0002**	1.270 (0.060)	1.289 (0.040)	0.22
Cortical GM DVR, median (IQR)	1.217 (1.194-1.229)	1.225 (1.201-1.272)	0.22	1.223 (1.193-1.250)	1.267 (1.205-1.277)	0.054
Brain stem DVR, mean (SD)	1.200 (0.061)	1.216 (0.059)	0.32	1.219 (0.057)	1.208 (0.066)	0.36
Amygdala DVR, median (IQR)	1.097 (1.038-1.150)	1.080 (1.043-1.114)	0.37	1.090 (1.057-1.118)	1.048 (1.021-1.108)	0.10
Thalamus DVR, mean (SD)	1.291 (0.060)	1.330 (0.074)	0.063	1.321 (0.070)	1.258 (0.081)	0.27
Pallidum DVR, mean (SD)	1.229 (0.061)	1.218 (0.074)	0.56	1.211 (0.067)	1.241 (0.092)	0.18
Ventral diencephalon DVR, mean (SD)	1.241 (0.071)	1.274 (0.063)	0.065	1.274 (0.058)	1.274 (0.080)	0.63
Active voxels in whole brain (*10^3), median (IQR)	74.93 (56.99-96.38)	99.33 (71.98-134.57)	**0.020**	89.53 (68.52-116.06)	150.13 (99.63-165.96)	**0.003**
Active voxels in NAWM (*10^3), median (IQR)	28.81 (22.54-37.79)	43.12 (28.98-55.45)	**0.010**	37.54 (26.88-47.67)	61.23 (49.92-73.68)	**0.002**
Active voxels in thalamus (*10^3), median (IQR)	2.91 (2.14-3.82)	3.14 (2.34-4.17)	0.25	2.95 (2.08-3.70)	4.20 (3.31-5.55)	**0.016**

Table 6. Specific [^{11}C]PK11195 binding in brain regions in DMT, no DMT, GFAP(low), and GFAP(high) groups. DMT groups had significantly higher DVR in whole brain, NAWM, occipital NAWM, and cortical GM as well as more active voxels in whole brain and NAWM compared to no DMT group. GFAP(low) group had significantly higher cortical GM DVR and more active voxels in whole brain and NAWM compared to GFAP(high), however GFAP(high) group had higher brain stem, pallidum, and ventral diencephalon DVRs. Division of MS patients to GFAP(low) and GFAP(high) groups was determined by the 80th percentile of the HC serum GFAP (90.47 pg/ml). All p-values have been calculated with Mann-Whitney U test. DVR, distribution volume ratio; GFAP, glial fibrillary acidic protein; GM, grey matter; IQR, interquartile range; MS, multiple sclerosis; NAWM, normal appearing white matter; SD, standard division; WM.

	DMT	**no DMT**	**p (DMT vs. no DMT)**	**GFAP(low)**	**GFAP(high)**	**p [GFAP(low) vs. GFAP(high)]**
Whole brain DVR, mean (SD)	1.209 (0.023)	1.183 (0.020)	**0.002**	1.210 (0.024)	1.194 (0.024)	0.052
NAWM DVR, mean (SD)	1.216 (0.048)	1.184 (0.044)	**0.044**	1.209 (0.044)	1.206 (0.053)	0.70
Parietal NAWM DVR, mean (SD)	1.302 (0.059)	1.260 (0.043)	0.053	1.306 (0.056)	1.277 (0.057)	0.079
Occipital NAWM DVR, mean (SD)	1.285 (0.059)	1.247 (0.034)	**0.036**	1.286 (0.055)	1.266 (0.056)	0.21
Cortical GM DVR, median (IQR)	1.246 (1.205-1.276)	1.205 (1.189-1.194)	**0.007**	1.263 (1.223-1.278)	1.207 (1.193-1.233)	**0.003**
Brain stem DVR, mean (SD)	1.205 (0.058)	1.246 (0.052)	0.071	1.196 (0.060)	1.233 (0.054)	**0.049**
Amygdala DVR, median (IQR)	1.080 (1.037-1.117)	1.079 (1.057-1.113)	0.84	1.056 (1.024-1.109)	1.097 (1.062-1.116)	0.088
Thalamus DVR, mean (SD)	1.330 (0.068)	1.330 (0.091)	0.82	1.316 (0.057)	1.342 (0.085)	0.35
Pallidum DVR, mean (SD)	1.215 (0.071)	1.227 (0.083)	0.70	1.191 (0.066)	1.241 (0.074)	**0.042**
Ventral diencephalon DVR, mean (SD)	1.270 (0.060)	1.286 (0.072)	0.61	1.250 (0.058)	1.294 (0.061)	**0.048**
Active voxels in whole brain (*10^3), median (IQR)	114.22 (86.38-149.40)	74.02 (54.68-96.31)	**0.007**	130.38 (82.24-153.21)	89.18 (67.15-112.11)	**0.026**
Active voxels in NAWM (*10^3), median (IQR)	46.58 (35.52-61.00)	28.30 (21.61-43.97)	**0.009**	52.46 (35.52-63.39)	37.40 (26.65-46.71)	**0.023**
Active voxels in thalamus (*10^3), median (IQR)	3.10 82.62-4.19)	3.17 (1.64-4.08)	0.49	2.98 (2.34-3.74)	3.17 (2.22-4.29)	0.65

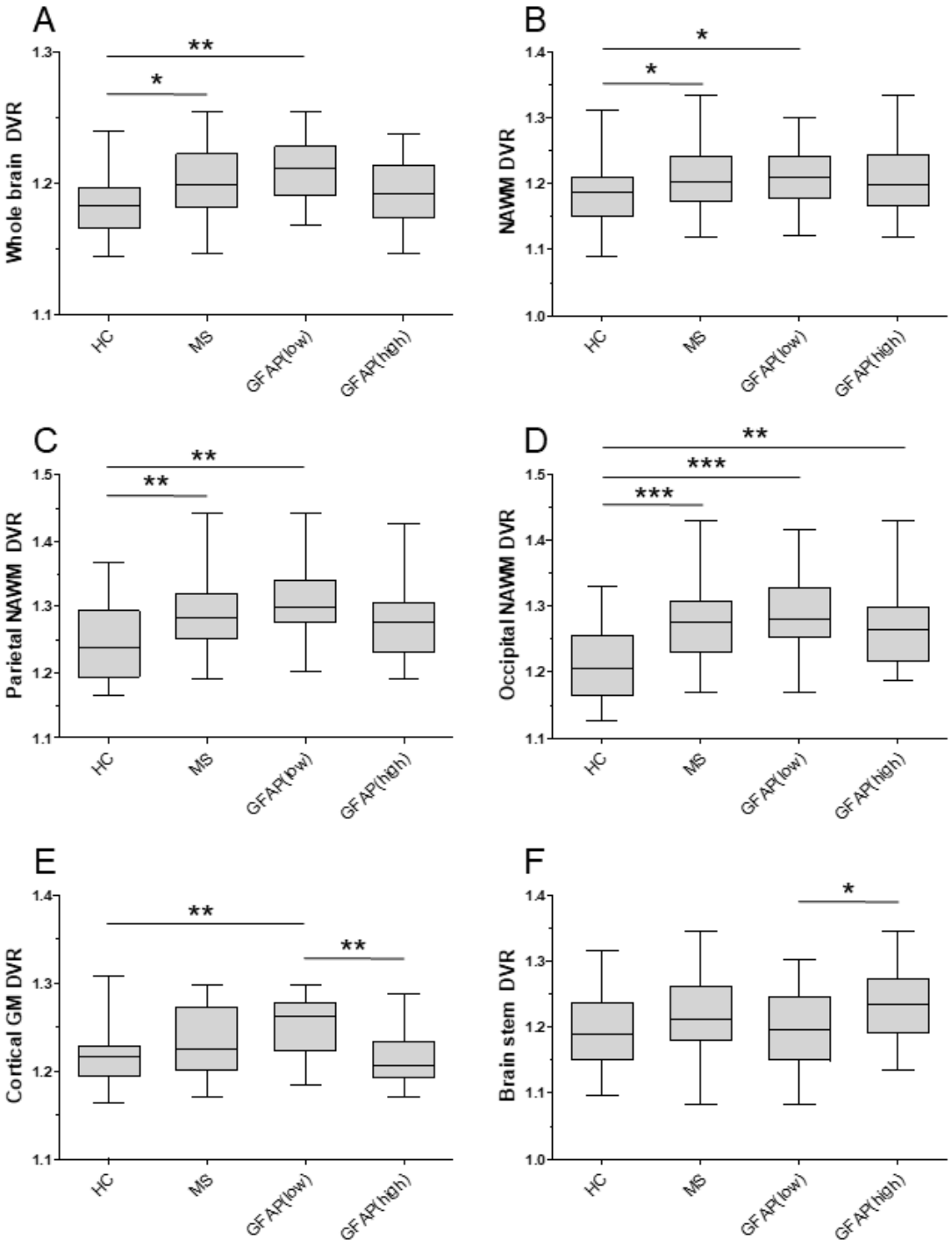

Figure 5. Specific [^{11}C]PK11195 binding in different brain regions in HCs and MS patients as well as GFAP(low) and GFAP(high) patient subgroups. A) HCs had lower whole brain DVR compared to MS patients and GFAP(low) group. B) HCs had lower NAWM DVR than MS patients as well as GFAP(low) group. C) Parietal NAWM DVR was higher in MS and GFAP(low) groups compared to HCs. D) MS patients, as well as MS subgroups GFAP(low) and GFAP(high), had higher occipital NAWM DVR compared to HCs. E) HCs and GFAP(high) group had lower cortical GM DVR compared to GFAP(low). F) GFAP(high) group had higher brain stem DVR compared to GFAP(low). Division of MS patients to GFAP(low) and GFAP(high) groups was determined by the 80th percentile of the HC serum GFAP (90.47 pg/ml). The DVRs are presented as box and whiskers (min, max). P-value explanation: * < 0.05; ** < 0.01; *** < 0.001. All p-values have been calculated with Mann-Whitney U test. DMT; disease modifying therapy; DVR, distribution volume ratio; GFAP, glial fibrillary acidic protein; GM, grey matter; HC, healthy control; MS, Multiple Sclerosis; NAWM, normal appearing white matter.

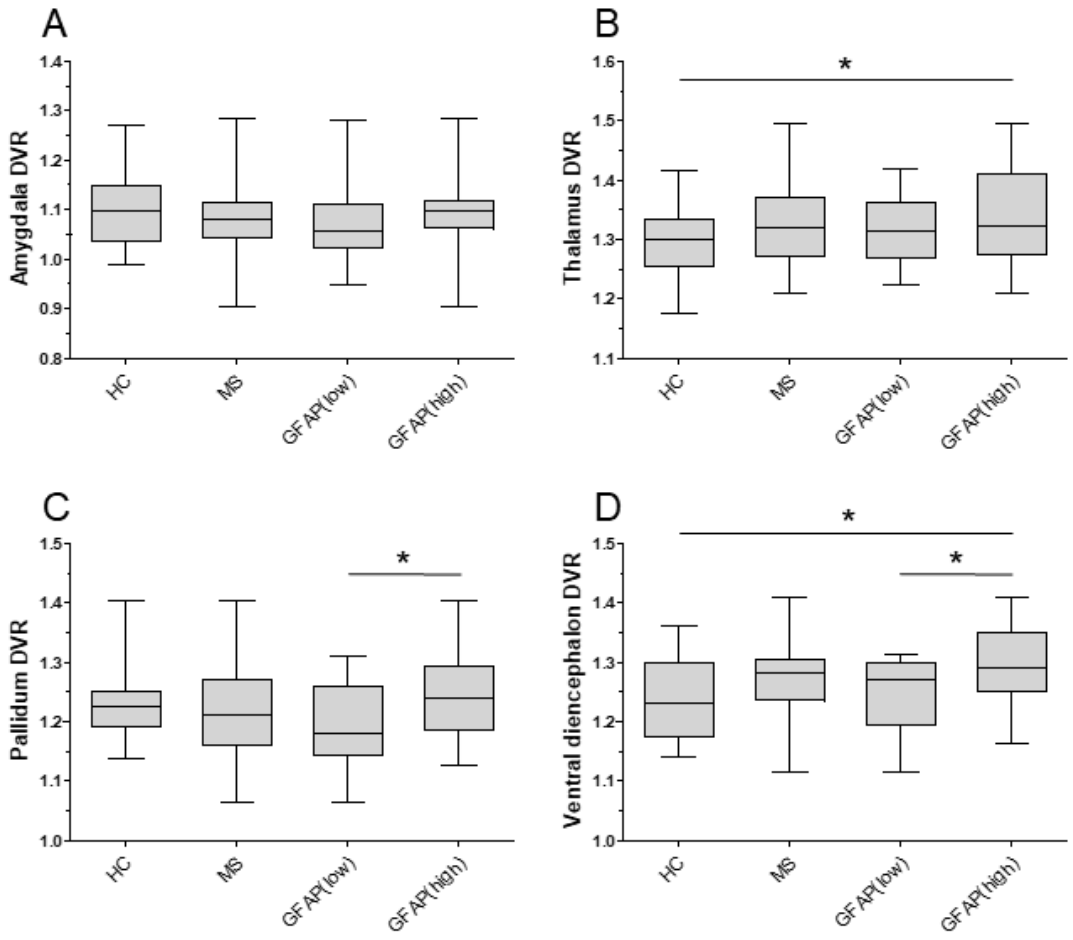

Figure 6. Specific [^{11}C]PK11195 binding in different brain regions in HCs and MS patients as well as GFAP(low) and GFAP(high) patient subgroups. A) No statistically significant differences were found in amygdala DVR between the groups. B) HCs had significantly lower thalamus DVR compared to GFAP(high) group. C) GFAP8low) group had lower pallidum DVR compared to GFAP(high). D) GFAP(high) group had higher ventricular diencephalon DVR compared to both HCs and GFAP(low) group. Division of MS patients to GFAP(low) and GFAP(high) groups was determined by the 80th percentile of the HC serum GFAP (90.47 pg/ml). The DVRs are presented as box and whiskers (min, max). P-value explanation: * < 0.05; ** < 0.01; *** < 0.001. All p-values have been calculated with Mann-Whitney U test. DMT; disease modifying therapy; DVR, distribution volume ratio; GFAP, glial fibrillary acidic protein; GM, grey matter; HC, healthy control; MS, Multiple Sclerosis; NAWM, normal appearing white matter.

Finally, the [^{11}C]PK11195 binding of HCs was also compared to different MS patient subgroups. Comparison revealed that male group had significantly higher whole brain DVR (p =0.006), NAWM DVR (p = 0.023), parietal NAWM DVR (p = 0.006), occipital NAWM DVR (p = 0.0008), and cortical GM DVR (p = 0.023), and lower thalamus DVR (p = 0.049) compared to HCs. Similarly, female patients had higher whole brain DVR (p = 0.048), parietal NAWM DVR (p = 0.031), and occipital NAWM (p = 0.001) compared to HCs. Compared to DMT group, HCs had lower whole brain DVR (p = 0.0009), NAWM DVR (p = 0.009), parietal

NAWM DVR ($p = 0.002$), occipital NAWM DVR ($p < 0.0001$), and cortical GM DVR ($p = 0.035$). Additionally, HCs had lower brain stem DVR compared to no DMT group ($p = 0.035$).

Statistically significant differences were also found between HCs and GFAP(low) and GFAP(high) groups. GFAP(low) group had higher whole brain DVR ($p = 0.002$), NAWM DVR ($p = 0.045$), parietal NAWM DVR ($p = 0.003$), occipital NAWM DVR ($p = 0.0004$), and cortical GM DVR ($p = 0.009$) compared to HCs (Figure 5A-E). GFAP(high) group, in turn, had higher occipital NAWM DVR ($p = 0.003$), thalamus DVR ($p = 0.047$), and ventral diencephalon DVR ($p = 0.013$) (Figure 5B, 6B,D).

2.4.2 Specific [^{11}C]PK11195 binding presented as active voxels

Specific [^{11}C]PK11195 binding in whole brain, NAWM, and thalamus was also studied as the number of active voxels which had unusually high activity. Group-specific statistics are presented in Tables 5 and 6.

Comparison of the number of active voxels revealed that MS patients had a higher number of active voxels in the whole brain ($p = 0.020$) and NAWM ($p = 0.010$) compared to HCs (Table 5, Figure 7A-B). The median number of active voxels ($*10^3$) was 99.33 in whole brain and 43.12 in NAWM in MS population. The respective values for HCs were 74.93 in whole brain and 28.81 in NAWM. There was no statistically significant difference in the number of active voxels in thalamus ($p = 0.25$) between MS patients and HCs (Table 5, Figure 7C).

When male and female patients were compared, it was found that male group had a significantly higher number of active voxels in the whole brain ($p = 0.003$), NAWM ($p = 0.002$) as well as thalamus ($p = 0.016$) compared to female patient group (Table 5). Male patients had a median number of active voxels ($*10^3$) in the whole brain of 150.13, in NAWM 61,23, and in thalamus 4.20. For female patients, the number of active voxels in whole brain, NAWM, and thalamus were 89.53, 37.54, and 2.95, respectively. Statistically significant differences ($p < 0.05$) in the number of the active voxels were present in whole brain and NAWM, but not in thalamus, even after the number of active voxels was proportioned by the number of all voxels in those specific regions.

DMT group had a significantly higher number of active voxels in the whole brain ($p = 0.007$) and NAWM ($p = 0.009$) compared to no DMT group (Table 6). The median number of active voxels ($*10^3$) in the whole brain was 114.22 in DMT group and 74.02 in no DMT group. In

NAWM, those values were 46.58 and 28.30, respectively. Statistically significant difference was not detected in thalamus (p = 0.49).

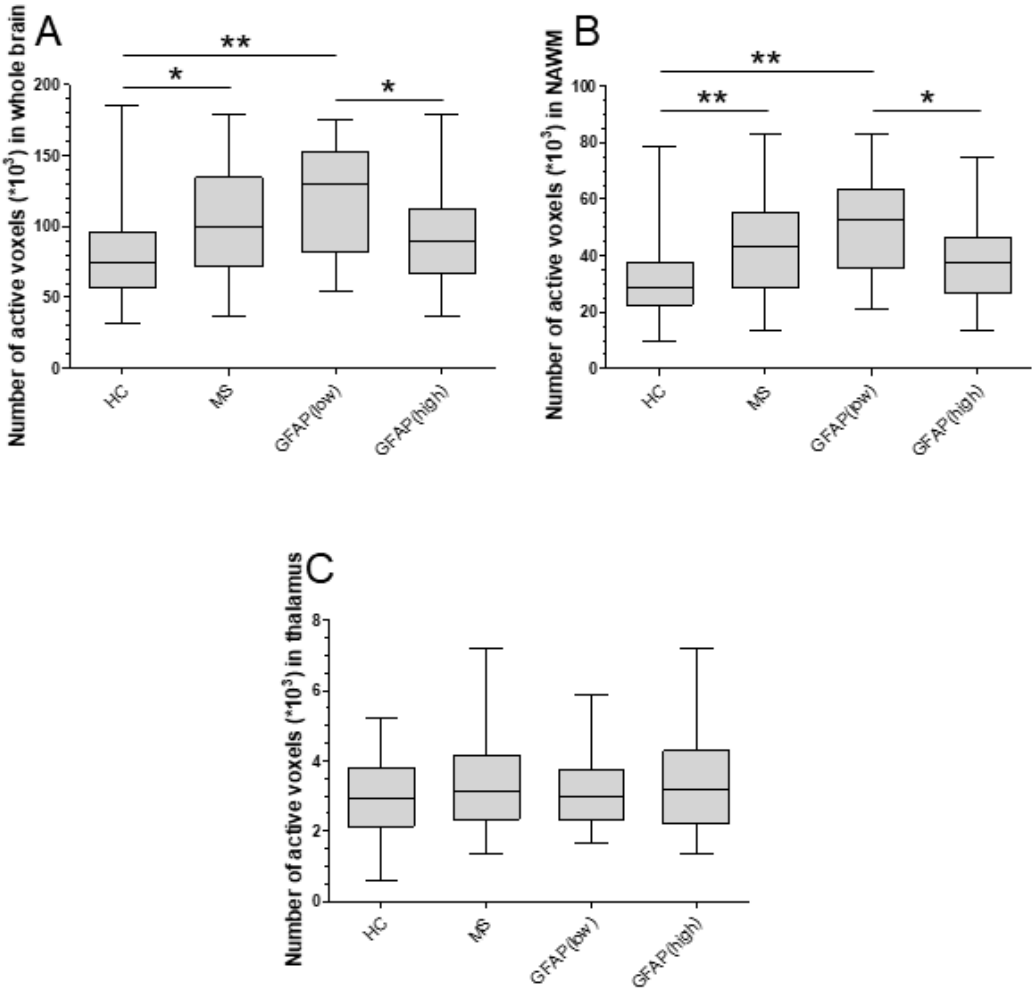

Figure 7. Number of active voxels in whole brain, NAWM, and thalamus in HCs and MS patients as well as GFAP(low) and GFAP(high) patient subgroups. A) MS patients had a higher number of active voxels in whole brain compared to HCs, and GFAP(low) group had more active voxels than GFAP(high). Additionally, GFAP(low) group had a higher number of active voxels in whole brain compared to HCs. B) MS patients had a higher number of active voxels in NAWM compared to HCs, and GFAP(low) group had more active voxels than GFAP(high). Additionally, GFAP(low) group had a higher number of active voxels in NAWM compared to HCs. C) Comparison of the number of active voxels in thalamus revealed no statistically significant differences between the groups. Division of MS patients to GFAP(low) and GFAP(high) groups was determined by the 80th percentile of the HC serum GFAP (90.47 pg/ml). The number of active voxels is presented as box and whiskers (min, max). P-value explanation: * < 0.05; ** < 0.01; *** < 0.001. All p-values have been calculated with Mann-Whitney U test. GFAP, glial fibrillary acidic protein; HC, healthy control; MS, multiple sclerosis; NAWM, normal appearing white matter.

GFAP(low) group had significantly more active voxels in the whole brain (p = 0.026) and NAWM (p = 0.023) compared to GFAP(high) (Table 6, Figure 7A-B). The median number of active voxels (*10^3) in the whole brain was 130.38 for GFAP(low) and 89.18 for GFAP(high) group. The median number of active voxels (*10^3) in NAWM were 52.46 and 37.40 for

GFAP(low) and GFAP(high) groups, respectively. There was no statistically significant difference in the number of active voxels in thalamus ($p = 0.65$) between these groups (Table 6, Figure 7C).

The active voxels of MS patient subgroups were also compared to HCs. HCs had a lower number of active voxels in whole brain ($p = 0.001$), NAWM ($p = 0.0006$), and thalamus ($p = 0.009$) compared to male patients. Similarly, when compared to DMT group, HCs had a lower number of active voxels in whole brain ($p = 0.002$) and NAWM ($p = 0.0007$). Compared to GFAP(low) group, HCs had a lower number of active voxels in whole brain ($p = 0.003$) and NAWM ($p = 0.001$) (Figure 7A-B). Other groups showed no statistically significant differences to HCs.

2.5 Lesion characteristics

The volume and DVR of T1 and T2 lesions as well as the DVR of T1 lesion rims and perilesional areas were analysed. The lesions were classified into rim-active, overall-active, and inactive phenotypes, and the number and volume of the lesions representing those phenotypes was determined. Group-specific statistics are presented in Tables 7 and 8.

MS patients had a total of 716 lesions out of which 98 (13.69%) were rim-active, 364 (50.84%) were overall-active, and 254 (35.47%) were inactive (Table 7). For all MS patients, the median number of rim-active lesions was one, number of overall-active was five, and the number of inactive lesions was five. In total, MS patients had a median of 10 lesions. The median of total volume of rim-active lesions was 0.052 cm^3, overall-active lesions 1.00 cm^3, and inactive lesions 0.48 cm^3 in MS patient population. The median total volume of lesions was 1.67 cm^3.

There were no statistically significant differences in any lesion-related results between female and male patients (Table 7), DMT and no DMT groups (Table 8), or GFAP(low) and GFAP(high) groups (Table 8).

Table 7. Lesion characteristics of all, female, and male MS patients. MS patients had a median of 10 lesions with a total volume of 1.670. The lesions were further divided to rim-active, overall-active, and inactive lesions, which MS patients had one, five, and five, respectively. No statistically significant differences in lesion characteristics were found between female and male patients. All p-values have been calculated with Mann-Whitney U test. DVR, distribution volume ratio; IQR, interquartile range; MS, Multiple Sclerosis; SD, standard division.

	MS	**Female (MS)**	**Male (MS)**	**p (female vs. male)**
T1 lesion DVR, median (IQR)	1.148 (1.086-1.233)	1.144 (1.086-1.232)	1.169 (0.997-1.265)	0.85
Lesion rim 0-2 mm DVR, mean (SD)	1.191 (0.088)	1.193 (0.088)	1.186 (0.092)	0.77
Perilesional area 2-6 mm DVR, mean (SD)	1.188 (0.079)	1.188 (0.079)	1.188 (0.085)	0.89
Perilesional area 4-6 mm DVR, mean (SD)	1.188 (0.076)	1.186 (0.076)	1.195 (0.079)	0.55
T2 lesion DVR, mean (SD)	1.140 (0.099)	1.138 (0.095)	1.146 (0.116)	0.91
Total number of lesions, median (IQR)	10 (6-21.75)	9 (5.5-23)	10 (6-20)	0.98
Total volume of lesions (cm^3), median (IQR)	1.67 (0.60-4.79)	1.53 (0.60-5.97)	1.97 (0.81-2.42)	1.00
Number of rim-active lesions, median (IQR)	1 (0-3.75)	1 (0-4)	1 (0-3)	0.89
Total volume of rim-active lesions (cm^3), median (IQR)	0.052 (0-0.27)	0.051 (0-0.30)	0.095 (0-0.26)	0.93
Number of overall-active lesions, median (IQR)	5 (2-11)	4 (2-12.50)	6 (1-10)	0.57
Total volume of overall-active lesions (cm^3), median (IQR)	1.00 (0.22-3.82)	0.81 (0.22-4.82)	1.25 (0.12-1.84)	0.81
Number of inactive lesions, median (IQR)	5 (2.25-7.75)	5 (2-8)	4 (3-7)	0.95
Total volume of inactive lesions (cm^3), median (IQR)	0.48 (0.17-0.77)	0.50 (0.17-0.78)	0.40 (0.19-0.58)	0.69

Table 8. Lesion characteristics of DMT, no DMT, GFAP(low), and GFAP(high) groups. There were no statistically significant differences between DMT and no DMT, or GFAP(low) and GFAP(high) groups. Division of MS patients to GFAP(low) and GFAP(high) groups was determined by the 80th percentile of the HC serum GFAP (90.47 pg/ml). All p-values have been calculated with Mann-Whitney U test. DMT; disease modifying therapy; DVR, distribution volume ratio; GFAP, glial fibrillary acidic protein; IQR, interquartile range; MS, Multiple Sclerosis; SD, standard division.

	DMT	**no DMT**	**p (DMT vs. no DMT)**	**GFAP(low)**	**GFAP(high)**	**p [GFAP(low) vs. GFAP(high)]**
T1 lesion DVR, median (IQR)	1.159 (1.082-1.233)	1.141 (1.098-1.238)	0.93	1.156 (1.088-1.228)	1.145 (1.082-1.239)	0.79
Lesion rim 0-2 mm DVR, mean (SD)	1.196 (0.086)	1.178 (0.096)	0.45	1.200 (0.083)	1.184 (0.093)	0.50
Perilesional area 2-6 mm DVR, mean (SD)	1.196 (0.080)	1.166 (0.076)	0.17	1.187 (0.080)	1.188 (0.080)	0.86
Perilesional area 4-6 mm DVR, mean (SD)	1.197 (0.079)	1.165 (0.065)	0.20	1.184 (0.078)	1.191 (0.076)	0.99
T2 lesion DVR, mean (SD)	1.143 (0.096)	1.131 (0.111)	0.64	1.137 (0.104)	1.142 (0.097)	0.77
Total number of lesions, median	10 (6.25-21)	13.5 (5.25-29.5)	0.95	10 (5.5-17.5)	13.5 (6-33.5)	0.29
Total volume of lesions, median	1.504 (0.620-2.902)	2.594 (0.603-8.101)	0.63	1.629 (0.338-2.394)	1.810 (0.719-9.413)	0.18
Number of rim-active lesions, median (IQR)	1 (0-2)	1.5 (0-4.75)	0.85	1 (0-1.75)	1.5 (0.5,75)	0.41
Total volume of rim-active lesions, median, (IQR)	0.051 (0-0.196)	0.072 (0-0.318)	0.99	0.051 (0-0.145)	0.090 (0-0.408)	0.62
Number of overall-active lesions, median (IQR)	5 (2-10.75)	5 (2-12.5)	0.97	5 (1.25-9)	6 (2-18.25)	0.32
Total volume of overall-active lesions, median (IQR)	0.90 (0.21-2.32)	1.13 (0.31-5.85)	0.61	0.72 (0.14-1.79)	1.09 (0.42-7.96)	0.17
Number of inactive lesions, median (IQR)	5 (2-7.75)	4.5 (3.25-7.75)	0.80	3.5 (2-7)	6 (3.25-8)	0.23
Total volume of inactive lesions, median (IQR)	0.50 (0.18-0.77)	0.37 (0.16-1.11)	1.00	0.37 (0.15-0.80)	0.48 (0.28-0.77)	0.53

2.6 Serum GFAP's correlation with other variables in MS patients and HCs as well as GFAP(low) and GFAP(high) subgroups

2.6.1 Demographic and clinical characteristics

In the MS patient population, serum GFAP levels correlated positively with EDSS (ρ = 0.38, p = 0.012, Figure 8A). However, serum GFAP's correlation to EDSS was not present in GFAP(low) (ρ = 0.081, p = 0.73, Figure 8B) and GFAP(high) (ρ = 0.15, p = 0.49, Figure 8C) groups.

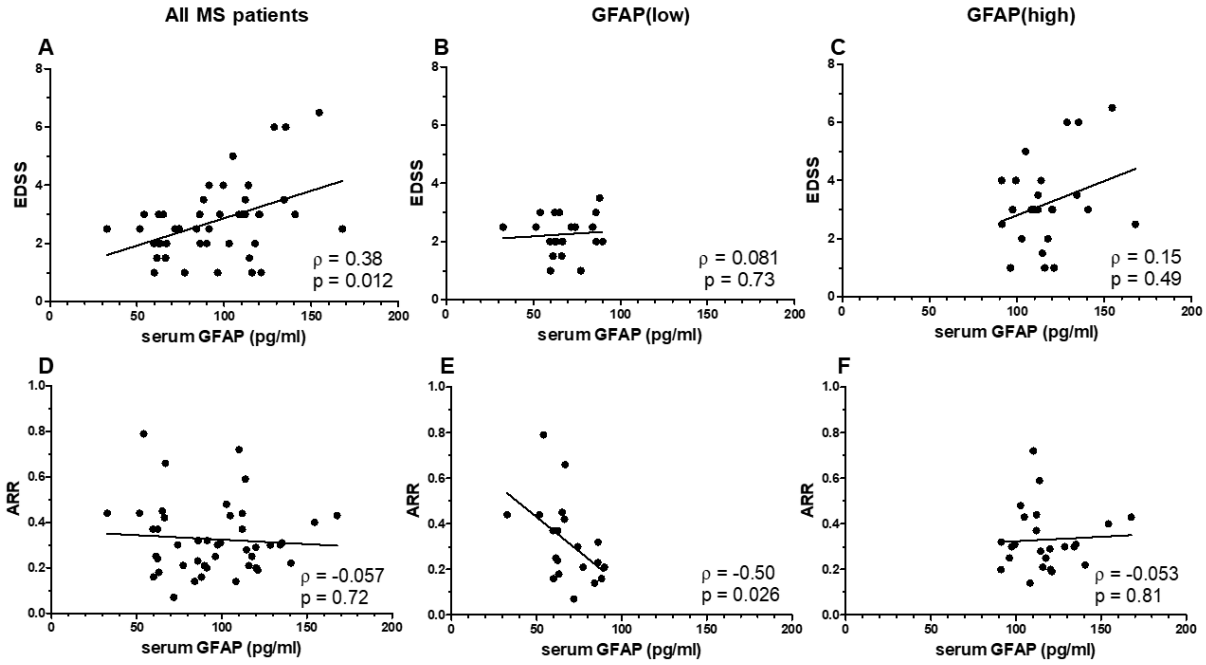

Figure 8. Serum GFAP's correlation to EDSS and ARR in all MS patients as well as GFAP(low) and GFAP(high) groups. A) Serum GFAP correlated positively with EDSS in whole MS patient population. B) Statistically significant correlation of EDSS and serum GFAP was not present in GFAP(low) group. C) No statistically significant correlation between serum GFAP and EDSS was found in GFAP(high) group. D) Correlation of serum GFAP and ARR was not present in all MS patients. E) In GFAP(low) group, serum GFAP correlated with ARR in a negative manner. F) No statistically significant correlation between serum GFAP and ARR was found in GFAP(high) group. Division of MS patients to GFAP(low) and GFAP(high) groups was determined by the 80th percentile of the HC serum GFAP (90.47 pg/ml). All correlations were calculated with Spearman's correlation analysis. ρ, Spearman's rank correlation coefficient; ARR, annualized relapse rate; EDSS, Expanded Disability Status Score; GFAP, glial fibrillary acidic protein; MS, multiple sclerosis.

In GFAP(low) group, higher serum GFAP was found to correlate with lower ARR (ρ = -0.50, p = 0.026, Figure 8E). Correlation between serum GFAP and ARR was not present in the whole MS patient population (ρ = -0.057, p = 0.72, Figure 8D) or in the GFAP(high) group (ρ = -0.053, p = 0.81, Figure 8F). Other correlations between serum GFAP and other demographic and clinical data (age, disease duration, age at onset, MSSS) were not found in the whole MS

population and its subgroups. Correlations between serum GFAP and demographic characteristics were not found in HCs.

2.6.2 [^{11}C]PK11195 binding presented as DVR

In the whole MS population, higher serum GFAP was found to correlate with lower parietal NAWM DVR (ρ = -0.31, p = 0.043, Figure 9A), however not with whole NAWM or other NAWM regions. A negative correlation was also found between serum GFAP and cortical GM DVR (ρ = -0.36, p = 0.018, Figure 9D). Serum GFAP was found to have a positive correlation to brain stem DVR (ρ = 0.37, p = 0.015, Figure 9G), amygdala DVR (ρ = 0.32, p = 0.036, Figure 10A), pallidum DVR (ρ = 0.30, p = 0.047, Figure 10D), and ventral diencephalon (ρ = 0.34, p = 0.023, Figure 10G).

No statistically significant correlations between serum GFAP and specific [^{11}C]PK11195 binding were detected in the GFAP(low) and GFAP(high) groups. However, there was a trend towards significance in the correlation between serum GFAP and ventral diencephalon DVR in the GFAP(high) group (ρ = 0.40, p = 0.053, Figure 10H).

Corresponding correlations were not found in the HC group. However, in the HC group, serum GFAP was found to correlate positively with corpus callosum DVR (ρ = 0.60, p = 0.025).

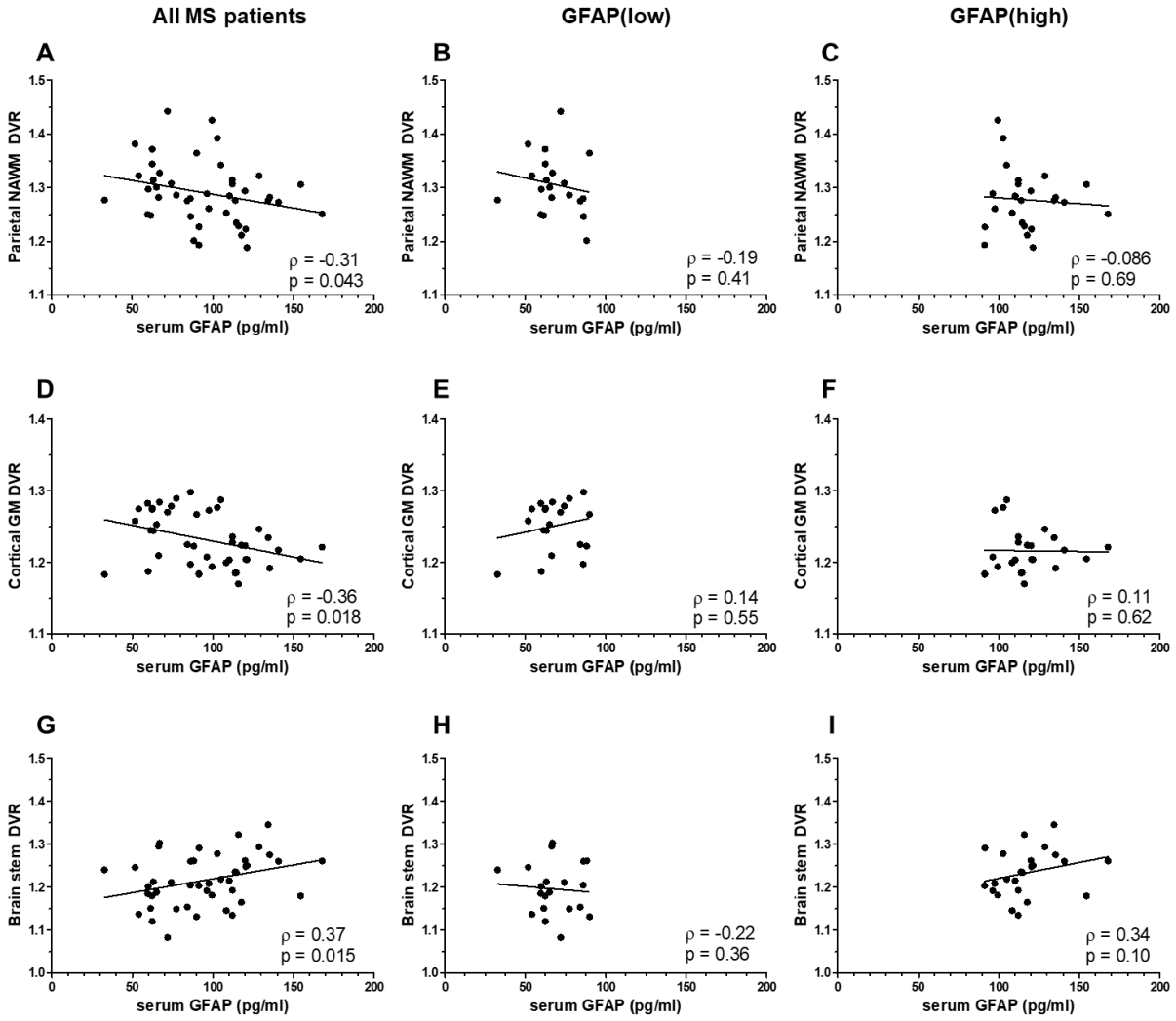

Figure 9. Serum GFAP's correlation to the DVR of parietal NAWM, cortical GM, and brain stem in all MS patients as well as GFAP(low) and GFAP(high) groups. A) Serum GFAP correlated negatively with parietal NAWM DVR in whole MS population. B) Statistically significant correlation of serum GFAP and parietal NAWM DVR was not present in GFAP(low) group. C) No statistically significant correlation between serum GFAP and parietal NAWM DVR was found in GFAP(high) group. D) In all MS patients, serum GFAP correlated negatively with cortical GM DVR. E) Serum GFAP did not correlate with cortical GM DVR in GFAP(low) group. F) No statistically significant correlation was found between serum GFAP and cortical GM DVR in GFAP(high) group. G) Serum GFAP correlated positively with brain stem DVR in whole MS population. H) Statistically significant correlation between serum GFAP and brain stem DVR was not present in GFAP(low) group. I) There was no statistically significant correlation between serum GFAP and brain stem DVR in GFAP(high) group. Division of MS patients to GFAP(low) and GFAP(high) groups was determined by the 80th percentile of the HC serum GFAP (90.47 pg/ml). All correlations were calculated with Spearman's correlation analysis. ρ, Spearman's rank correlation coefficient; DVR; distribution volume ratio; GFAP, glial fibrillary acidic protein; GM, grey matter; MS, multiple sclerosis; NAWM; normal appearing white matter.

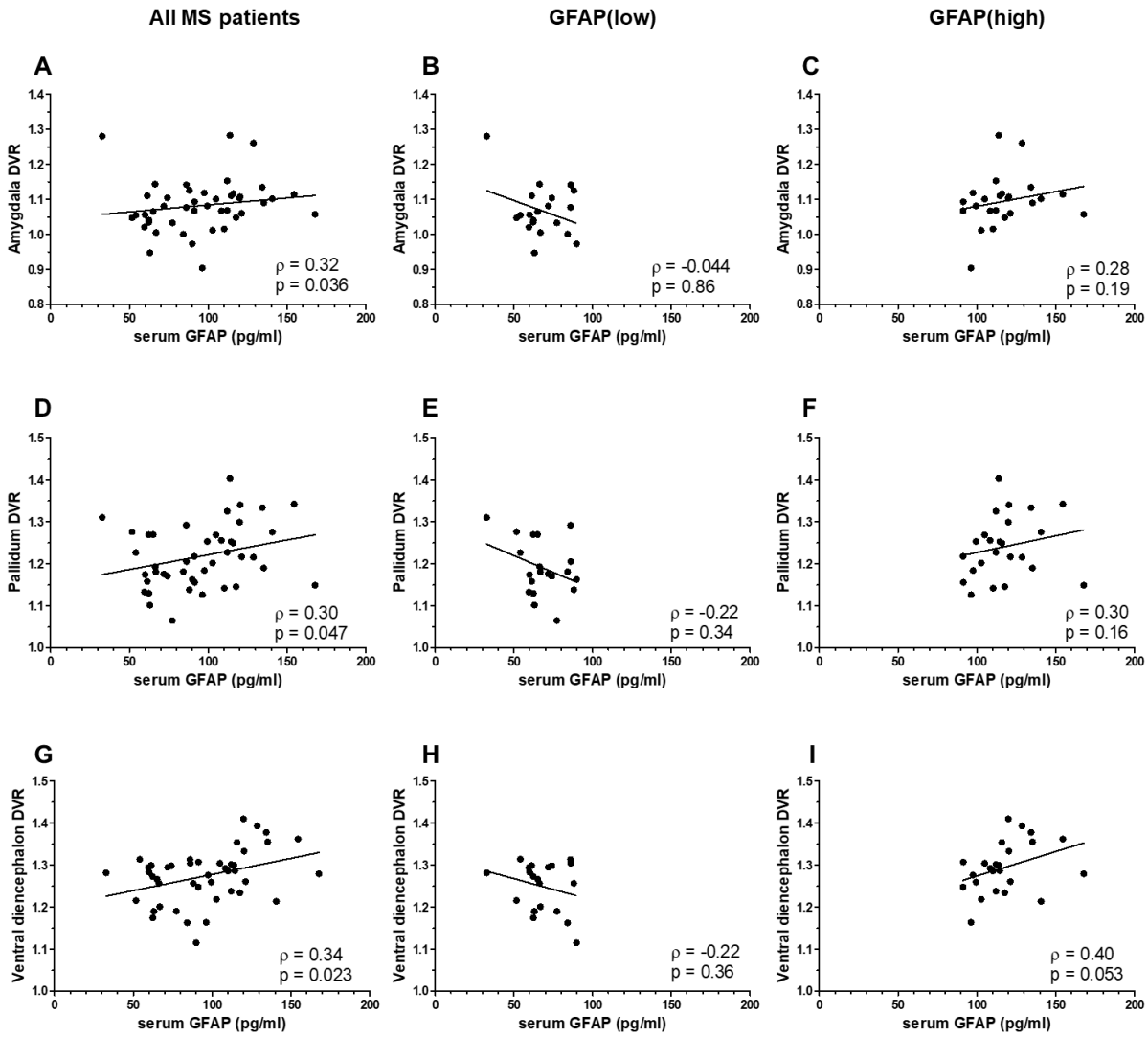

Figure 10. Serum GFAP's correlation to the DVR of amygdala, pallidum, and ventral diencephalon in all MS patients as well as GFAP(low) and GFAP(high) groups. A) Serum GFAP correlated positively with amygdala DVR in MS patients. B) There was no statistically significant correlation between serum GFAP and amygdala DVR in the GFAP(low) group, however unlike in the whole MS population, the correlation in GFAP(low) group was negative. C) Serum GFAP did not correlate with amygdala DVR in the GFAP(high) group. D) In the whole MS population, serum GFAP correlated positively with pallidum DVR. E) In GFAP(low) group, there was no statistically significant correlation between serum GFAP and pallidum DVR but the correlation was negative unlike in the whole MS population. F) No statistically significant correlation was found between serum GFAP and pallidum DVR in the GFAP(high) group. G) Serum GFAP correlated positively with the DVR in ventral diencephalon in all MS patients. H) No statistically significant correlation was found between serum GFAP and ventral diencephalon DVR in the GFAP(low) group but again the correlation was negative. I) There was a trend towards significance in the correlation between serum GFAP and ventral diencephalon DVR in the GFAP(high) group. Division of MS patients to GFAP(low) and GFAP(high) groups was determined by the 80th percentile of the HC serum GFAP (90.47 pg/ml). All correlations were calculated with Spearman's correlation analysis. ρ, Spearman's rank correlation coefficient; DVR; distribution volume ratio; GFAP, glial fibrillary acidic protein; MS, multiple sclerosis.

2.6.3 [^{11}C]PK11195 binding presented as active voxels

In whole MS patient group, serum GFAP correlated with the number of active voxels in the whole brain (ρ = -0.30, p = 0.045, Figure 11A) and NAWM (ρ = -0.30, p = 0.048, Figure 11D) in a negative manner. However, serum GFAP did not correlate with the number of active voxels in the whole brain or NAWM in GFAP(low) and GFAP(high) subgroup (Figure 11B-C, E-F).

Additionally, higher serum GFAP levels were found to correlate with a higher number of active voxels in thalamus of GFAP(high) group (ρ = 0.45, p =0.028, Figure 11I) but not in the whole MS population (ρ = 0.18, p = 0.23, Figure 11G) or GFAP(low) group (ρ = -0.065, p = 0.79, Figure 11H). Corresponding correlations were not found in HCs.

2.6.4 Lesion characteristics

In the whole MS population, there was a positive correlation between serum GFAP and the percentage of total overall-active lesion volume out of total lesion volume (ρ = 0.30, p = 0.046, Figure 12D). Correlation between serum GFAP and the percentage of total overall-active lesion volume out of total lesion volume was also found in the GFAP(high) group (ρ = 0.61, p = 0.002, Figure 12F) but not in GFAP(low) group (ρ = -0.075, p = 0.75).

A negative correlation between serum GFAP and the percentage of total inactive lesion volume out of total lesion volume was found in GFAP(high) group (ρ = -0.50, p = 0.012, Figure 12I). Additionally, there was a trend towards significance in the whole MS patient population between serum GFAP and the percentage of total inactive lesion volume out of total lesion volume (ρ = -0.29, p = 0.056, Figure 12G). GFAP(low) group showed no correlation between serum GFAP and the percentage of total inactive lesion volume out of total lesion volume (ρ = 0.023, p = 0.92).

Serum GFAP did not correlate with the percentage of total rim-active lesion volume out of total lesion volume (Figure 12A-C). No correlations between serum GFAP and other lesion characteristics (Tables 7 and 8) were found.

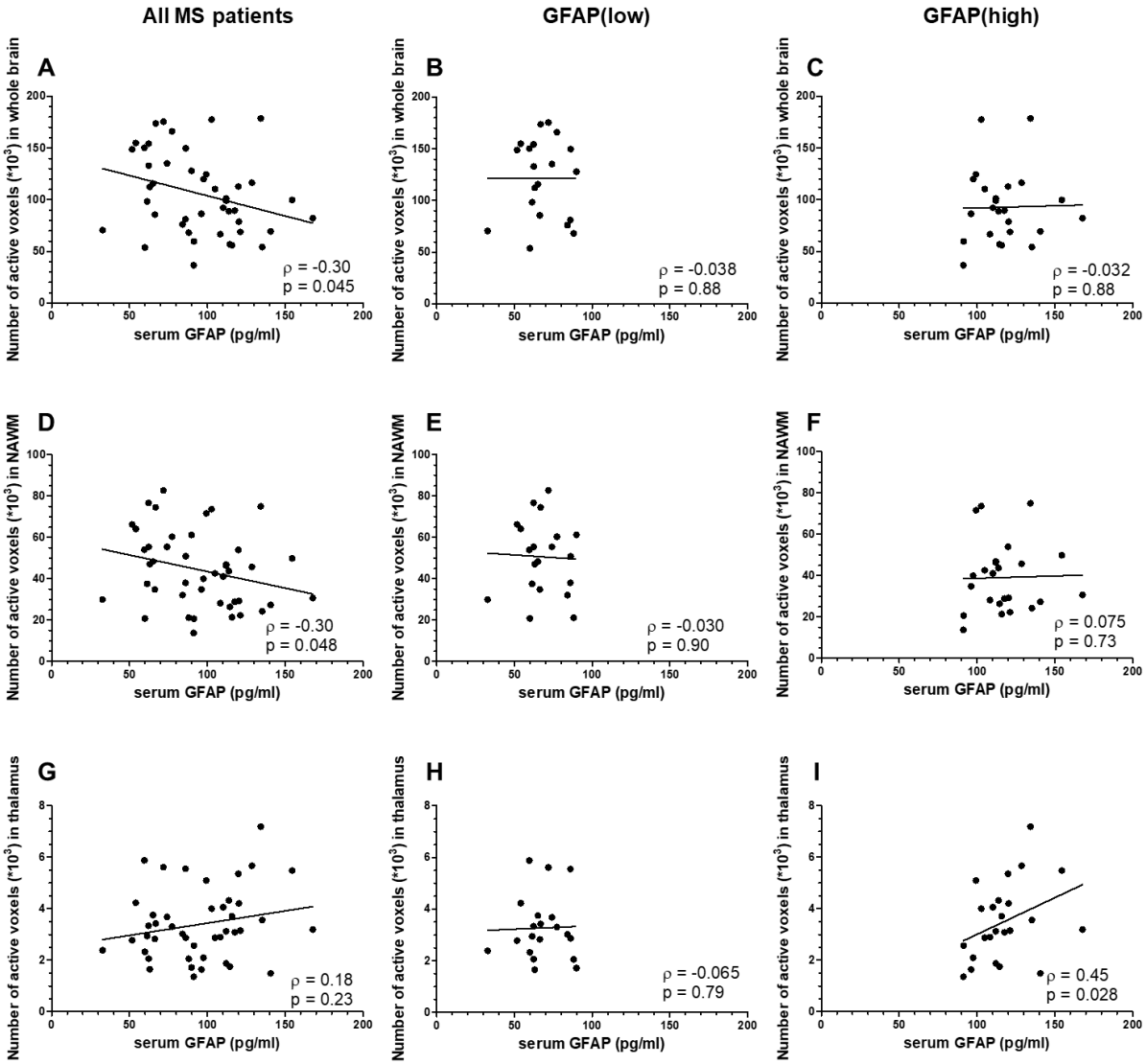

Figure 11. Serum GFAP's correlation to the number of active voxels (*10^3) in whole brain, NAWM, and thalamus in all MS patients as well as GFAP(low) and GFAP(high) groups. A) Serum GFAP correlated negatively with the number of active voxels in whole brain in the whole MS population. B) There was no correlation between serum GFAP and the number of active voxels in whole brain in GFAP(low) group. C) There was no correlation between serum GFAP and the number of active voxels in whole brain in GFAP(high) group. D) Serum GFAP correlated negatively with the number of active voxels in NAWM in the whole MS population. E) There was no correlation between serum GFAP and the number of active voxels in NAWM in GFAP(low) group. F) There was no correlation between serum GFAP and the number of active voxels in NAWM in GFAP(high) group. G) There was no correlation between serum GFAP and the number of active voxels in thalamus in the whole MS population group. H) There was no correlation between serum GFAP and the number of active voxels in thalamus in GFAP(low) group. I) Serum GFAP correlated positively with the number of active voxels in thalamus in GFAP(high) group. Division of MS patients to GFAP(low) and GFAP(high) groups was determined by the 80th percentile of the HC serum GFAP (90.47 pg/ml). All correlations were calculated with Spearman's correlation analysis. ρ, Spearman's rank correlation coefficient; GFAP, glial fibrillary acidic protein; MS, multiple sclerosis; NAWM, normal appearing white matter.

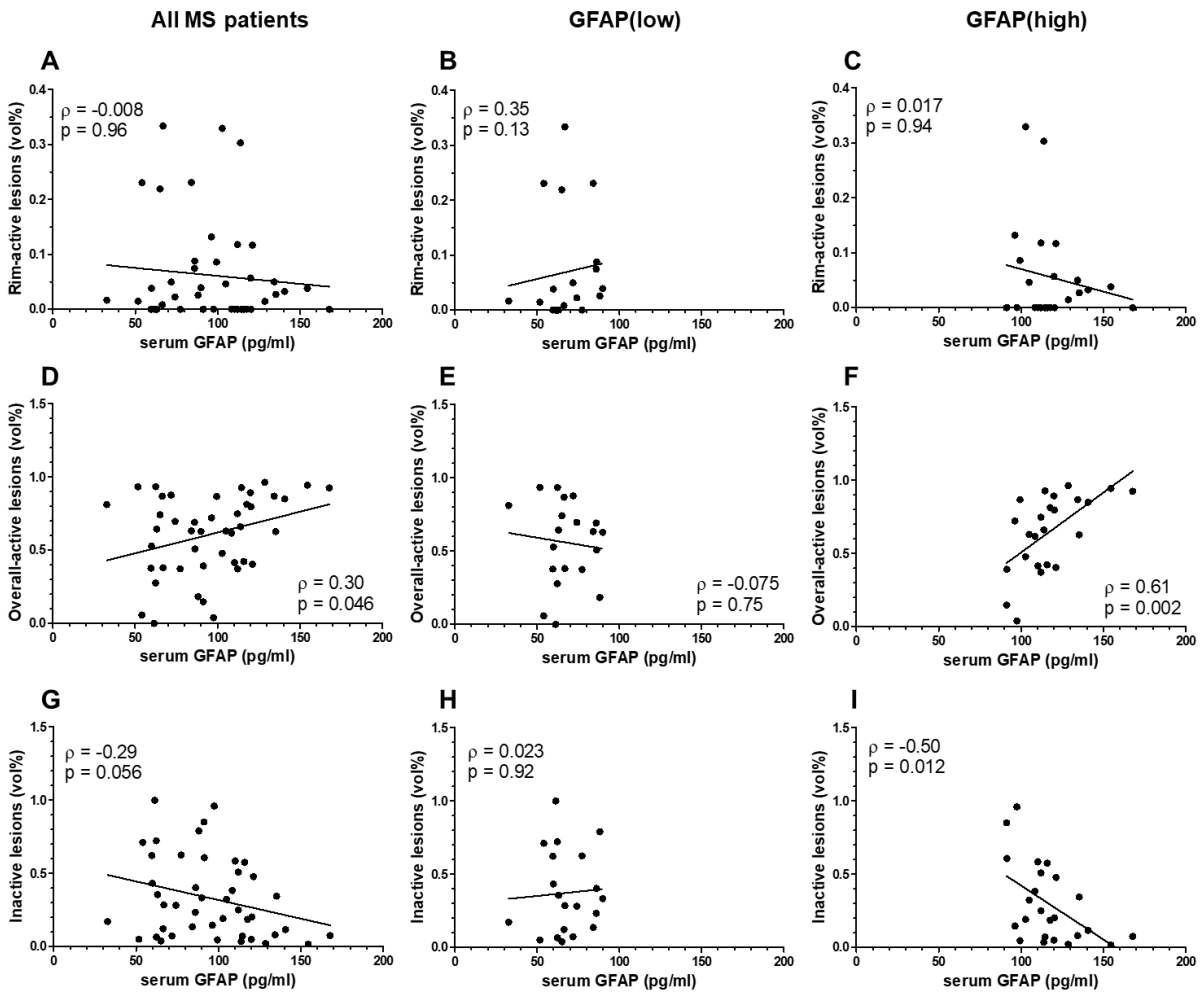

Figure 12. Serum GFAP's correlation to the percentage of total rim-active, overall-active, and inactive lesion volume out of the total volume lesion volume in all MS patients as well as GFAP(low) and GFAP(high) groups. D) Serum GFAP correlated positively with the percentage of total overall-active lesion volume out of the total lesion volume in MS patient population. E) Statistically significant correlation between overall active lesions (vol%) and serum GFAP was not found in GFAP(low) group. F) In GFAP(high) group, serum GFAP correlated positively with the percentage of total overall-active lesion volume out of total lesion volume. G) There was a trend towards statistical significance in the correlation of the percentage of total inactive lesion volume out of total lesion volume in MS patient population. H) No statistically significant correlation was found in GFAP(low) group. I) A negative correlation between inactive lesions (vol%) and serum GFAP was found in GFAP(high) group. Division of MS patients to GFAP(low) and GFAP(high) groups was determined by the 80th percentile of the HC serum GFAP (90.47 pg/ml). All correlations were calculated with Spearman's correlation analysis. ρ, Spearman's rank correlation coefficient; GFAP, glial fibrillary acidic protein; MS, multiple sclerosis; vol%, percentage out of the total lesion volume.

3 Discussion

MS is a chronic, life-altering disease that targets the CNS, causing neuroinflammation, multifocal demyelination, and progressive neurodegeneration that are presumably a result of a self-antigen targeting autoimmune reaction (Nylander & Hafler, 2012). Unfortunately, the pathogenesis of MS is still not fully known, and despite recent advancements and a growing interest in developing new and effective treatment options, there is still an unmet medical need. Thus, it is utmost important to research the underlying mechanisms and factors behind the key driver of MS, neuroinflammation.

The aim of this master's thesis project was to study the association between microglial and astrocytic activation. They are the two key players of neuroinflammation in MS, and therapeutic targets of interest as suggested by prior literature (Brandi et al., 2022; Brosnan & Raine, 2013; Liddelow et al., 2017; Ponath et al., 2018; Tan et al., 2020). Microglial activation was assessed by TSPO-PET imaging, a widely used method for studying neuroinflammation and microgliosis (Y. Lee et al., 2020). PET imaging enables *in vivo* research of MS patients, and offers quantitative information on the inflammatory and functional changes in the brain (Högel et al., 2018; Nylund et al., 2021; Poutiainen et al., 2016). Reactive astrogliosis was studied as serum GFAP since reactive astrocytes are known to overexpress GFAP (Zamanian et al., 2012) (Sofroniew, 2015). GFAP can be released from the cell and found from the blood stream (Agostini et al., 2021), making serum GFAP is an easy and only mildly invasive method for assessing reactive astrogliosis. GFAP levels were determined with SIMOA, a commonly used and highly sensitive method (Abdelhak et al., 2018, 2019; Aktas et al., 2021; Ayrignac et al., 2020; Högel et al., 2020; Meier et al., 2023; Tybirk et al., 2022).

Previous studies have reported elevated serum GFAP levels in MS patients indicating increased astrocyte activity (Abdelhak et al., 2018; Högel et al., 2020; Meier et al., 2023; Niiranen et al., 2021). The results of this study are in line with those previous findings as serum GFAP levels were higher in MS patients compared to HCs. This finding favours the idea of reactive astrogliosis and BBB disturbance being part of MS pathogenesis. However, the difference in individual serum GFAP levels between different analyses raises a concern regarding the reliability of the results, and thus the inconsistencies should be further investigated. The differences could be explained by the different analysis kits, despite both analyses were done with SIMOA technology. The reason may also be the prolonged freezing samples had to endure, as it has been reported to affect the stability of the compound (Tybirk et al., 2022). However,

this does not explain why patients had both higher and lower serum GFAP levels in the later analysis.

An even more drastic difference in serum GFAP was found between HCs and patients who did not receive any DMT, as patients who did not receive any DMT had significantly higher serum GFAP levels compared to those who did. Again, this has been documented in prior research (Högel et al., 2020) although there are also reports on serum GFAP not being dependent on DMT status (Abdelhak et al., 2018, 2019; Ayrignac et al., 2020). However, a study with patients with untreated benign and treated aggressive RRMS found no difference in serum GFAP between these groups (Niiranen et al., 2021), suggesting that serum GFAP levels could be altered with effective treatment and treatment response could be monitored with this biomarker.

Serum GFAP is also considered to be an indicator of disease progression (Abdelhak et al., 2018, 2019; Axelsson et al., 2011; Ayrignac et al., 2020; Barro et al., 2023; Högel et al., 2020; E. J. Lee et al., 2020). In line with prior research, serum GFAP levels were found to correlate with disability, assessed by EDSS, in whole MS population, as patients with high serum GFAP levels had higher EDSS scores. Previous studies have also reported serum GFAP to correlate with age and disease duration (Abdelhak et al., 2018, 2019; Ayrignac et al., 2020; Barro et al., 2023; Högel et al., 2020; E. J. Lee et al., 2020), however those associations were not found in this cohort. This could be due to a small sample size and narrow IQRs of the variables in this study. Serum GFAP's correlation to MSSS has also been previously suggested (Axelsson et al., 2011), but that could not be detected in this study much like in others (Abdelhak et al., 2019; Högel et al., 2020). Serum GFAP's correlation to EDSS but not MSSS in this study is most likely due to the lack of correlation to disease duration.

Relapses have also been reported to affect GFAP levels, although the true relationship between acute relapses and serum GFAP is still a mystery, as studies have reported differing results (Aktas et al., 2021; Burman et al., 2014; Högel et al., 2020; Watanabe et al., 2019). To minimize the effects a recent relapse may have on the GFAP levels, all patients included in this study had been relapse-free for the previous 120 days. The correlation analysis between serum GFAP and ARR revealed a negative relationship between the two in the GFAP(low) group. This finding, together with serum GFAP correlating with EDSS, is in line with serum GFAP's suggested association with relapse-independent disease progression (Meier et al., 2023). However, although also negative, the correlations in all MS patients and GFAP(high) group were not statistically significant which raises the question whether this is a coincidental finding due to

the small sample size or if low serum GFAP really is indicative of less frequent relapses but only in low concentrations.

Not only were the serum GFAP levels higher in MS patients compared to HCs, but specific [^{11}C]PK11195 binding, measured as DVR and voxels with anomalously high activity, was also greater in the whole brain as well as the NAWM of patients compared to HCs. Previous studies have also reported on higher [^{11}C]PK11195 binding, suggestive of innate immune cell activity, in the NAWM of MS patients, especially SPMS patients and even CIS subjects, compared to HCs (Bezukladova et al., 2020; Giannetti et al., 2015; Kang et al., 2021; Nylund et al., 2021; Rissanen et al., 2014). These findings support the idea of microglia and neuroinflammation contributing to MS pathophysiology.

Between GFAP(low) and GFAP(high) groups, statistically significant differences in DVR were detected in brain stem, pallidum, and ventral diencephalon, with GFAP(low) group having lower DVRs in all. In line with these results, serum GFAP was found to positively correlate with brain stem, amygdala, pallidum, and ventral diencephalon DVRs in the whole MS population. These results support our hypothesis of higher microglial activation being associated with higher astrocytic activity. However, cortical GM DVR was higher in GFAP(low) group. In addition, although no statistically significant differences were detected in whole brain or NAWM DVR, GFAP(low) group had a higher number of active voxels in those regions, and there was a trend towards significance in the whole brain and parietal NAWM DVRs with GFAP(low) group having higher mean values. Accordingly, correlation analyses showed serum GFAP to correlate negatively with the number of active voxels in whole brain and NAWM, as well as the cortical GM and parietal NAWM DVRs in the whole MS population. These findings are not in line with the hypothesis as higher serum GFAP was thought to be associated with higher [^{11}C]PK11195 binding.

Contrary to expectations, serum GFAP did not correlate with NAWM DVR, and its correlation with the number of active voxels in NAWM was negative. These findings are not in line with prior research and other results, as in this study serum GFAP correlated positively with EDSS, and higher EDSS scores have been linked to increased [^{11}C]PK11195 binding in the NAWM (Bezukladova et al., 2020; Giannetti et al., 2015; Rissanen et al., 2018; Saraste et al., 2022). Higher EDSS score correlated with higher NAWM DVR in this study, too (data not shown). This discrepancy however could be explained by the small sample size and low correlation

coefficients. Additionally, glial activity is a much more dynamic variable compared to EDSS, and that could create variance in their association.

The association between TSPO-PET measurable microglial activation and serum GFAP in MS has not been previously reported on. The results of this study regarding serum GFAP's correlation to [^{11}C]PK11195 binding in different regions are interesting, as if the differences are not caused by abnormalities in the cohort or small sample sizes, it suggests that the association between serum GFAP and [^{11}C]PK11195 binding would not automatically be positive or negative but rather dependent of the brain region. They also raise the question whether these differences could be caused by pro- and anti-inflammatory microglia affecting in different regions or based on disease progression.

Prior research has reported astrocytes to have regional differences that could also affect their GFAP content (Batiuk et al., 2020; Ben Haim & Rowitch, 2016; Griemsmann et al., 2015). It is possible that different astrocyte subpopulations could affect the pathology differently, and their effects could be dependent on the disease stage, too (Wheeler et al., 2020). Study conducted with post-mortem brain samples found that GFAP concentrations were highest in spinal cord, brain stem, and hippocampus, and lowest in cerebral cortex and WM (Sjölin et al., 2022). If a region with high GFAP concentration was damaged due to a MS lesion, it could result in relatively higher serum GFAP concentration, as well as a stronger positive correlation between microglial and astrocytic activity in that specific region. In line with this, the strongest positive correlations between serum GFAP and [^{11}C]PK11195 binding (DVR) in this study were seen in brain stem, and other inner regions such as amygdala and ventral diencephalon.

The region-dependent heterogeneity of microglia has also been widely researched, and while differences can be detected in healthy brain, some heterogeneity is consequent on pathogenesis (J. Lee et al., 2022; Tan et al., 2020). For example, a mouse study reported TSPO expression to vary between brain regions with highest expression localizing to inner regions of the brain as well as WM having higher expression levels compared to GM (Betlazar et al., 2018) . Additionally, another mouse study has suggested astrocyte and microglia heterogeneity to result in different inflammatory responses in case of a pro-inflammatory stimulus with higher density and activation in amygdala, for instance (Brandi et al., 2022). Taken together, this could lead to regional differences in the [^{11}C]PK11195 as well as in the association of serum GFAP and [^{11}C]PK11195 binding. However, to confirm whether there actually is regional variance in the association between microglia and astrocytes, further research is warranted.

There was a positive correlation between serum GFAP and the percentage of total overall-active lesion volume out of total lesion volume in whole MS population. A negative correlation was found between serum GFAP and the percentage of total inactive lesion volume out of total lesion volume in GFAP(high) group and almost significantly in the whole MS patient group. In active lesions and at the rim of chronic active lesions, almost all TSPO-expressing cells are microglia or macrophages (Nutma et al., 2021) while TSPO-expressing astrocytes are abundant in inactive lesions as well as in the cores of chronic active lesions (Nutma et al., 2019). Also, most MS lesions are located in the perivascular area of the brain (Tallantyre et al., 2008), aiding the release of GFAP to the blood stream. Taken together, it could be hypothesized that the association between microglial activity and reactive astrogliosis is more prominent in the MS lesions compared to other regions.

Despite these correlations, no statistically significant differences were found in the lesion characteristics when patient groups with high and low serum GFAP levels were compared. Lesion load, phenotypes, or activity inside the lesion and at the lesion rim did not seem to affect the serum GFAP levels, although correlation between serum GFAP and lesion load has been previously reported (Ayrignac et al., 2020; Högel et al., 2020).

Just like treatment status affects the serum GFAP levels, its affects can also be seen in microglial activation presented as DVR. DMT group had higher DVRs in whole brain and cortical GM as well as NAWM and its subregions compared to no DMT group, in addition to which they had more active voxels in whole brain and NAWM, too. These findings are surprising as use of DMTs has shown to reduce microglial activity (Ratchford et al., 2012; Sucksdorff et al., 2019). However, these previous longitudinal studies are about glatiramer acetate and natalizumab. In our cohort, only six out of the 32 treated patients (19 %) used glatiramer acetate or natalizumab. Also, it is possible that the treated patients have more active disease which requires them to use medication, whereas patients with less active disease types, and less microgliosis, do not need medication. This could also explain why, against expectations, GFAP(low) group had greater [^{11}C]PK11195 binding than GFAP(high) group since GFAP(low) group had significantly more treated patients. It is also important to note that TSPO-PET imaging alone is not able to distinguish pro- and anti-inflammatory microglia (Bonsack et al., 2016), and as many MS medications are suggested to cause microglial conversion from M1 to M2 phenotype (De Kleijn & Martens, 2020), it may be possible that in the areas where DMT group had higher DVRs, microglia had taken on more of an anti-inflammatory phenotype.

As MS affects more women than men (Ghasemi et al., 2017), gender should also be considered a factor when studying MS pathophysiology. Comparison of female and male patients revealed that in this study cohort, female patients have a longer disease duration. This could be explained by multiple factors; i) although not statistically significant, female patients had a higher mean age; ii) disease duration was calculated from the first sign of symptoms which can be inaccurate as patients may not remember the exact times or even recognize the early symptoms; iii) women are considered more likely to report their symptoms (Barsky et al., 2001). Analyses also show male patients having greater WM, NAWM, and cortical GM volumes compared to female patients which is consistent with men having a larger brains (Ritchie et al., 2018; Ruigrok et al., 2014).

Although the results of this thesis can be considered indicative of the association between serum GFAP and microglial activation in the CNS, this study does have its limitations. Firstly, the study cohort is quite small as it includes only 44 patients. Especially the division of patients to smaller subgroups such as GFAP(low) and GFAP(high) groups results in quite small group sizes which could have led to lack of power. This is suggested by serum GFAP's correlations to different DVRs being present in the whole MS patient population but not in GFAP(low) and GFAP(high) groups. Secondly, the two analyses of serum GFAP gave different results. It is also possible that the small sample size may have affected the differences and unexpected correlation results. However, as serum GFAP has been suggested as a biomarker of individual patients, more research is required regarding its storage and reflectiveness of pathological changes, for instance. Thirdly, although many correlations between serum GFAP and [^{11}C]PK11195 binding as well as active voxels were statistically significant, they were not very strong, which is why definite conclusions on their association cannot be drawn. And lastly, it is important to remember that although TSPO-PET is used to measure microglial activation, other cells, such as activated astrocytes, are known to express TSPO (Jacobs et al., 2012; Kuhlmann & Guilarte, 2000; Nutma et al., 2019, 2021; Rizzo et al., 2014; Rupprecht et al., 2010; Varlow et al., 2022), and this should be considered when interpreting the results.

Further research on the association between microglial activation and serum GFAP is still required for us to fully understand the role of microglia and astrocytes in MS pathophysiology. In future studies, the differences between MS subtypes should also be considered as serum GFAP and microglial activation are known to be more prevalent in progressive MS types compared to RRMS (Abdelhak et al., 2018; Högel et al., 2020; Meier et al., 2023). Additionally, the association between serum GFAP and [^{11}C]PK11195 binding should be studied over time

to understand the possible changes in glial activity during the disease progression and activity stages. Advancement in the distinguishing of pro- and anti-inflammatory cells is also required, as TSPO-PET imaging alone cannot differentiate them (Bonsack et al., 2016) in addition to which the role of GFAP and its use as a biomarker in MS should be further studied as studies about it have mainly focused on TBI.

In conclusion, glial activity is increased in MS pathology as indicated by increased [^{11}C]PK11195 binding and serum GFAP. Serum GFAP also correlates with EDSS, suggesting it being a biomarker of disability progression. The association between microglial and astrocytic activity remains somewhat elusive as correlation coefficients were not very strong, and they were both positive and negative in nature, depending on the brain region. More research is required to find out whether glial activation in MS is dependent on the brain regions or if these were coincidental findings. However, serum GFAP and TSPO can be considered viable biomarkers of glial activity in future research regarding the association between astrocytic and microglial activity.

4 Materials and methods

4.1 Ethical approval and participant consent

The study was conducted following ethical standards set by the Declaration of Helsinki and was approved by the ethics committee. To participate in this study, study subjects were required to give their written, informed, and voluntary consent. Obligation of secrecy regarding patient information was taken into account.

4.2 Study participants

The study cohort included 44 MS patients (40 RRMS, 4 SPMS) who were recruited between 2016-2019 from the outpatient clinic of the Division of Clinical Neurosciences at University Hospital of Turku, Finland. The participants were required to have a MS diagnosis based on current criteria and be willing to participate in PET imaging. Additionally, the study included 22 age- and sex-matched HCs with no known neurological symptoms or diseases.

Study participants participated in [^{11}C]PK11195-PET imaging to detect immune cell activation in the brain, MRI to be used as anatomical reference and evaluate MS-related pathology, and blood sampling. In addition, MS patients had a clinical assessment performed by an experienced clinician to determine their EDSS score based on the standardized examination form (neurostatus.net). Other clinical variables included disease duration, MSSS, and ARR. Disease duration was calculated from the first symptoms to the imaging, MSSS was determined based on disease duration and EDSS, and ARR was calculated by dividing the total number of relapses from the first relapse to the imaging by the disease duration.

For this study, inclusion criteria for MS patients were maximum of 180 days between the obtaining the blood sample and PET imaging. Blood samples were obtained from 14 HCs, too. Exclusion criteria was intolerability of MRI or PET, pregnancy, a clinical relapse (new neurological symptoms lasting $\geq$ 24 hours) within 120 days prior to participation and/or gadolinium enhancing lesions.

4.3 MRI and PET acquisition

Brain MRI scanning of MS patients was done in Turku PET Centre with a 3 T Ingenuity TF PET/MR System scanner (Philips Healthcare, Cleveland, OH). With a spatial resolution of 1 x 1 x 1 mm, the acquired sequences were axial T2, 3D fluid-attenuated inversion recovery

(FLAIR), 3D T1, and gadolinium-enhanced 3D T1. An 8-channel SENSE head coil was utilized. Detailed MRI protocol has been previously described (Bezukladova et al., 2020). MRI scans of HCs were performed in Turku, Finland with the following scanners: Gyroscan Intera 1.5 T Nova Dual scanner (n = 8), 3 T Ingenuity TF PET/MR System scanner (n = 9) or 3 T Ingenia (n = 5) scanner (Philips Healthcare, Cleveland, OH).

PET scans of both MS patients and HCs were done with a brain-dedicated ECAT HRRT scanner (CTI/Siemens) with an intrinsic spatial resolution of 2.5 mm. The process has been previously described (Nylund et al., 2021). The radioligand, [^{11}C]PK11195, was synthesized as previously described (Rissanen et al., 2018). The mean (SD) injected doses of [^{11}C]PK11195 for MS patients and HCs were 488 (14.8) MBq and 489 (16.5) MBq, respectively (p = 0.9).

4.4 MRI and PET data pre-processing and analysis

The semi-automated method to create a combined T2 lesion region of interest (ROI) and a combined T1 lesion ROI mask images has been described in detail previously (Bezukladova et al., 2020). In summary, T2 lesions were initially identified from FLAIR images with Lesion Segmentation Tool (LST, www.statistical-modelling.de/lst.html, a toolbox running in SPM8). With the help of these T2 lesions, T1 hypointense lesions were then identified visually from the 3D T1 images. The identification of T1 lesion ROI masks was performed by manually shaping the masks slice by slice using CarimasCE software (https://turkupetcentre.fi/carimas/). Creation of binary brain ROI and segmentation of GM and WM were performed with Freesurfer 5.3 software (http://surfer.nmr.mgh.harvard.edu/).

Included in the whole brain ROI were cerebellum, cerebrum, and brain stem but not ventricles. Lesion rim and perilesional ROIs were created by dilatating the T1 lesion ROI masks after which the T1 lesion ROI was removed. In the 0-2 mm lesion rim ROI, the T1 lesion ROI was dilated by 2 voxels. In the 2-6 mm and 4-6 mm lesion rim ROIs, in addition to removing the T1 lesion ROI, also the 0-2 mm and 0-4 mm lesion ROIs were removed, respectively. The NAWM ROI was obtained by removing the combined T1 lesion mask, 0-2 mm lesion rim mask, cerebellar WM, and brain matter from the WM ROI. Other ROIs included cortical GM, brain stem, amygdala, thalamus, pallidum, and ventral diencephalon, and were obtained directly from Freesurfer software. Ventral diencephalon ROI was defined to include hypothalamus, sublenticular extended amygdala, basal forebrain, and portion of the ventral tegmentum. Volumes (cm^3) of NAWM, cortical GM, and lesions were obtained with Freesurfer software as previously described (Rissanen et al., 2018).

The created ROIs were used to determine and evaluate the location and intensity of specific [^{11}C]PK11195 binding that indicates innate immune cell activation. This binding was presented as distribution volume ratio (DVR) which was determined with a supervised cluster algorithm (SuperPK software, SVCA4 classification) (Yaqub et al., 2012). DVRs were calculated for the pre-specified ROIs. The reconstruction, smoothing, partial volume correction and co-registration of PET images was performed as previously described (Rissanen et al., 2014; Sucksdorff et al., 2020). Active voxels were determined based on the average of mean+1.96*SD DVRs of 18 HCs with a threshold DVR value of 1.56, as previously described (Nylund et al., 2021).

4.5 Categorization of lesions

Categorization of T1 hypointense lesions was done by comparing the proportion of active voxels in the lesion and at the lesion rim as previously described (Nylund et al., 2021). Based on this, the lesions were divided into the following subtypes: rim-active lesions, overall-active lesions, and inactive lesions. Rim-active phenotype required the that if 5-20 % of the active voxels are in the lesion core, there must be double the percentage of active voxels at the rim. Alternatively, if maximum of 5 % of the active voxels in the core, rim had to have ≥ 5 % more active voxels compared to the core. Inactive lesions were determined by 0 % active voxels in the lesion core and 0 % at the rim. Lesions that did not fit in these two categories were classified as overall-active. T1 lesions included in this phenotyping were larger than 27 mm^3 and were located within cerebral WM.

4.6 Measurement of serum GFAP

Blood samples of 44 MS patients and 14 HCs were collected in 10 ml Vacuette® serum clot-activator tubes (Greiner Bio-one, product number 455092) before 12 AM. The blood was then allowed to clot for 30 minutes at room temperature before the serum was stored in aliquots at -80 °C in the Auria Biobank (Turku, Finland) within two hours of sampling. The frozen samples were shipped in dry ice to Basel, Switzerland, where the serum GFAP levels were determined by University of Basel with SIMOA (single-molecule array) assay kits (Quanterix Corporation, Lexington, MA, USA) called GFAP (1st measurement) and NEUROLOGY 2-PLEX B (2nd measurement). The 1st analysis was performed a mean of 2.9 years after the sampling, and the 2nd analysis was done 2.5 years after the 1st one.

In the analysis, samples and calibrators were measured in duplicates with seven non-zero calibrators. Additionally, there were three native serum controls from the biobank of University of Basel in each analysis. The mean concentrations (inter-assay coefficient of variation) of the controls we 61.2 pg/ml (7.4%), 85.8 pg/ml (6.0%), and 94.8 pg/ml (4.06%) in the first analysis, and 85.3 pg/ml (12.6%), 105.5 pg/ml (9.1%), and 500.2 (7.5%) in the second one. Concentrations of all samples were higher than the concentration of the lowest calibrator meeting acceptance criteria and lower than the concentration of the highest calibrator meeting acceptance criteria (Valentin et al., 2011).

4.7 Statistical analysis

Statistical analysis was performed with GraphPad Prism software (version 5.01). Normality of data was tested using Shapiro-Wilk normality test. Based on the normality test results, variables are presented as either mean with standard deviation (SD) or range, or median with interquartile range (IQR) in the Tables 1-8. Differences between different groups were analysed with Mann-Whitney U (Wilcoxon rank-sum) test. Statistical differences were determined for multiple variables including clinical and demographic characteristics, MRI volumes, DVR of different brain regions, and lesion characteristics. Correlation analyses, using Spearman's rank correlation coefficient (ρ), were performed to study the relationships between variables. Correlation was studied between serum GFAP and other variables in MS patients and HCs as well as GFAP(low) and GFAP(high) subgroups. These statistical tests were selected due to high alternation of normal and non-normal distribution in variables between different groups as well as the rather small and disproportioned group sizes. All the performed tests were two-tailed and used a p-value of <0.05 for statistical significance.

For analysis, the whole study population was divided into different subgroups which were then compared: MS patients vs. HCs, female vs. male MS patients, and MS patients receiving some disease modifying therapy (DMT) vs. patients with no DMT. DMT status was determined by the therapy at the time of participation to imaging and/or within prior two months. Additionally, MS patients were divided into GFAP(low) and GFAP(high) subgroups. The cut-off value was determined by the 80^{th} percentile of the HC serum GFAP (90.47 pg/ml).

5 Acknowledgements

I would like to acknowledge and thank my supervisors Laura Airas and Maija Saraste, as well as the whole Airas group, for welcoming me to the research group and guiding me through this process. I am forever grateful for the help I received during this experience. Also, a special thank you to Marjo Nylund and Eveliina Honkonen for teaching me how to draw the lesion masks, and Markus Matilainen for guiding me through the statistical analyses.

I would also like to thank my family and friends for supporting, encouraging, and motivating me during this project. Lastly, like all clinical research, this project would not have been possible without the study participants, so I owe my gratitude to those who volunteered.

6 References

Abdelhak, A., Foschi, M., Abu-Rumeileh, S., Yue, J. K., DAnna, L., Huss, A., Oeckl, P., Ludolph, A. C., Kuhle, J., Petzold, A., Manley, G. T., Green, A. J., Otto, M., & Tumani, H. (2022). Blood GFAP as an emerging biomarker in brain and spinal cord disorders. *Nature Reviews Neurology*, *18*, 158–172. https://doi.org/10.1038/s41582-021-00616-3

Abdelhak, A., Hottenrott, T., Morenas-Rodríguez, E., Suárez-Calvet, M., Zettl, U. K., Haass, C., Meuth, S. G., Rauer, S., Otto, M., Tumani, H., & Huss, A. (2019). Glial Activation Markers in CSF and Serum From Patients With Primary Progressive Multiple Sclerosis: Potential of Serum GFAP as Disease Severity Marker? *Frontiers in Neurology*, *10*, 280. https://doi.org/10.3389/fneur.2019.00280

Abdelhak, A., Huss, A., Kassubek, J., Tumani, H., & Otto, & M. (2018). Serum GFAP as a biomarker for disease severity in multiple sclerosis. *Scientific Reports*, *8*(14798). https://doi.org/10.1038/s41598-018-33158-8

Absinta, M., Maric, D., Gharagozloo, M., Garton, T., Smith, M. D., Jin, J., Fitzgerald, K. C., Song, A., Liu, P., Lin, J., Wu, T., Johnson, K. R., Mcgavern, D. B., Schafer, D. P., Calabresi, P. A., & Reich, D. S. (2021). A lymphocyte – microglia – astrocyte axis in chronic active multiple sclerosis. *Nature*, *597*, 709–714. https://doi.org/10.1038/s41586-021-03892-7

Agostini, M., Amato, F., Vieri, M. L., Greco, G., Tonazzini, I., Baroncelli, L., Caleo, M., Vannini, E., Santi, M., Signore, G., & Cecchini, M. (2021). Glial-fibrillary-acidic-protein (GFAP) biomarker detection in serum-matrix: Functionalization strategies and detection by an ultra-high-frequency surface-acoustic-wave (UHF-SAW) lab-on-chip. *Biosensors and Bioelectronics*, *172*, 112774. https://doi.org/10.1016/J.BIOS.2020.112774

Ahmed, T. (2022). Neural stem cell engineering for the treatment of multiple sclerosis. *Biomedical Engineering Advances*, *4*, 100053. https://doi.org/10.1016/J.BEA.2022.100053

Airas, L., & Yong, V. W. (2022). Microglia in multiple sclerosis - Pathogenesis and imaging. *Current Opinion in Neurology*, *35*(3), 299–306. https://doi.org/10.1097/WCO.0000000000001045

Aktas, O., Smith, M. A., Rees, W. A., Bennett, J. L., She, D., Katz, E., Cree, B. A. C., Fujihara, K., Paul, F., Hartung, H. P., Marignier, R., Kim, H. J., Weinshenker, B. G., Pittock, S. J., Wingerchuk, D. M., Cutter, G. R., Green, A. J., Mealy, M. A., & Drappa, J. (2021). Serum Glial Fibrillary Acidic Protein: A Neuromyelitis Optica Spectrum

Disorder Biomarker. *Annals of Neurology*, *89*(5), 895–910. https://doi.org/10.1002/ana.26067

Aloisi, F., Ria, F., Penna, G., & Adorini, L. (1998). Microglia are more efficient than astrocytes in antigen processing and in Th1 but not Th2 cell activation. *Journal of Immunology*, *160*(10), 4671–4680.

Axelsson, M., Malmeström, • C, Nilsson, • S, Haghighi, • S, Rosengren, • L, & Lycke, • J. (2011). Glial fibrillary acidic protein: a potential biomarker for progression in multiple sclerosis. *Journal of Neurology*, *258*, 882–888. https://doi.org/10.1007/s00415-010-5863-2

Aykaç, S., & Eliaçık, S. (2022). What are the trends in the treatment of multiple sclerosis in recent studies? – A bibliometric analysis with global productivity during 1980–2021. *Multiple Sclerosis and Related Disorders*, *68*, 104185. https://doi.org/10.1016/J.MSARD.2022.104185

Ayrignac, X., Le Bars, E., Duflos, C., Hirtz, C., Maleska Maceski, A., Carra-Dallière, C., Charif, M., Pinna, F., Prin, P., Menjot de Champfleur, N., Deverdun, J., Kober, T., Marechal, B., Fartaria, M. J., Corredor Jerez, R., Labauge, P., & Lehmann, S. (2020). Serum GFAP in multiple sclerosis: correlation with disease type and MRI markers of disease severity. *Scientific Reports*, *10*, 10923. https://doi.org/10.1038/s41598-020-67934-2

Baecher-Allan, C., Kaskow, B. J., & Weiner, H. L. (2018). Multiple Sclerosis: Mechanisms and Immunotherapy. *Neuron*, *97*(4), 742–768. https://doi.org/10.1016/j.neuron.2018.01.021

Banati, R. B., Newcombe, J., Gunn, R. N., Cagnin, A., Turkheimer, F., Heppner, F., Price, G., Wegner, F., Giovannoni, G., Miller, D. H., Perkin, G. D., Smith, T., Hewson, A. K., Bydder, G., Kreutzberg, G. W., Jones, T., Cuzner, M. L., & Myers, R. (2000). The peripheral benzodiazepine binding site in the brain in multiple sclerosis. Quantitative in vivo imaging of microglia as a measure of disease activity. *Brain*, *123*(11), 2321–2337. https://doi.org/10.1093/brain/123.11.2321

Barro, C., Healy, B. C., Liu, Y., Saxena, S., Paul, A., Polgar-Turcsanyi, M., Guttmann, C. R. G., Bakshi, R., Kropshofer, H., Weiner, H. L., & Chitnis, T. (2023). Serum GFAP and NfL Levels Differentiate Subsequent Progression and Disease Activity in Patients With Progressive Multiple Sclerosis. *Neurology Neuroimmunology & Neuroinflammation*, *10*(e200052). https://doi.org/10.1212/NXI.0000000000200052

Barsky, A., Peekna, H., & Borus, J. (2001). Somatic Symptom Reporting in Women and Men.

Journal of General Internal Medicine, *16*(4), 266–275. http://www.ncbi.nlm.nih.gov/pubmed/11318929

Batiuk, M. Y., Martirosyan, A., Wahis, J., de Vin, F., Marneffe, C., Kusserow, C., Koeppen, J., Viana, J. F., Oliveira, J. F., Voet, T., Ponting, C. P., Belgard, T. G., & Holt, M. G. (2020). Identification of region-specific astrocyte subtypes at single cell resolution. *Nature Communications*, *11*. https://doi.org/10.1038/s41467-019-14198-8

Ben Haim, L., & Rowitch, D. H. (2016). Functional diversity of astrocytes in neural circuit regulation. *Nature Reviews Neuroscience*, *18*(1), 31–41. https://doi.org/10.1038/nrn.2016.159

Bergström, M., Mosskin, M., Ericson, K., Ehrin, E., Thorell, J. O., von Holst, H., Norén, G., Persson, A., Halldin, C., & Stone-Elander, S. (1986). Peripheral benzodiazepine binding sites in human gliomas evaluated with positron emission tomography. *Acta Radiologica. Supplementum*, *369*, 409—411.

Betlazar, C., Harrison-Brown, M., Middleton, R. J., Banati, R., & Liu, G. J. (2018). Cellular sources and regional variations in the expression of the neuroinflammatory marker translocator protein (TSPO) in the normal brain. *International Journal of Molecular Sciences*, *19*(9), 2707. https://doi.org/10.3390/ijms19092707

Beynon, V., George, I. C., Elliott, C., Arnold, D. L., Ke, J., Chen, H., Zhu, L., Ke, C., Giovannoni, G., Scaramozza, M., Campbell, N., Bradley, D. P., Franchimont, N., Gafson, A., & Belachew, S. (2022). Chronic lesion activity and disability progression in secondary progressive multiple sclerosis. *BMJ Neurology Open*, *4*, e000240. https://doi.org/10.1136/bmjno-2021-000240

Bezukladova, S., Tuisku, J., Matilainen, M., Vuorimaa, A., Nylund, M., Smith, S., Sucksdorff, M., Mohammadian, M., Saunavaara, V., Laaksonen, S., Rokka, J., Rinne, J. O., Rissanen, E., & Airas, L. (2020). Insights into disseminated MS brain pathology with multimodal diffusion tensor and PET imaging. *Neurol Neuroimmunol Neuroinflamm*, *7*(3). https://doi.org/10.1212/NXI.0000000000000691

Bonsack, F., Alleyne, C. H., & Sukumari-Ramesh, S. (2016). Augmented expression of TSPO after intracerebral hemorrhage: A role in inflammation? *Journal of Neuroinflammation*, *13*(151). https://doi.org/10.1186/s12974-016-0619-2

Braestrup, C., Albrechsten, R., & Squires, R. F. (1977). High densities of benzodiazepine receptors in human cortical areas. *Nature*, *269*, 702–704.

Brandi, E., Torres-Garcia, L., Svanbergsson, A., Haikal, C., Liu, D., Li, W., & Li, J. Y. (2022). Brain region-specific microglial and astrocytic activation in response to systemic

lipopolysaccharides exposure. *Frontiers in Aging Neuroscience*, *14*, 910988. https://doi.org/10.3389/fnagi.2022.910988

Brosnan, C. F., & Raine, C. S. (2013). The Astrocyte in Multiple Sclerosis Revisited. *GLIA*, *61*(4), 453–465. https://doi.org/10.1002/glia.22443

Burman, J., Zetterberg, H., Fransson, M., Loskog, A. S., Raininko, R., & Fagius, J. (2014). Assessing tissue damage in multiple sclerosis: A biomarker approach. *Acta Neurologica Scandinavica*, *130*(2), 81–89. https://doi.org/10.1111/ane.12239

Chaudhuri, A., & Behan, P. O. (2004). Multiple Sclerosis Is Not an Autoimmune Disease. *Archives of Neurology*, *61*, 1610–1612.

Christopherson, K. S., Ullian, E. M., Stokes, C. C. A., Mullowney, C. E., Hell, J. W., Agah, A., Lawler, J., Mosher, D. F., Bornstein, P., & Barres, B. A. (2005). Thrombospondins are astrocyte-secreted proteins that promote CNS synaptogenesis. *Cell*, *120*(3), 421–433. https://doi.org/10.1016/j.cell.2004.12.020

Ciccarelli, O., Barkhof, F., Bodini, B., De Stefano, N., Golay, X., Nicolay, K., Pelletier, D., Pouwels, P. J. W., Smith, S. A., Wheeler-Kingshott, C. A. M., Stankoff, B., Yousry, T., & Miller, D. H. (2014). Pathogenesis of multiple sclerosis: insights from molecular and metabolic imaging. *The Lancet Neurology*, *13*, 807–822. https://doi.org/10.1016/S1474-4422(14)70101-2

Colonna, M., & Butovsky, O. (2017). Microglia Function in the Central Nervous System During Health and Neurodegeneration. *Annual Review of Immunology*, *35*, 441–468. https://doi.org/10.1146/annurev-immunol

Correale, J. (2021). BTK inhibitors as potential therapies for multiple sclerosis. *The Lancet Neurology*, *20*(9), 689–691. https://doi.org/10.1016/S1474-4422(21)00250-7

Cosenza-Nashat, M., Zhao, M. L., Suh, H. S., Morgan, J., Natividad, R., Morgello, S., & Lee, S. C. (2009). Expression of the translocator protein of 18 kDa by microglia, macrophages and astrocytes based on immunohistochemical localization in abnormal human brain. *Neuropathology and Applied Neurobiology*, *35*(3), 306–328. https://doi.org/10.1111/j.1365-2990.2008.01006.x

De Groot, C. J. A., Bergers, E., Kamphorst, W., Ravid, R., Polman, C. H., Barkhof, F., & Van Der Valk, P. (2001). Post-mortem MRI-guided sampling of multiple sclerosis brain lesions: Increased yield of active demyelinating and (p)reactive lesions. *Brain*, *124*(8), 1635–1645. https://doi.org/10.1093/brain/124.8.1635

De Kleijn, K. M. A., & Martens, G. J. M. (2020). Molecular effects of FDA-approved multiple sclerosis drugs on glial cells and neurons of the central nervous system.

International Journal of Molecular Sciences, *21*(4229). https://doi.org/10.3390/ijms21124229

Dobson, R., & Giovannoni, G. (2019). Multiple sclerosis - a review. *European Journal of Neurology*, *26*, 27–40. https://doi.org/10.1111/ene.13819

Dong, Y., & Wee Yong, V. (2019). When encephalitogenic T cells collaborate with microglia in multiple sclerosis. *Nature Reviews Neurology*, *15*, 704–717. https://doi.org/10.1038/s41582-019-0253-6

Eng, L. F., Ghirnikar, R. S., & Lee, Y. L. (2000). Glial Fibrillary Acidic Protein: GFAP-Thirty-One Years (1969-2000)*. *Neurochemical Research*, *25*(9/10), 1439–1451. https://doi.org/10.1023/a:1007677003387

Eng, L. F., Vanderhaeghen, J. J., Bignami, A., & Gerstl, B. (1971). An acidic protein isolated from fibrous astrocytes. *Brain Research*, *28*(2), 351–354. https://doi.org/10.1016/0006-8993(71)90668-8

Enzinger, C., Barkhof, F., Ciccarelli, O., Filippi, M., Kappos, L., Rocca, M. A., Ropele, S., Rovira, À., Schneider, T., De Stefano, N., Vrenken, H., Wheeler-Kingshott, C., Wuerfel, J., & Fazekas, F. (2015). Nonconventional MRI and microstructural cerebral changes in multiple sclerosis. *Nature Reviews Neurology*, *11*, 676–686. https://doi.org/10.1038/nrneurol.2015.194

Escartin, C., Galea, E., Lakatos, A., O'Callaghan, J. P., Petzold, G. C., Serrano-Pozo, A., Steinhäuser, C., Volterra, A., Carmignoto, G., Agarwal, A., Allen, N. J., Araque, A., Barbeito, L., Barzilai, A., Bergles, D. E., Bonvento, G., Butt, A. M., Chen, W. T., Cohen-Salmon, M., … Verkhratsky, A. (2021). Reactive astrocyte nomenclature, definitions, and future directions. *Nature Neuroscience*, *24*, 312–325. https://doi.org/10.1038/s41593-020-00783-4

Faulkner, J. R., Herrmann, J. E., Woo, M. J., Tansey, K. E., Doan, N. B., & Sofroniew, M. V. (2004). Reactive Astrocytes Protect Tissue and Preserve Function after Spinal Cord Injury. *The Journal of Neuroscience*, *24*(9), 2143–2155. https://doi.org/10.1523/JNEUROSCI.3547-03.2004

Fisniku, L. K., Brex, P. A., Altmann, D. R., Miszkiel, K. A., Benton, C. E., Lanyon, R., Thompson, A. J., Miller, D. H., & Fisniku, L. (2008). Disability and T 2 MRI lesions: a 20-year follow-up of patients with relapse onset of multiple sclerosis. *Brain*, *131*, 808–817. https://doi.org/10.1093/brain/awm329

Ghasemi, N., Razavi, S., & Nikzad, E. (2017). Multiple Sclerosis: Pathogenesis, Symptoms, Diagnoses and Cell-Based Therapy. In *CELL JOURNAL* (Vol. 19, Issue 1).

https://doi.org/https://doi.org/10.22074/cellj.2016.4867

Giannetti, P., Politis, M., Su, P., Turkheimer, F. E., Malik, O., Keihaninejad, S., Wu, K., Waldman, A., Reynolds, R., Nicholas, R., & Piccini, P. (2015). Increased PK11195-PET binding in normal-appearing white matter in clinically isolated syndrome. *Brain: A Journal of Neurology*, *138*, 110–119. https://doi.org/10.1093/brain/awu331

Goldenberg, M. M. (2012). Multiple Sclerosis Review. *P & T : A Peer-Reviewed Journal for Formulary Management*, *37*(3), 175–183.

Griemsmann, S., Höft, S. P., Bedner, P., Zhang, J., Von Staden, E., Beinhauer, A., Degen, J., Dublin, P., Cope, D. W., Richter, N., Crunelli, V., Jabs, R., Willecke, K., Theis, M., Seifert, G., Kettenmann, H., & Steinhäuser, C. (2015). Characterization of panglial gap junction networks in the thalamus, neocortex, and hippocampus reveals a unique population of glial cells. *Cerebral Cortex*, *25*(10), 3420–3433. https://doi.org/10.1093/cercor/bhu157

Guilarte, T. R. (2019). TSPO in diverse CNS pathologies and psychiatric disease: A critical review and a way forward. *Pharmacology & Therapeutics*, *194*, 44–58. https://doi.org/10.1016/J.PHARMTHERA.2018.09.003

Hauser, S. L., & Cree, B. A. C. (2020). Treatment of Multiple Sclerosis: A Review. *The American Journal of Medicine*, *133*(12), 1380-1390.e2. https://doi.org/10.1016/J.AMJMED.2020.05.049

Högel, H., Rissanen, E., Barro, C., Matilainen, M., Nylund, M., Kuhle, J., & Airas, L. (2020). Serum glial fibrillary acidic protein correlates with multiple sclerosis disease severity. *Multiple Sclerosis Journal*, *26*(2), 210–219. https://doi.org/10.1177/1352458518819380

Högel, H., Rissanen, E., Vuorimaa, A., & Airas, L. (2018). Positron emission tomography imaging in evaluation of MS pathology in vivo. *Multiple Sclerosis Journal*, *24*(11), 1399–1412. https://doi.org/10.1177/1352458518791680

International Multiple Sclerosis Genetics Consortium (IMSGC), Beecham, A., & Patsopoulos, N. et al. (2013). Analysis of immune-related loci identifies 48 new susceptibility variants for multiple sclerosis. *Nature Genetics*, *45*(11), 1353–1360. https://doi.org/10.1038/ng.2770

Jacobs, A. H., Tavitian, B., & Consortium, I. (2012). Noninvasive molecular imaging of neuroinflammation. *J Cereb Blood Flow Metab.*, *32*(7), 1393–1415. https://doi.org/10.1038/jcbfm.2012.53

Joyce, N., Annett, G., Wirthlin, L., Olson, S., Bauer, G., & Nolta, J. A. (2010). Mesenchymal stem cells for the treatment of neurodegenerative disease. *Regenerative Medicine*, *5*(6),

933–946. https://doi.org/https://doi.org/10.2217/rme.10.72

Kamma, E., Lasisi, W., Libner, C., Shin Ng, H., & Plemel, J. R. (2021). Brain profiling in murine colitis and human epilepsy reveals neutrophils and TNFα as mediators of neuronal hyperexcitability. *Journal of Neuroinflammation*, *19*, 45. https://doi.org/10.1186/s12974-022-02408-y

Kang, Y., Pandya, S., Zinger, N., Michaelson, N., & Gauthier, S. A. (2021). Longitudinal change in TSPO PET imaging in progressive multiple sclerosis. *Annals of Clinical and Translational Neurology*, *8*(8), 1755–1759. https://doi.org/10.1002/acn3.51431

Kaunzner, U. W., Kang, Y., Monohan, E., Kothari, P. J., Nealon, N., Perumal, J., Vartanian, T., Kuceyeski, A., Vallabhajosula, S., Mozley, P. D., Riley, C. S., Newman, S. M., & Gauthier, S. A. (2017). Reduction of PK11195 uptake observed in multiple sclerosis lesions after natalizumab initiation. *Multiple Sclerosis and Related Disorders*, *15*, 27–33. https://doi.org/10.1016/j.msard.2017.04.008

Kim, T., & Pae, A. N. (2016). Translocator protein (TSPO) ligands for the diagnosis or treatment of neurodegenerative diseases: a patent review (2010-2015; part 1). *Expert Opinion on Therapeutic Patents*, *26*(11), 1325–1351. https://doi.org/10.1080/13543776.2016.1230606

Kodama, L., & Gan, L. (2019). Do Microglial Sex Differences Contribute to Sex Differences in Neurodegenerative Diseases? *Trends in Molecular Medicine*, *25*(9), 741–749. https://doi.org/10.1016/j.molmed.2019.05.001

Krumbholz, (M, Hohlfeld, R., Meinl, E., Krumbholz, M., Derfuss, T., Hohlfeld, R., & Meinl, E. (2012). B cells and antibodies in multiple sclerosis pathogenesis and therapy. *Nature Reviews Neurology*, *8*, 613–623. https://doi.org/10.1038/nrneurol.2012.203

Kuhlmann, A. C., & Guilarte, T. R. (2000). Cellular and Subcellular Localization of Peripheral Benzodiazepine Receptors After Trimethyltin Neurotoxicity. *Journal of Neurochemistry*, *74*(4), 1694–1704. https://doi.org/https://doi.org/10.1046/j.1471-4159.2000.0741694.x

Kurtzke, J. F. (1983). Rating neurologic impairment in multiple sclerosis: An expanded disability status scale (EDSS). *Neurology*, *33*(11), 1444–1452. https://doi.org/10.1212/wnl.33.11.1444

Lavisse, S., Guillermier, M., Hérard, A. S., Petit, F., Delahaye, M., Van Camp, N. V., Haim, L. Ben, Lebon, V., Remy, P., Dollé, F., Delzescaux, T., Bonvento, G., Hantraye, P., & Escartin, C. (2012). Reactive astrocytes overexpress TSPO and are detected by TSPO positron emission tomography imaging. *The Journal of Neuroscience*, *32*(32), 10809–

10818. https://doi.org/https://doi.org/10.1523/JNEUROSCI.1487-12.2012

Lee, E. J., Lim, Y. M., Kim, S., Choi, L., Kim, H., Kim, K., Kim, H. W., Lee, J. S., & Kim, K. K. (2020). Clinical implication of serum biomarkers and patient age in inflammatory demyelinating diseases. *Annals of Clinical and Translational Neurology*, *7*(6), 992–1001. https://doi.org/10.1002/acn3.51070

Lee, J., Kim, S. W., & Kim, K. T. (2022). Region-Specific Characteristics of Astrocytes and Microglia: A Possible Involvement in Aging and Diseases. *Cells*, *11*(12), 1902. https://doi.org/10.3390/cells11121902

Lee, Y., Park, Y., Nam, H., Lee, J. W., & Yu, S. W. (2020). Translocator protein (TSPO): The new story of the old protein in neuroinflammation. *BMB Reports*, *53*(1), 20–27. https://doi.org/10.5483/BMBRep.2020.53.1.273

Liddelow, S., Guttenplan, K., Clarke, L. E., Bennett, F., Bohlen, C., Schirmer, L., Bennett, M. L., Münch, alexandra E., Chung, W.-S., Peterson, T., Wilton, D. K., Frouin, A., Napier, B., Stevens, B., & Barres, B. (2017). Neurotoxic reactive astrocytes are induced by activated microglia. *Nature*, *541*(7638), 481–487. https://doi.org/10.1038/nature21029

Logan, J., Fowler, J. S., Volkow, D., Wang, G., Ding, Y., & Alexoff, D. L. (1996). Distribution Volume Ratios Without Blood Sampling from Graphical Analysis of PET Data. *Journal of Cerebral Blood Flow & Metabolism*, *16*, 834–840.

Ludwin, S. K., Rao, V. T., Moore, graig S., & Antel, J. P. (2016). Astrocytes in multiple sclerosis. *Multiple Sclerosis Journal*, *22*(9), 1114–1124. https://doi.org/10.1177/1352458516643396

Lutz, S. E., Zhao, Y., Gulinello, M., Lee, S. C., Raine, C. S., & Brosnan, C. F. (2009). Deletion of astrocyte connexins 43 and 30 leads to a dysmyelinating phenotype and hippocampal CA1 vacuolation. *Journal of Neuroscience*, *29*(24), 7743–7752. https://doi.org/10.1523/JNEUROSCI.0341-09.2009

Maeda, J., Higuchi, M., Inaji, M., Ji, B., Haneda, E., Okauchi, T., Zhang, M. R., Suzuki, K., & Suhara, T. (2007). Phase-dependent roles of reactive microglia and astrocytes in nervous system injury as delineated by imaging of peripheral benzodiazepine receptor. *Brain Research*, *1157*(1), 100–111. https://doi.org/10.1016/j.brainres.2007.04.054

Meier, S., Willemse, E. A. J., Schaedelin, S., Oechtering, J., Lorscheider, J., Melie-Garcia, L., Cagol, A., Barakovic, M., Galbusera, R., Subramaniam, S., Barro, C., Abdelhak, A., Thebault, S., Achtnichts, L., Lalive, P., Müller, S., Pot, C., Salmen, A., Disanto, G., … Kuhle, J. (2023). Serum Glial Fibrillary Acidic Protein Compared With Neurofilament Light Chain as a Biomarker for Disease Progression in Multiple Sclerosis. *JAMA*

Neurology. https://doi.org/10.1001/jamaneurol.2022.5250

Messing, A., & Brenner, M. (2020). GFAP at 50. *American Society for Neurochemistry*, *Jan-Dec*(12), 1759091420949680. https://doi.org/10.1177/1759091420949680

Michell-Robinson, M. A., Touil, H., Healy, L. M., Owen, D. R., Durafourt, B. A., Bar-Or, A., Antel, J. P., & Moore, C. S. (2015). Roles of microglia in brain development, tissue maintenance and repair. *Brain*, *138*(5), 1138–1159. https://doi.org/10.1093/brain/awv066

Middeldorp, J., & Hol, E. M. (2011). GFAP in health and disease. In *Progress in Neurobiology* (Vol. 93, Issue 3, pp. 421–443). Pergamon. https://doi.org/10.1016/j.pneurobio.2011.01.005

Miljkovic, D., & Spasojevic, I. (2013). Multiple Sclerosis: Molecular Mechanisms and Therapeutic Opportunities. *Antioxidants & Redox Signalling*, *19*(18), 2286–2334. https://doi.org/10.1089/ars.2012.5068

Min, K. J., Yang, M. S., Kim, S. U., Jou, I., & Joe, E. H. (2006). Astrocytes induce hemeoxygenase-1 expression in microglia: A feasible mechanism for preventing excessive brain inflammation. *Journal of Neuroscience*, *26*(6), 1880–1887. https://doi.org/10.1523/JNEUROSCI.3696-05.2006

Nichols, N. R., Day, J. R., Laping, N. J., Johnson, S. A., & Finch, C. E. (1993). GFAP mRNA increases with age in rat and human brain. *Neurobiology of Aging*, *14*(5), 421–429.

Niiranen, M., Kontkanen, A., Jääskeläinen, O., Tertsunen, H. M., Selander, T., Hartikainen, P., Huber, N., Solje, E., Haapasalo, A., Kokkola, T., Lohioja, T., Herukka, S. K., Simula, S., & Remes, A. M. (2021). Serum GFAP and NfL levels in benign relapsing-remitting multiple sclerosis. *Multiple Sclerosis and Related Disorders*, *56*(103280). https://doi.org/https://doi.org/10.1016/j.msard.2021.103280

Notter, T., Coughlin, J. M., Sawa, A., & Meyer, U. (2018). Reconceptualization of translocator protein as a biomarker of neuroinflammation in psychiatry. *Molecular Psychiatry*, *23*, 36–47. https://doi.org/10.1038/mp.2017.232

Notter, T., Schalbetter, S. M., Clifton, N. E., Mattei, D., Richetto, J., Thomas, K., Meyer, U., & Hall, J. (2021). Neuronal activity increases translocator protein (TSPO) levels. *Molecular Psychiatry*, *26*, 2025–2037. https://doi.org/10.1038/s41380-020-0745-1

Nutma, E., Gebro, E., Marzin, M. C., van der Valk, P., Matthews, P. M., Owen, D. R., & Amor, S. (2021). Activated microglia do not increase 18 kDa translocator protein (TSPO) expression in the multiple sclerosis brain. *Glia*, *69*(10), 2447–2458. https://doi.org/10.1002/glia.24052

Nutma, E., Stephenson, J. A., Gorter, R. P., De Bruin, J., Boucherie, D. M., Donat, C. K.,

Breur, M., Van Der Valk, P., Matthews, P. M., Owen, D. R., & Amor, S. (2019). A quantitative neuropathological assessment of translocator protein expression in multiple sclerosis. *Brain*, *142*(11), 3440–3455. https://doi.org/10.1093/brain/awz287

Nylander, A., & Hafler, D. A. (2012). Multiple sclerosis. *The Journal of Clinical Investigation*, *122*(4), 1180–1188. https://doi.org/https://doi.org/10.1172/JCI58649

Nylund, M., Sucksdorff, M., Matilainen, M., Polvinen, E., Tuisku, J., & Airas, L. (2021). Phenotyping of multiple sclerosis lesions according to innate immune cell activation using 18 kDa translocator protein-PET. *Brain Communications*, *4*(1). https://doi.org/10.1093/braincomms/fcab301

Ontaneda, D., Fox, R. J., & Chataway, J. (2015). Clinical trials in progressive multiple sclerosis: lessons learned and future persectives. *Lancet Neurology*, *14*(2), 208–223. https://doi.org/10.1016/S1474-4422(14)70264-9

Owen, D. R., Narayan, N., Wells, L., Healy, L., Smyth, E., Rabiner, E. A., Galloway, D., Williams, J. B., Lehr, J., Mandhair, H., Peferoen, L. A. N., Taylor, P. C., Amor, S., Antel, J. P., Matthews, P. M., & Moore, C. S. (2017). Pro-inflammatory activation of primary microglia and macrophages increases 18 kDa translocator protein expression in rodents but not humans. *Journal of Cerebral Blood Flow and Metabolism*, *37*(8), 2679–2690. https://doi.org/10.1177/0271678X17710182

Owen, D. R., Yeo, A. J., Gunn, R. N., Song, K., Wadsworth, G., Lewis, A., Rhodes, C., Pulford, D. J., Bennacef, I., Parker, C. A., Stjean, P. L., Cardon, L. R., Mooser, V. E., Matthews, P. M., Rabiner, E. A., & Rubio, J. P. (2012). An 18-kDa Translocator Protein (TSPO) polymorphism explains differences in binding affinity of the PET radioligand PBR28. *Journal of Cerebral Blood Flow & Metabolism*, *32*, 1–5. https://doi.org/10.1038/jcbfm.2011.147

Pappata, S., Cornu, P., Samson, Y., Prenant, C., Benavides, J., Scatton, B., Crouzel, C., Hauw, J. J., & Syrota, A. (1991). PET study of carbon-11-PK 11195 binding to peripheral type benzodiazepine sites in glioblastoma: A case report. *Journal of Nuclear Medicine*, *32*(8), 1608–1610.

Pérez, C. A., Cuascut, F. X., & Hutton, G. J. (2023). Immunopathogenesis, Diagnosis, and Treatment of Multiple Sclerosis: A Clinical Update. *Neurologic Clinics*, *41*(1), 87–106. https://doi.org/10.1016/J.NCL.2022.05.004

Polman, C. H., O'Connor, P. W., Havrdova, E., Hutchinson, M., Kappos, L., Miller, D. H., Phillips, J. T., Lublin, F. D., Giovannoni, G., Wajgt, A., Toal, M., Lynn, F., Panzara, M. A., & Sandrock, A. W. (2006). A Randomized, Placebo-Controlled Trial of Natalizymab

for Relapsing Multiple Sclerosis. *The New England Journal of Medicine*, *354*(9), 899–910. https://doi.org/10.1056/NEJMoa044397

Ponath, G., Park, C., & Pitt, D. (2018). The Role of Astrocytes in Multiple Sclerosis. *Frontiers in Immunology*, *9:2017*. https://doi.org/10.3389/fimmu.2018.00217

Poutiainen, P., Jaronen, M., Quintana, F. J., & Brownell, A. L. (2016). Precision medicine in multiple sclerosis: Future of PET imaging of inflammation and reactive astrocytes. In *Frontiers in Molecular Neuroscience* (Vol. 9, Issue 85). https://doi.org/10.3389/fnmol.2016.00085

Powell, E. M., & Geller, H. M. (1999). Dissection of Astrocyte-Mediated Cues in Neuronal Guidance and Process Extension. *GLIA*, *26*(1), 73–83. https://doi.org/10.1002/(SICI)1098-1136(199903)26:1<73::AID-GLIA8>3.0.CO;2-S

Preziosa, P., Hristova, M., Brennan, F. H., Ramaglia, V., Morgan, B. P., & Gommerman, J. L. (2021). An "Outside-In" and "Inside-Out" Consideration of Complement in the Multiple Sclerosis Brain: Lessons From Development and Neurodegenerative Diseases. *Frontiers in Cellular Neuroscience*, *14*, 600656. https://doi.org/10.3389/fncel.2020.600656

Ransohoff, R. M. (2016). A polarizing question: do M1 and M2 microglia exist? *Nature Neuroscience*, *19*(8), 987–991. https://doi.org/10.1038/nn.4338

Ratchford, J. N., Endres, C. J., Hammoud, D. A., Pomper, M. G., Shiee, N., McGready, J., Pham, D. L., & Calabresi, P. A. (2012). Decreased microglial activation in MS patients treated with glatiramer acetate. *Journal of Neurology*, *259*(6), 1199–1205. https://doi.org/10.1007/s00415-011-6337-x

Rissanen, E., Tuisku, J., Rokka, J., Paavilainen, T., Parkkola, R., Rinne, J. O., & Airas, L. (2014). In vivo detection of diffuse inflammation in secondary progressive multiple sclerosis using PET imaging and the radioligand 11C-PK11195. *Journal of Nuclear Medicine*, *55*(6), 939–944. https://doi.org/10.2967/jnumed.113.131698

Rissanen, E., Tuisku, J., Vahlberg, T., Sucksdorff, M., Paavilainen, T., Parkkola, R., Rokka, J., Gerhard, A., Hinz, R., Talbot, P. S., Rinne, J. O., & Airas, L. (2018). Microglial activation, white matter tract damage, and disability in MS. *Neurology - Neuroimmunology Neuroinflammation*, *5*(3), e443. https://doi.org/10.1212/nxi.0000000000000443

Ritchie, S. J., Cox, S. R., Shen, X., Lombardo, M. V, Reus, L. M., Clara, A., Harris, M. A., Alderson, H. L., Hunter, S., Neilson, E., Liewald, D. C. M., Auyeung, B., Whalley, H. C., Lawrie, S. M., Gale, C. R., Bastin, M. E., McIntosh, A. M., & Deary, I. J. (2018). Sex Differences in the Adult Human Brain: Evidence from 5216 UK Biobank Participants.

Cerebral Cortex, *28*(8), 2959–2975. https://doi.org/10.1093/cercor/bhy109

Rizzo, G., Veronese, M., Tonietto, M., Zanotti-Fregonara, P., Turkheimer, F. E., & Bertoldo, A. (2014). Kinetic modeling without accounting for the vascular component impairs the quantification of [11 C]PBR28 brain PET data. *Journal of Cerebral Blood Flow & Metabolism*, *34*, 1060–1069. https://doi.org/10.1038/jcbfm.2014.55

Rolak, L. A. (2003). Multiple sclerosis: it's not the disease you thought it was. *Clinical Medicine & Research*, *1*(1), 57–60. https://doi.org/10.3121/cmr.1.1.57

Roxburgh, R. H. S. R., Seaman, S. R., Masterman, T., Hensiek, A. E., Sawcer, S. J., Vukusic, S., Achiti, I., Confavreux, C., Coustans, M., Le Page, E., Edan, G., McDonnell, G. V., Hawkins, S., Trojano, M., Liguori, M., Cocco, E., Marrosu, M. G., Tesser, F., Leone, M. A., … Compston, D. A. S. (2005). Multiple sclerosis severity score: Using disability and disease duration to rate disease severity. *Neurology*, *64*(7), 1144–1151. https://doi.org/10.1212/01.WNL.0000156155.19270.F8

Ruigrok, A. N. V., Salimi-Khorshidi, G., Lai, M. C., Baron-Cohen, S., Lombardo, M. V., Tait, R. J., & Suckling, J. (2014). A meta-analysis of sex differences in human brain structure. *Neuroscience and Biobehavioral Reviews*, *39*, 34–50. https://doi.org/10.1016/j.neubiorev.2013.12.004

Rupprecht, R., Papadopoulos, V., Rammes, G., Baghai, T. C., Fan, J., Akula, N., Groyer, G., Adams, D., & Schumacher, M. (2010). Translocator protein (18 kDa) (TSPO) as a therapeutic target for neurological and psychiatric disorders. *Nature Reviews Drug Discovery*, *9*, 971–988. https://doi.org/10.1038/nrd3295

Saraste, M., Matilainen, M., Rajda, C., Galla, Z., Sucksdorff, M., Vécsei, L., & Airas, L. (2022). Association between microglial activation and serum kynurenine pathway metabolites in multiple sclerosis patients. *Multiple Sclerosis and Related Disorders*, *59*, 103667. https://doi.org/10.1016/J.MSARD.2022.103667

Singh, S., Metz, I., Amor, S., Van Der Valk, P., Stadelmann, C., & Brü, W. (2013). Microglial nodules in early multiple sclerosis white matter are associated with degenerating axons. *Acta Neuropathologica*, *125*(4), 595–608. https://doi.org/10.1007/s00401-013-1082-0

Sjölin, K., Kultima, K., Larsson, A., Freyhult, E., Zjukovskaja, C., Alkass, K., & Burman, J. (2022). Distribution of five clinically important neuroglial proteins in the human brain. *Molecular Brain*, *15*(1), 1–8. https://doi.org/10.1186/s13041-022-00935-6

Sofroniew, M. V. (2009). Molecular dissection of reactive astrogliosis and glial scar formation. *Trends in Neurosciences*, *32*(12), 638–647.

https://doi.org/10.1016/j.tins.2009.08.002

Sofroniew, M. V., & Vinters, H. V. (2010). Astrocytes: Biology and pathology. *Acta Neuropathologica*, *119*(1), 7–35. https://doi.org/10.1007/s00401-009-0619-8

Sofroniew, M. V. (2015). Astrogliosis. *Cold Spring Harbor Perspectives in Biology*, *7*(2). https://doi.org/10.1101/cshperspect.a020420

Stephenson, D. T., Schober, D. A., Smalstig, E. B., Mincy, R. E., Gehlert, D. R., & Clemens, J. A. (1995). Peripheral benzodiazepine receptors are colocalized with activated microglia following transient global forebrain ischemia in the rat. *Journal of Neuroscience*, *15*(7), 5263–5274. https://doi.org/10.1523/jneurosci.15-07-05263.1995

Stys, P. K., Zamponi, G. W., van Minnen, J., & Geurts, J. J. G. (2012). Neuroscience Autoimmunity Cytodegeneration "Inside-out" model "Outside-in" model. *Nature Reviews Neuroscience*, *13*, 507–514.

Sucksdorff, M., Matilainen, M., Tuisku, J., Polvinen, E., Vuorimaa, A., Rokka, J., Nylund, M., Rissanen, E., & Airas, L. (2020). Brain TSPO-PET predicts later disease progression independent of relapses in multiple sclerosis. *Brain*, *143*(11), 3318–3330. https://doi.org/10.1093/brain/awaa275

Sucksdorff, M., Tuisku, J., Matilainen, M., Vuorimaa, A., Smith, S., Keitilä, J., Rokka, J., Parkkola, R., Nylund, M., Rinne, J., Rissanen, E., & Airas, L. (2019). Natalizumab treatment reduces microglial activation in the white matter of the MS brain. *Neurology: Neuroimmunology and NeuroInflammation*, *6*(e574). https://doi.org/10.1212/NXI.0000000000000574

Tallantyre, E. C., Brookes, M. J., Dixon, J. E., Morgan, P. S., Evangelou, N., & Morris, P. G. (2008). Demonstrating the perivascular distribution of ms lesions in vivo with 7-tesla MRI. *Neurology*, *70*(22), 2076–2078. https://doi.org/10.1212/01.wnl.0000313377.49555.2e

Tan, Y. L., Yuan, Y., & Tian, L. (2020). Microglial regional heterogeneity and its role in the brain. *Molecular Psychiatry*, *25*, 351–367. https://doi.org/10.1038/s41380-019-0609-8

Thompson, A. J., Banwell, B. L., Barkhof, F., Carroll, W. M., Coetzee, T., Comi, G., Correale, J., Fazekas, F., Filippi, M., Freedman, M. S., Fujihara, K., Galetta, S. L., Hartung, H. P., Kappos, L., Lublin, F. D., Marrie, R. A., Miller, A. E., Miller, D. H., Montalban, X., … Cohen, J. A. (2018). Diagnosis of multiple sclerosis: 2017 revisions of the McDonald criteria. *The Lancet Neurology*, *17*(2), 162–173. https://doi.org/10.1016/S1474-4422(17)30470-2

Titus, H. E., Chen, Y., Podojil, J. R., Robinson, A. P., Balabanov, R., Popko, B., & Miller, S.

D. (2020). Pre-clinical and Clinical Implications of “Inside-Out” vs. “Outside-In” Paradigms in Multiple Sclerosis Etiopathogenesis. *Frontiers in Cellular Neuroscience*, *14*, 599717. https://doi.org/10.3389/fncel.2020.599717

Tybirk, L., Hviid, C. V. B., Knudsen, C. S., & Parkner, T. (2022). Serum GFAP - reference interval and preanalytical properties in Danish adults. *Clinical Chemistry and Laboratory Medicine*, *60*(11), 1830–1838. https://doi.org/10.1515/cclm-2022-0646

Valentin, M. A., Ma, S., Zhao, A., Legay, F., & Avrameas, A. (2011). Validation of immunoassay for protein biomarkers: Bioanalytical study plan implementation to support pre-clinical and clinical studies. *Journal of Pharmaceutical and Biomedical Analysis*, *55*(5), 869–877. https://doi.org/10.1016/J.JPBA.2011.03.033

Varlow, C., Knight, A. C., McQuade, P., & Vasdev, N. (2022). Characterization of neuroinflammatory positron emission tomography biomarkers in chronic traumatic encephalopathy. *Brain Communications*, *4*(1), 1–12. https://doi.org/10.1093/braincomms/fcac019

Venneti, S., Lopresti, B. J., & Wiley, C. A. (2006). The peripheral benzodiazepine receptor (Translocator protein 18 kDa) in microglia: From pathology to imaging. *Progress in Neurobiology*, *80*(6), 308–322. https://doi.org/10.1016/J.PNEUROBIO.2006.10.002

Voß, E. V., Škuljec, J., Gudi, V., Skripuletz, T., Pul, R., Trebst, C., & Stangel, M. (2012). Characterisation of microglia during de- and remyelination: Can they create a repair promoting environment? *Neurobiology of Disease*, *45*(1), 519–528. https://doi.org/10.1016/j.nbd.2011.09.008

Walton, C., King, R., Recthman, L., Kaye, W., Leray, E., Ann Marrie, R., & et al. (2020). Rising prevalence of multiple sclerosis worldwide: Insights from the Atlas of MS, third edition. *Multiple Sclerosis Journal*, *26*(15), 1816–1821. https://doi.org/10.1177/1352458520970841

Watanabe, M., Nakamura, Y., Michalak, Z., Isobe, N., Barro, C., Leppert, D., Matsushita, T., Hayashi, F., Yamasaki, R., Kuhle, J., & Kira, J. (2019). Serum GFAP and neurofilament light as biomarkers of disease activity and disability in NMOSD. *Neurology*, *93*(13), e1299 LP-e1311. https://doi.org/10.1212/WNL.0000000000008160

Wheeler, M. A., Clark, I. C., Tjon, E. C., Li, Z., Zandee, S. E. J., Couturier, C. P., Watson, B. R., Scalisi, G., Alkwai, S., Rothhammer, V., Rotem, A., Heyman, J. A., Thaploo, S., Sanmarco, L. M., Ragoussis, J., Weitz, D. A., Petrecca, K., Moffitt, J. R., Becher, B., … Quintana, F. J. (2020). MAFG-driven astrocytes promote CNS inflammation. *Nature*, *578*(7796), 593–599. https://doi.org/10.1038/s41586-020-1999-0

Williams, A., Platon, G., & Lubetzki, C. (2007). Astrocytes - Friends or Foes in Multiple Sclerosis? *Glia*, *55*, 1300–1312. https://doi.org/10.1002/glia

Wirths, O., Kummer, M. P., Zhou, X., Boddeke, E., Raj, D., Yin, Z., Breur, M., Doorduin, J., Holtman, I. R., Olah, M., Mantingh-Otter, I. J., Van Dam, D., De Deyn, P. P., den Dunnen, W., L Eggen, B. J., & Amor, S. (2017). Increased White Matter Inflammation in Aging- and Alzheimer's Disease Brain. *Frontiers in Molecular Neuroscience*, *10*, 206. https://doi.org/10.3389/fnmol.2017.00206

Wootla, B., Eriguchi, M., & Rodriguez, M. (2012). Is Multiple Sclerosis an Autoimmune Disease? *Autoimmune Diseases*, *2012*(969657). https://doi.org/10.1155/2012/969657

Xiao, B. G., & Link, H. (1999). Is there a balance between microglia and astrocytes in regulating Th1/Th2-cell responses and neuropathologies? *Immunology Today*, *20*(11), 477–479. https://doi.org/10.1016/S0167-5699(99)01501-7

Yang, Z., & Wang, K. K. W. (2015). Glial fibrillary acidic protein: From intermediate filament assembly and gliosis to neurobiomarker. *Trends in Neurosciences*, *38*(6), 364–374. https://doi.org/10.1016/j.tins.2015.04.003

Yaqub, M., Van Berckel, B. N. M., Schuitemaker, A., Hinz, R., Turkheimer, F. E., Tomasi, G., Lammertsma, A. A., & Boellaard, R. (2012). Optimization of supervised cluster analysis for extracting reference tissue input curves in (R)-[11C]PK11195 brain PET studies. *Journal of Cerebral Blood Flow and Metabolism*, *32*(8), 1600–1608. https://doi.org/10.1038/jcbfm.2012.59

Zamanian, J. L., Xu, L., Foo, L. C., Nouri, N., Zhou, L., Giffard, R. G., & Barres, B. A. (2012). Genomic analysis of reactive astrogliosis. *Journal of Neuroscience*, *32*(18), 6391–6410. https://doi.org/10.1523/JNEUROSCI.6221-11.2012

Zeis, T., Graumann, U., Reynolds, R., & Schaeren-Wiemers, N. (2008). Normal-appearing white matter in multiple sclerosis is in a subtle balance between inflammation and neuroprotection. *Brain*, *131*(1), 288–303. https://doi.org/10.1093/brain/awm291

Zrzavy, T., Hametner, S., Wimmer, I., Butovsky, O., Weiner, H. L., & Lassmann, H. (2017). Loss of "homeostatic" microglia and patterns of their activation in active multiple sclerosis. *Brain*, *140*, 1900–1913. https://doi.org/10.1093/brain/awx113